Subversion of MHC-II antigen presentation by *Toxoplasma gondii* involves parasite secretory organelles and the modulation of host immune effectors in the endocytic pathway

Louis-Philippe Leroux

Institute of Parasitology

McGill University, Montreal

Submitted December 2012

A thesis submitted to McGill University in partial fulfillment of the requirement of the degree of PhD in parasitology

Abstract

The obligate intracellular protozoan parasite *Toxoplasma gondii*, the causative agent of toxoplasmosis, is a highly ubiquitous pathogen that infects virtually any warm-blooded animal. Although the infection generally remains asymptomatic in healthy individuals, the parasite invariably encysts. It has been shown that *T. gondii* is able to achieve this goal at least by interfering with MHC-II antigen presentation to dampen the development of the $CD4^+$ T helper cell response and gain a head start on the host adaptive immune system. Previous reports have shown that *T. gondii* inhibits transcription of MHC-II and several other related genes, but the causative inhibitory molecules have yet to be identified.

In an attempt to identify these molecules, a forward genetic screening strategy was initially elaborated, with a genome-wide insertional mutagenesis carried out in order to disrupt the genes encoding for the inhibitory molecules followed. By specifically isolating mutants unable to inhibit MHC-II expression and antigen presentation by flow cytometry, isolation of the disrupted loci and database mining could have enabled the identification by of the encoded inhibitory molecules. However, the screen was not carried out due to experimental limitations.

Biochemical analyses were employed to further characterize the MHC-II inhibitory activity, revealing that this activity segregated with the high-speed supernatant (HSS) prepared from sonicated parasites and was enriched with increasing centrifugal speeds. The inhibitory activity was protein dose-dependent and was completely abrogated when the HSS was treated with a broad-spectrum protease. Subcellular fractionation revealed that the inhibitory activity was found in fractions enriched with secretory organelles, specifically rhoptries (ROP) and/or dense granules (GRA). Furthermore, excreted-secreted antigens (ESA) from freshly egressed tachyzoites displayed inhibitory activity. Proteins from ESA preparations were separated by a two-step fractionation using ion exchange chromatography followed size-exclusion chromatography, and analyzed by

tandem mass spectrometry (MS/MS). Database mining of the MS/MS results generated a list of possible candidates, the majority of which originated from secretory organelles.

Although MHC-II expression was inhibited, low levels of MHC-II molecules were still detected in infected or lysate-treated cells. Experimental results argued that the first layer of transcriptional regulation has to be complemented by a post-translational layer of interference in the host cell endocytic pathway, involving the MHC-II associated invariant chain (Ii), and peptide editor H2-DM. Ii mRNA and protein levels were induced in *T. gondii*-infected cells, while MHC-II and H2-DM IFNγ-induced expression was down-regulated. Ii accumulated in infected cells from 20 hour post-infection until host cell lysis, mainly in the ER. In Ii KO cells, the absence of Ii restored the ability of infected bone marrow-derived dendritic cells to present a parasite antigen in the context of MHC-II, arguing that Ii acts as a dominant negative on MHC-II-restricted antigen presentation of endogenously acquired parasite antigens. Keys host proteases, namely legumain, and cathepsins L and S, and the acidification of endosomal compartments were modulated by the parasite, pointing toward a wider manipulation of the host endocytic pathway by *T. gondii*. Opposing expression patterns of Ii and H2-DM had a drastic effect *in vivo* not only on parasite dissemination towards lymphoid organs, $CD4^+$ T cell activation, and IFNγ production during acute infection, but also on cyst numbers and survival at the chronic phase of the infection. Altogether, these findings reveal a broader manipulation of host cell processes by *T. gondii*, and shed new light on the intricate interactions between intracellular pathogens and host cells, and their ability to subvert immune functions to establish successful infections.

Résumé

Le parasite protozoaire intracellulaire obligatoire *Toxoplasma gondii*, l'agent causant la toxoplasmose, est un pathogène ubiquitaire capable d'infecter tout animal à sang chaud. En dépit du fait que l'infection reste généralement asymptomatique chez les individus en bonne santé, le parasite s'enkyste inévitablement. Il a été démontré que *T. gondii* est capable d'atteindre ce but en partie en interférant avec la présentation d'antigène par le complexe majeur d'histocompatibilité (CMH)-II pour diminuer le développement de la réponse des cellules T $CD4^+$ et pour ainsi devancer la réponse adaptative du système immunitaire. Il a été démontré que *T. gondii* inhibe la transcription de CMH-II et autres gènes liés, mais les molécules inhibitrices causatives restent inconnues.

Pour identifier ces molécules, une stratégie pour un criblage génétique avait été élaborée. Une mutagénèse insertionelle à travers le génome devait être conduite pour perturber les gènes codant pour ces molécules inhibitrices, suivie d'un tri par cytométrie en flux de cellules infectées avec des mutants. En isolant les mutants incapables d'inhiber l'expression de CMH-II, l'isolement des locus génétiques et l'exploration des bases de données auraient pu permettre l'identification des molécules codées. Cependant, ce criblage ne fut complété dû à des limitations expérimentales.

Des analyses biochimiques ont démontré que l'activité inhibitrice se retrouvait dans le surnageant d'haute-vitesse (HSS) préparé à partir de parasites soniqués, et était enrichie avec des vitesses de centrifugation croissantes. L'activité inhibitrice était dose-dépendante de protéines et était complètement abrogée lorsque le SHV était préalablement traité avec une protéase. Un fractionnement subcellulaire révéla que l'activité se retrouvait dans les fractions enrichies d'organelles sécrétoires (rhoptries et granules denses). Aussi, des antigènes excrétés-sécrétés (ESA) obtenus de tachyzoïtes fraîchement lysés possédaient une activité inhibitrice. Les protéines d'ESA furent séparées par fractionnement en deux étapes, commençant par une chromatographie par échange d'ions, suivi par une chromatographie d'exclusion par taille et analysées

par spectrométrie de masse en tandem (MS/MS). Les résultats obtenus furent comparés aux bases de données, et une liste fut dressée avec de candidats potentiels, la majorité d'entre eux provenant d'organelles de sécrétion.

Malgré l'expression réduite, quelques molécules de CMH-II étaient détectés dans les cellules infectées ou traitées. Nos résultats démontrent que la régulation transcriptionelle doit être complémentée par une interférence au niveau post-traductionel dans la voie endocytique de la cellule hôte qui implique la chaîne invariante associée au CMH-II (Ii) et l'éditeur de peptide H2-DM. Les niveaux d'ARNm et de protéines d'Ii étaient induits dans les cellules infectées, alors que ceux de CMH-II et d'H2-DM étaient inhibés. Ii s'accumulait dans les cellules infectées dès 20 heures post-infection, principalement dans le RE. Dans les cellules Ii KO, l'absence d'Ii rétablit la capacité de cellules dendritiques à présenter un antigène du parasite dans le contexte de CMH-II, proposant ainsi qu'Ii agit comme un dominant négatif sur la présentation d'antigènes endogènes provenant du parasite. Des protéases de l'hôte (légumaine, cathepsines L et S) et l'acidification des compartiments endosomaux étaient modulées par le parasite, révélant une manipulation plus étendue de la voie endocytique. Les modes d'expression opposés d'Ii et H2-DM avaient un effet *in vivo* sur la dissémination des parasites vers des organes lymphoïdes, l'activation des cellules T $CD4^+$, la production d'IFNγ, le nombre de kystes et la survie. Collectivement, nos résultats montrent l'étendue des processus de manipulation par *T. gondii*, révélant de complexes interactions avec l'hôte et sa capacité de subvertir les fonctions immunitaires pour établir une infection chronique.

Acknowledgements

First and foremost, I would like to extend my deepest gratitude to my supervisor Dr. Florence Dzierszinski for allowing me to joint her laboratory and overseeing the successful completion of my studies. Her guidance in designing and elaborating the experimental procedures, as well as her scientific insights were essential to my research. She has offered me tremendous opportunities from which my academic and scientific development has undoubtedly benefited.

I sincerely thank Dr. Armando Jardim for agreeing to acts as my interim supervisor since January 2012 as well as being part of my advisory committee since the very beginning of my graduate studies. I owe to him the completion of my thesis free of any impediments. Also, I would like to thank the other members of my advisory committee, Drs. Paula Ribeiro and Reza Salavati, for their constructive criticism and dedication to me and my fellow students and our academic research.

Also, I would like to thank Dr. Manami Nishi, former post-doctoral fellow, for training me in different laboratory skills. Furthermore, I would like to express my appreciation to her as well as other former students, Dayal Dasanayake, Sandy El Hage, Clément Trunet, Gregory Kaiman, and Teresa Plegge for contributing to our research with experimental results. Other members of the Institute of Parasitology deserve my recognition; Dr. Petra Rohrbach for letting me use her confocal microscope and helping me with image analysis, Mr. Serghei Dernovici and Mrs. Kristi Bangs for being instrumental in perfecting my flow cytometry skills, and Dr. Timothy Geary for his kind words and wise advice.

I would like to acknowledge the contributions from our collaborators Drs David Bzik and Barbara Fox (Dartmouth Medical School), Elizabeth Bikoff (University of Oxford), Hidde Ploegh (Whitehead Institute), Jean-François Dubremetz (University of Montpellier), Dominique Soldati-Favre (University of Geneva), Jean Gosselin (Laval University), Albert Descoteaux (Centre INRS-Institut Armand Frappier), Salman Qureshi, Jörg Fritz and Hervé Le Moual

(McGill University) for sharing invaluable reagents and material with our laboratory. Their contributions had a significant impact on my experiments, extending the thoroughness of my research.

My graduate studies and my research could not have been possible without the funds granted by the different funding agencies: the Fonds de recherche du Québec Nature et technologies (FQRNT), the Lynden Laird Lyster Memorial Fellowship in Parasitology, the March of Dimes Foundation, the Canada Research Chairs (CRC), the Natural Sciences and Engineering Research Council (NSERC), the Centre for Host-Parasite Interactions (CHPI), and the Graduate Research Enhancement and Travel (GREAT) Awards.

Finalement, j'aimerais profiter de l'occasion pour remercier ma famille, mes parents Pierre et Jacinte, mon frère Mathieu et ma sœur Marie-Élise, et ma grand-mère Gervaise pour le support et leur amour inconditionnels. Je vous remercie de tout cœur pour m'avoir encouragé pendant toutes ces années; je vous aime et je vous dédie cet ouvrage. A very special thank you to Missy Hansen-Murphy for putting up with my late nights and odd hours in the lab and for listening to me when I was incessantly blabbing about my little parasites.

To all mentioned above, I shall be forever grateful. Thank you. Merci.

- Louis-Philippe Leroux

List of Abbreviations

ACN: acetonitrile

AEBSF: 4-(2-aminoethyl) benzenesulfonyl fluoride hydrochloride

AEP: asparaginyl endopeptidase

AIDS: acquired immunodeficiency syndrome

AP1 and **2:** adaptor protein 1 and 2

APC: allophycocyanine

BCA: bicinchoninic acid

BMDC: bone marrow-derived dendritic cell

BMMΦ: bone marrow-derived macrophage

bp: base pair

BRG1: brahma-related gene 1

BSA: bovine serum albumin

CARM1: co-activator-associated arginine methyltransferase 1

CAT: chloramphenicol acetyl transferase

CBP: CREB-binding protein

CD: cluster of differentiation

CDC: Centers for Disease Control and Prevention

CHAPS: 3-[(3-cholamidopropyl) dimethylammonio]-1-propanesulfonate

CIITA: class-II major histocompatibility complex transactivator

CLIP: class II-associated invariant chain peptide

CNS: central nervous system

cpsII: carbamoyl phosphate synthetase II

CREB: cyclic-AMP-responsive-element-binding protein (CREB)

CTL: cytotoxic T lymphocyte

Cy: cyanine

CytD: cytochalasin D

DAPI: 4’,6-diamidino-2-phenylindole dilactate

DC: dendritic cell

DDAO-SE: 7-hydroxy-9H(I,3-dichloro-9,9-dimethylacridin-2-one succinimidyl ester

DHFR*-TS: dihydrofolate reductase-thymidylate synthase

DIC: differential interference contrast

DMEM: Dulbecco's modified Eagle's medium

DMSO: dimethyl sulfoxide

DNA: deoxyribonucleic acid

DTT: dithiothreitol

EDTA: ethylenediaminetetraacetic acid

EE: early endosome

egr2: early growth response 2

ELISA: enzyme-linked immunosorbent assay

EMEM: Eagle's minimum essential medium

ENU: N-nitroso-N-ethylurea

ER: endoplasmic reticulum

ESA: excreted-secreted antigen

ExoA: exotoxin A

FACS: fluorescence-activated cell sorting

FBS: fetal bovine serum

FITC: fluorescein isothiocyanate

GAS: IFNγ-activated site

GFP: green fluorescent protein

GM-CSF: granulocyte macrophage colony-stimulating factor

GRA: dense granule

HAART: highly active anti-retroviral therapy

HEPES: 4-(2-hydroxyethyl)-1-piperazineethanesulfonic acid

HFF: human foreskin fibroblast

HIV: human immunodeficiency virus

HK: heat-killed

HLA: human leukocyte antigen

HRP: horseradish peroxidase

HSC70: heat-shock chaperone 70

HSP: heat-shock protein

HSS: high-speed supernatant

Ii: invariant chain

IFNα, β, or γ: interferon alpha, beta, or gamma

IFNγRα and β: interferon gamma receptor alpha and beta chains

IL: interleukin

***i*NKT:** invariant natural killer T cell

iNOS: inducible nitric oxide synthase

IRF1 and **IRF2:** IFN-regulatory factor 1 and 2

IRF-3: IRF-element

IRG: immunity-related GTPase

ISG: Immature secretory organelle

JAK1 and **2:** Janus kinase 1 and 2

KO: knock-out

lacZ: β-galactosidase

LC: liquid chromatography

LE: late endosome

LPS: lipopolysaccharide

MAPK: mitogen activated-protein kinase

MHC-II: major histocompatibility complex class II

MIC: microneme

MIF: macrophage migration inhibitory factor

MIIC: MHC-II compartment

MLN: mesenteric lymph node

MOI: multiplicity of infection

MS/MS: tandem mass spectrometry

NF-κB: nuclear factor kappa B

NFY: nuclear transcription factor Y

NK: natural killer cell

NOD: nucleotide-binding oligomerization domain

nt: nucleotide

OVA: ovalbumin

pAPC: profession antigen presenting cell

PBS: phosphate buffered saline

PCAF: p300/CBP-associated factor

PCR: polymerase chain reaction

pDC: plasmacytoid dendritic cell

PDG: Percoll density gradient

PE: phycoerythrin

PerCP: peridinin chlorophyll

PFA: paraformaldehyde

PI: propidium iodide

PLV: plant-like vacuole

PV: parasitophorous vacuole

PVM: parasitophorous vacuole membrane

RFP: red fluorescent protein

RFXANK: regulatory factor X-associated ankyrin-containing protein

RFXAP: regulatory factor X-associated protein

RFX5: regulatory factor X5

RON: rhoptry neck protein

ROP: rhoptry

RPMI: Roswell Parl Memorial Institute medium

RT: reverse transcription

RT-PCR: real-time polymerase chain reaction

SAG1: surface antigen 1

SDS-PAGE: sodium dodecyl sulfate polyacrylamide gel electrophoresis

SOCS1: suppressor of cytokine signaling 1

STAT: signal transducer and activator of transcription

TAP: transporter associated with antigen processing

TCEP: Tris (2-carboxethyl) phosphine

TCR: T cell receptor

TE: toxoplasmic encephalitis

TEC: thymic epithelial cell

TGFβ: tumor growth factor beta

TGN: trans-Golgi network

TIR: Toll/interleukin-1 receptor

TLR: Toll-like receptor

TNFα: tumor necrosis factor alpha

T_{reg}: regulatory T cell

TTBS: Tween-Tris buffered saline

UPRT: uracil phosphoribosyltransferase

USF1: upstream transcription factor 1

UTR: untranslated region

WHO: World Health Organization

WT: wild-type

YFP: yellow fluorescent protein

X-Gal: 5-bromo-4-chloro-indolyl-β-D-galactopyranoside

Statement of Originality

Chapter 2: Elaboration of a forward genetic screening strategy to identify *T. gondii* genes coding molecules inhibiting MHC-II expression.

In this chapter, the details of a forward genetic screening strategy are described. This strategy consisted of performing a random genome-wide insertional mutagenesis using a highly efficient plasmid based on the dihydrofolate reductase thymidylate synthase (DHFR*-TS) cDNA (Roos, Sullivan et al. 1997). It was predicted that every single gene within the genome can be disrupted by this method given the size of the insertional plasmid, the high rate of nonhomologous recombination events, and the haploid nature of *T. gondii* tachyzoites (Donald and Roos 1995) (Roos, Sullivan et al. 1997), making this approach unbiased and sufficiently broad to uncover the genes of interest. Following the mutagenesis, mutant parasites found to be unable to inhibit IFNγ-induced MHC-II expression in pAPCs were to be isolated by flow cytometry cell sorting. The disrupted genetic loci were to be identified by either inverse PCR (Roos, Sullivan et al. 1997) or by plasmid rescue (Donald and Roos 1995) (Roos, Sullivan et al. 1997), and once the sequence was to be obtained, database mining using numerous computational tools available on the *Toxoplasma gondii* database (http://toxodb.org) could have helped identify the genes, and ultimately give clues as to the mechanisms of inhibition. A previous forward genetic screening using a chemical mutagen, N-nitroso-N-ethylurea (ENU), was able to identify genes involved in the *T. gondii* cell cycle (Gubbels, Lehmann et al. 2008), but our multidisciplinary approach using insertional mutagenesis outlined herein is the first to set as a goal the identification of parasite molecules involved in the inhibition of MHC-II expression.

Chapter 3 - Manuscript I: Louis-Philippe Leroux, Dayal Dasanayake, Manami Nishi, Barbara A. Fox, David J. Bzik, Armando Jardim, Florence S. Dzierszinski (to be submitted for publication). Excreted-secreted antigens from *Toxoplasma gondii* secretory organelles inhibit interferon gamma-mediated MHC-II up-regulation in bone marrow-derived macrophages.

In this manuscript, biochemical analyses were carried out in an attempt to identify *Toxoplasma gondii* molecules involved in the inhibition of MHC-II expression. Several reports had previously revealed that soluble *T. gondii* antigens (STAg) modulate cytokine production and responsiveness by immune cells (Reis e Sousa, Hieny et al. 1997) (Aliberti, Reis e Sousa et al. 2000) (Scanga, Aliberti et al. 2002) (McKee, Dzierszinski et al. 2004) (Lee, Heo et al. 2008). In 2006, Lang and associates had reported that a pronase-sensitive, PBS-soluble fraction prepared from parasite lysates inhibited MHC-II expression in RAW 264.7 cells (Lang, Algner et al. 2006). Our work expanded on these findings by refining the lysates preparation and by tracing the origin of the inhibitory molecules back to secretory organelles, either rhoptries (ROP) or dense granules (GRA). A series of ROP and GRA knock-outs not previously assessed for their ability to inhibit MHC-II were tested. Also, our experimental procedures were carried out using a different cell type, bone marrow-derived macrophages (BMMΦ). Although no molecules have been definitively identified, a list of 24 potential candidates, including many with yet unknown functions, has been generated.

Chapter 4 - Manuscript II: Louis-Philippe Leroux, Manami Nishi, Sandy El-Hage, Barbara A. Fox, David J. Bzik, Florence S. Dzierszinski. The invariant chain (Ii) and the peptide editor H2-DM modulate MHC-II antigen presentation and $CD4^+$ T cell effectors during infection by *Toxoplasma gondii*.

Although it is well known that *T. gondii* inhibits MHC-II expression in professional antigen presenting cells (pAPCs), the current literature has focused mainly on the transcriptional regulation by the parasites. However, mature MHC-II molecules are detected in infected cells (Luder, Lang et al. 1998), albeit at low levels. Yet, these latter remain unable to efficiently present parasite-derived antigens to cognate $CD4^+$ T helper cell (Luder, Walter et al. 2001) (McKee, Dzierszinski et al. 2004). In this second manuscript, we present evidence of a second, post-translational layer of regulation by *T. gondii* that complements the transcriptional inhibition to efficiently block antigen presentation. This second

layer involved the MHC-II associated invariant chain (Ii), and the findings described here constitute the first report of the induction of Ii by a pathogen to block presentation of endogenously-acquired parasite-derived antigens by MHC-II molecules. In addition, we present novel findings relating a wider manipulation of the endocytic pathway by the parasite with regards to some of its properties, specifically the acidification and enzymatic activities of resident proteases. These findings argue that suboptimal processing of antigens and Ii could contribute to the parasite's ability to block MHC-II presentation. Furthermore, we assessed the impact of Ii and the peptide editor H2-DM, both critical players of the MHC-II pathway, on $CD4^+$ T cell activation, IFNγ production, parasite dissemination, brain cyst burden, and survival in the chronic phase following *T. gondii* infection in an animal model.

Author's Contributions

The design and execution of the experiments reported in this thesis were carried out by the author under the supervision of Dr. Florence S. Dzierszinski. Also, Dr. Armando Jardim partly contributed to the design of some experiments in the first manuscript (Chapter 3). In this manuscript, excreted-secreted antigen (ESA) production, parasite viability testing, ion-exchange and size-exclusion chromatography experiments were performed by Dayal Dasanayake, generation of the ROP and GRA knock-outs was accomplished by Drs. Barbara A. Fox and David J. Bzik (Dartmouth Medical School, Lebanon, NH), however, all flow cytometry experiments performed following these procedures were performed by the author. Liquid chromatography and tandem mass spectrometry (LC-MS/MS) was carried out at the L'institut de recherche en immunologie et cancérologie (IRIC) at the Université de Montréal (Montréal, Canada). However, results and discussion sections were written by the author.

In the second manuscript (Chapter 4), all of the experiments were accomplished by the author, except microscopy monitoring the kinetics of Ii expression was performed by Dr. Manami Nishi, real-time PCR reactions measuring host cell gene expression were done by Sandy El Hage, generation of toxostatins 1 and 2 knock-outs was accomplished by Drs. Barbara A. Fox and David J. Bzik, while processing and staining of brain tissue for histology was carried out by the Histopathology Services at Charles River (Wilmington, MA).

Table of Contents

List of Figures

List of Tables

Introduction

Pathogens have evolved very diverse ways to establish a successful infection and to allow their transmission from one host to another (Lange and Ferguson 2009). Transmission requires pathogens to withstand the retaliation by the host immune system, to adapt their life cycles, and to persist long enough without killing their host until another host is available to be infected. Co-evolution along with their hosts and their immune system meant developing strategies to subvert and interfere with processes of both the innate and adaptive immune systems. Where the immune system falls short in overcoming a disease, chemotherapeutic medication and vaccination have been invaluable solutions to ensure human population health.

Although chemotherapeutic treatment has saved countless lives and it is still in great part efficacious against many diseases, emergence of drug resistance is an increasingly problematic situation (Wright 2007). As an alternative or a complement to chemotherapy, vaccination has long been successful in fighting certain diseases (Hilleman 2000). In fact, the success of vaccination was best demonstrated by the eradication of smallpox in humans (Ellner 1998).

However, all currently available, rationally-designed vaccines in humans are based on humoral immunity, while cellular or T cell-based vaccines have yet to be successfully designed (Robinson and Amara 2005). The challenges in developing a potent cell-mediated vaccine, which would prove useful against intracellular pathogens, highlight the need to thoroughly understand the interactions between host and pathogen, and to decipher the different biological mechanisms employed by harmful organisms to subvert normal immune functions.

In recent years, the protozoan parasite *Toxoplasma gondii* has become a useful model not only for apicomplexans, but also for intracellular parasitism in general for many reasons. First, this parasite displays an impressive range of natural hosts, which includes virtually any warm-blooded animal (Dubey,

Storandt et al. 1999) (Tenter, Heckeroth et al. 2000) (Dubey 2004), making research performed in laboratory animals relevant. Second, genetic manipulation of the parasite is readily achievable due to its haploid genome during most of its life stages, the availability of its completely sequenced genome, and its ease of culture *in vitro* (Roos, Donald et al. 1994) (Donald and Roos 1995) (Kissinger, Gajria et al. 2003) (Kim and Weiss 2004) (Gajria, Bahl et al. 2008). Third, the parasite is able to infect any nucleated cell, including those of the immune system (Kim and Weiss 2004). Lastly, natural infection by *T. gondii* elicits a strong Th1-type immune response that depends on the cellular arm of the immune system (Suzuki, Orellana et al. 1988) (Gazzinelli, Hakim et al. 1991) (Denkers and Gazzinelli 1998), which makes research relevant in the development of T cell-based vaccines, and is fairly well controlled in otherwise healthy hosts.

Over the past 20 years, research on *T. gondii* has uncovered numerous ways the parasite is able to subvert the host immune response, from favoring the production anti-inflammatory over pro-inflammatory cytokines to establishing a niche in immune-privileged sites (Lang, Gross et al. 2007). Another area of interest is the parasite's ability to inhibit antigen presentation and to initially dampen the development of a T cell response (Luder, Lang et al. 1998) (Luder, Walter et al. 2001) (McKee, Dzierszinski et al. 2004). A fundamental immunology paradigm states that antigens must be processed and presented on major histocompatibility complex (MHC) molecules, whereby MHC-I molecules present antigens to $CD8^+$ cytotoxic T lymphocytes (CTL) while MHC-II present antigens to $CD4^+$ T helper (T_h) cells (Janeway 2001). The latter subset of T cells has long been identified as being instrumental in the mounting and regulation of an adequate adaptive immune response against invading pathogens. Hence, it is of great interest knowing how *T. gondii* is able to inhibit MHC-II antigen presentation and how this impacts the immune response.

The original initiative of the work detailed in this thesis was to identify *T. gondii* molecules involved in the inhibition of MHC-II expression in professional antigen presenting cells (pAPCs). Although expression and activity of many host

molecules implicated in MHC-II expression have been shown to be modulated during infection, no definitive *T. gondii* molecules have been linked directly to the inhibition of MHC-II so far. Nonetheless, the first manuscript herein details the biochemical analyses that have allowed us to gain significant knowledge on the nature of the inhibitory activity on MHC-II expression and to narrow down the list of possible molecules. Certainly, the results reported will guide future research, and ultimately, the identification of molecules involved in antigen presentation interference and maturation of pAPCs will help the identification of related molecules in other pathogen species.

According to the literature, inhibition of MHC-II expression by *T. gondii* is mainly achieved by interfering with transcription of MHC-II and other related genes (Luder, Lang et al. 2003) (Lang, Algner et al. 2006). However, we show that this appears to be an incomplete picture since some MHC-II molecules can mature and be detected in infected cells. In the second manuscript, we provide evidence that the first transcriptional layer of regulation, that appears not to inhibit expression completely, has to be complemented with a second, post-translational layer of regulation by the parasite. The experimental results revealed an uncoordinated expression of an important component of the MHC-II pathway, namely the invariant chain, with the rest of the class II genes (MHC-II and the peptide editor H2-DM). Indeed, the data presented here argue for a wider manipulation of the host endocytic pathway that stretches beyond simple transcriptional regulation. *In vivo* studies were carried out to assess the impact of these two components (Ii and H2-DM) highlighting their contributions to development of immune response against toxoplasmosis.

Overall, the findings detailed in this thesis shed new light on the intricate interactions between an intracellular pathogen, *Toxoplasma gondii*, and its host cell, and on the strategies deployed by a pathogen to subvert the immune system and to establish a successful infection. Understanding these processes will bring new insights into the development of novel therapy strategies against intracellular pathogens.

Chapter 1. Literature Review

1.1. *Toxoplasma gondii* biology, transmission, and disease

Toxoplasma gondii is an obligate intracellular protozoan parasite of the phylum Apicomplexa (Levine 1988). This phylum includes over 5,000 different species, the majority of which are intracellular parasites. Notable apicomplexans include *Plasmodium* sp, the causative agents of malaria, *Cryptosporidium* sp, *Eimeria* sp, and *Neospora* sp. Although these pathogens are evolutionarily related, they exhibit different host specificities, life cycles, and cause different pathologies. Animals of the Felidae family act as definitive hosts to *T. gondii* in which the parasite can complete its sexual life cycle, while virtually any warm-blooded vertebrate, including mice and humans, can serve as intermediate hosts to allow asexual replication (Frenkel, Dubey et al. 1970) (Dubey, Miller et al. 1970). Considering that an estimated one-third of the human population is at some point exposed to *Toxoplasma* and that this parasite displays an impressive host range, from pigs, sheep, goats, rabbits, dogs, wild coyotes, red and gray foxes, cattle, deer, to marsupials, sea otters, chickens, and pigeons (Dubey, Storandt et al. 1999) (Tenter, Heckeroth et al. 2000) (Dubey 2004), *T. gondii* has undoubtedly evolved an elaborate panel of strategies to ensure its survival in innumerable hosts making it one of the most successful and ubiquitous parasite (Saeij, Boyle et al. 2005).

Toxoplasma gondii is considered a food and waterborne pathogen, whereby infection occurs through the fecal-oral route when infective oocysts containing sporozoites are shed in feline feces, contaminating potable water or vegetables, and are ingested by subsequent hosts (Dubey 1986; Dubey 2004) (Figure 1.1). In most cases, infection occurs after consuming raw or undercooked meat that contains tissue cysts. Furthermore, toxoplasmosis can be transmitted transplacentally from an acutely infected mother to her fetus. During the acute phase of the infection, rapidly-dividing tachyzoites will invade any nucleated cell, including cells of the immune system. It will reside and replicate by endodyogeny in a non-fusogenic vacuole called the parasitophorous vacuole (PV),

egress and invade a new cell, eventually going through multiple rounds of cell invasion and lysis while disseminating throughout the host (Dubey 2004). Even though the PV membrane is formed from the host cell membrane, it does not fuse to other host organelles most likely due to the selective exclusion of host membrane proteins during its formation (Jones, Yeh et al. 1972) (Joiner, Fuhrman et al. 1990).

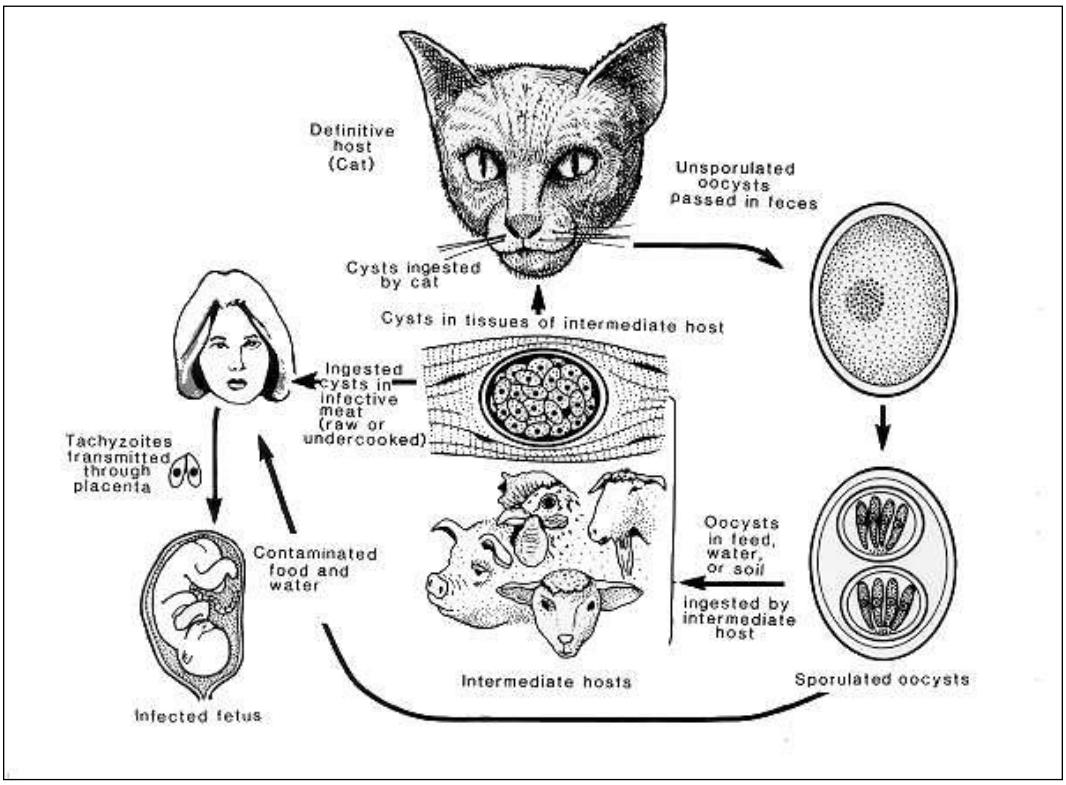

Figure 1.1: *Toxoplasma gondii* life cycle (Dubey 1986).

There are three possible migratory pathways utilized by *T. gondii* to cross cellular barriers, such as the placenta, the intestinal epithelium, the blood-brain, blood-retina and blood-testis barriers, and to disseminate throughout the host (Lambert and Barragan 2010) (Elsheikha and Khan 2010). First, extracellular tachyzoites, powered by their own motility apparatus (Dobrowolski and Sibley 1996), can traverse epithelial layers without disrupting their integrity via a paracellular pathway. Second, the parasite can actively invade (Morisaki, Heuser et al. 1995) and penetrate through the apical side of an epithelial cell and exit through the basolateral side without establishing a replicative vacuole, a process

referred to as transcellular traversal. Third, *T. gondii* can resort to leukocyte-assisted transfer, also known as the Trojan horse mechanism, whereby infected circulating leukocytes carry the parasites they bear across cellular barriers and to lymphoid organs allowing parasite dissemination (Courret, Darche et al. 2006) (Lambert, Hitziger et al. 2006).

Soon after the start of the infection, tachyzoites reach muscle tissues and immune privileged sites, notably the brain, and convert to more latent bradyzoites that encyst (Dubey 2004). These encysted parasites can remain dormant for the remainder of the host's life. In felines, these tissues cysts are the best precursors to the sexual cycle (Dubey 1998) and are extremely refractory to drug treatments (Boyer and McLeod 2002). Encystation can occur as early as six to nine days post-infection (Dubey, Speer et al. 1997) concomitant with the development of a parasite-specific adaptive immune response and environmental stress (Weiss and Kim 2000).

In immunocompetent hosts, acute toxoplasmosis triggers a strong immune response that limits the infection and remains generally asymptomatic. However, congenital toxoplasmosis can cause serious birth defects including hydrocephaly, mental retardation, blindness, and chorioretinitis (Remington, McLeod et al. 2000). Also, increasing evidence has linked postnatally, rather than congenitally, acquired ocular toxoplasmosis in otherwise healthy individuals (Glasner, Silveira et al. 1992) (Montoya and Remington 1996) with atypical strains of the parasite (Grigg, Ganatra et al. 2001). These atypical or "exotic" strains have been found to harbor unique polymorphisms and, at some loci, dimorphic allele patterns (Su, Evans et al. 2003). It is believe that these strains have introgressed with the typical clonal lineages through subsequent crosses (David Sibley 2003), making it difficult to relate any of these strains to the three main lineages (Ajzenberg, Banuls et al. 2004). Furthermore, spontaneous reactivation of dormant cysts can occur in immunosuppressed individuals such as patients with acquired immunodeficiency syndrome (AIDS), receiving chemotherapy against cancer or immunosuppressive drugs during organ transplant, or elderly people with a

waning immune system (Luft and Remington 1992) (Dubey 2004). In fact, toxoplasmic encephalitis (TE), a condition characterized by lesions caused by reactivating cysts in the brain, is the most important opportunistic disease of the central nervous system (CNS) in AIDS patients even with the availability of the highly active anti-retroviral therapy (HAART) (Abgrall, Rabaud et al. 2001) (Bonnet, Lewden et al. 2005). The fact that the human immunodeficiency virus (HIV) primarily infects and depletes $CD4^+$ T cells (Alimonti, Ball et al. 2003) and that the onset of TE coincides with lowered levels of this lymphocyte population (Oksenhendler, Charreau et al. 1994) confirms the importance of the latter in the control of *Toxoplasma gondii* and prevention of pathology. Prevalence of the chronic form of the infection amongst the human population varies drastically depending on the geographical location and socio-culture habits, ranging from 30 to 80% (Tenter, Heckeroth et al. 2000). These striking numbers highlight the fact that *T. gondii* has evolved to be a successful parasite, but they also serve as a reminder that this protozoa represents a risk to many people specifically to those mentioned above.

According to population genetics classifications, there are three major clonal lineages of *Toxoplasma gondii*, typically referred to as type I, II, and III (Howe and Sibley 1995). Although strains from all three lineages have been isolated from humans, type II strains are the most common culprits for human toxoplasmosis. Type I strains are linked to acute virulence with a lethal dose (LD_{100}) of a single infectious organism in mice, while type II and III strains are usually qualified as avirulence with an LD_{100} ranging from 10^3 to 10^5 (Sibley and Boothroyd 1992). Despite the clonal propagation and contrasting extent of virulence, the lineages only defer by a few percent at the DNA level for any given locus (Howe and Sibley 1995). Genetic crosses between the different lineages and surveying virulence in laboratory mice helped map five virulence (*VIR*) loci (Saeij, Boyle et al. 2006). These loci are located on chromosomes XII (VIR_1), X (VIR_2), VIIa (VIR_3), VIIb (VIR_4), and XII (VIR_5). Within these *VIR*s, polymorphic genes coding for rhoptry proteins including ROP16 and ROP18 (Saeij, Boyle et al. 2006) and a tandem cluster of alleles of ROP5 (Behnke, Khan et al. 2011), as

well as dense granule protein GRA15 (Rosowski, Lu et al. 2011) have been linked directly to the virulence differences observed so far. In part, these findings bring forth the importance of the parasite's arsenal of secretory proteins during infection, as discussed below.

1.2. *T. gondii* morphology and secretory organelles

Toxoplasma gondii is a crescent-shaped zoite measuring around 7 µm in length and 3 µm in width. In fact, its genus name derives from its morphology: *toxo* (arc or bow) and *plasma* (life) (Dubey 2008). Its species name comes from the first animal it was isolated from by Nicolle and Manceaux in 1908, the gundi (*Ctenodactulys gundi*). This eukaryotic parasite possesses a single nucleus, a single mitochondrion, a single interconnected endoplasmic reticulum (ER) network, a single Golgi stack, and an apicoplast (Figure 1.2). The apicoplast is a nonphotosynthetic plastid believed to originate from an ancient event of endosymbiosis during which an alga was ingested or internalized by the apicomplexan ancestor (McFadden, Reith et al. 1996). Recently, a novel organelle was identified in *T. gondii* that was eventually dubbed the plant-like vacuole (PLV) given the features it shares with the plant vacuole (Miranda, Pace et al. 2010). The PLV seems to play a role in homeostatis and calcium storage during the extracellular stage as well as containing transporters like an aquaporin and a vacuolar proton ATPase usually found in the plant vacuole membrane (tonoplast).

One of the defining morphological features is the apical complex. In fact, the name of the phylum Apicomplexa derives from this biological structure. The apical complex includes three secretory organelles, namely the micronemes (MIC), rhoptries (ROP) (which also includes rhoptry neck proteins or RON), and dense granules (GRA), and the conoid. Micronemes and rhoptries are clustered at the apical end of the parasite, while dense granules are scattered throughout its cytoplasm. These organelles discharge their contents sequentially in a stringently

controlled fashion that coincides with different steps in the host invasion process: microneme exocytosis occurs upon host cell binding, rhoptry secretion during host cell invasion, and dense granule release during PV formation and parasite maturation (Carruthers and Sibley 1997). For example, microneme proteins such as MIC1, MIC2, MIC4, and MIC6 are involved in invasion and vacuole formation (Soldati, Dubremetz et al. 2001), rhoptry proteins like ROP2, and dense granule proteins GRA3 and GRA5 lead to organelle hijacking and associate with the host mitochondria (Sinai and Joiner 2001) and ER (Ahn, Kim et al. 2006), respectively.

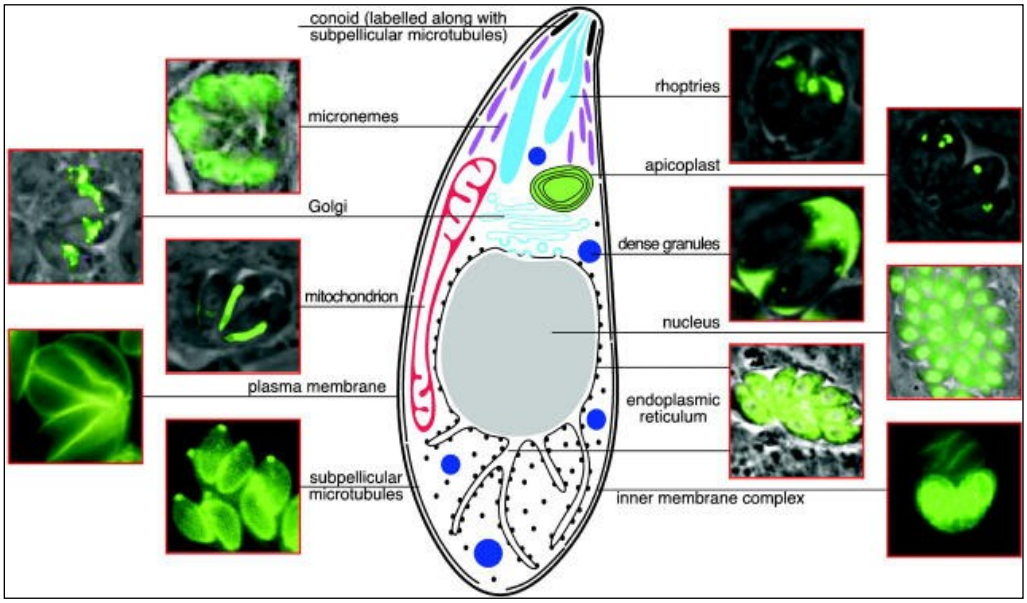

Figure 1.2: *Toxoplasma gondii* morphology and subcellular organelles (Joiner and Roos 2002).

Importantly, virulence differences between the archetypical types have been linked to different proteins from the secretory organelles and the secreted products are known to affect numerous host cell functions including apoptosis, signaling pathways, and immunity (Laliberte and Carruthers 2008). For instance, polymorphic ROP16 and ROP18 have received considerable attention over the past few years since they were shown to be linked to the virulence *VIR* loci (Saeij, Boyle et al. 2006). Type I and III ROP16, a protein kinase, has been shown to make its way to the host cell nucleus upon invasion, and to phosphorylate STAT3 and 6 (Saeij, Coller et al. 2007) (Ong, Reese et al. 2010). STAT3/6 have been

shown to suppress STAT1- and NF-κB-dependent transcription of pro-inflammatory genes (Ohmori and Hamilton 2000) (discussed below), partially explaining the decreased IL-12 production in cells infected with type I or III-expressing parasites (Saeij, Coller et al. 2007). ROP18, another serine-threonine kinase, has been shown to phosphorylate and deactivate murine immunity-related GTPases (IRG), Irga6, Irgb6, and Irgb10, to thwart the accumulation of these IRGs and stripping of the PV membrane, and to prevent elimination of the parasites (Fentress, Behnke et al. 2010) (Steinfeldt, Konen-Waisman et al. 2010), but recent evidence suggests that a virulent allele and expression of ROP5 is required (Niedelman, Gold et al. 2012). GRA15 was shown to modulate activation of NF-κB in infected cells (Rosowski, Lu et al. 2011). Interestingly, this modulation displays a type-dependency due to GRA15 polymorphisms, whereby GRA15 from type II strains activate NF-κB at high levels, while type I and III strains do not. Collectively, these reports highlight the differences in virulence between the three lineages and the intricacy of the modulation of the cell by the parasite.

Thus, it is likely that many functions for these secreted molecules will be uncovered and will explain some of the phenotypes observed during the course of infection and help understanding the underlying biology, and potentially be used as novel target for treatment or vaccine design.

1.3. Chemotherapy and vaccines

Current chemotherapeutic treatment against toxoplasmosis relies on the combination of pyrimethamine, sulfadiazine, and leucovorin (folinic acid). Although proven effective, the first two drugs display some level of toxicity, hence immunocompetent adults and children diagnosed with toxoplasmosis are usually not treated unless symptoms prove to be severe and persistent, or if the infection occurred in laboratory settings (Montoya and Liesenfeld 2004) (Schmidt, Hogh et al. 2006). Pyrimethamine and sulfadiazine act by inhibiting

folic acid synthesis through different mechanisms. To limit depletion of folic acid in the patient, supplements are usually administered during treatment (Soheilian, Sadoughi et al. 2005). According to the World Health Organization (WHO) and the Centers for Disease Control and Prevention (CDC) recommendations, this drug combination is currently the standard for treating congenital toxoplasmosis (Rorman, Zamir et al. 2006) and decreasing its adverse signs and symptoms (McLeod, Boyer et al. 2006). However, pyrimethamine and sulfadizine have potential teratogenic effects, notably if given during the first trimester (Dorangeon, Marx-Chemla et al. 1992). Alternatively, spiramycin can be given instead during this critical period to prevent transplacental transmission (Kaye 2011). Also, clindamycin can replace sulfadiazine for people sensitive to sulfonamides drugs (Montoya and Liesenfeld 2004).

Unfortunately, no vaccines against *T. gondii* are available in humans. Early vaccination methods were attempted using killed *T. gondii*, lysates or crude extracts, but all failed to succeed to confer protective immunity and prevent cyst formation (Jongert, Roberts et al. 2009). Several trials were carried out using either purified or recombinant proteins, notably the immunodominant stage-specific surface antigen 1 (SAG1) (Bulow and Boothroyd 1991) (Khan, Ely et al. 1991) (Debard, Buzoni-Gatel et al. 1996) (Velge-Roussel, Marcelo et al. 2000), microneme proteins MIC1 and MIC4 (Lourenco, Bernardes et al. 2006), and mixtures of dense granule protein GRA2 and GRA6 (Golkar, Shokrgozar et al. 2007), GRA4 with rhoptry protein ROP2 (Martin, Supanitsky et al. 2004), or GRA7 with a MIC2-MIC3-SAG1 chimeric protein (Jongert, Melkebeek et al. 2008). Although these different vaccination attempts provided higher survival rates and significant reduction in brain cyst loads, complete protection against acute or chronic toxoplasmosis was only achieved with the use of strong adjuvants such as Freud's Complete Adjuvant and QuilA (Khan, Ely et al. 1991) (Brinkmann, Remington et al. 1993) (Mishima, Xuan et al. 2001). However, protein-based vaccines are known to induce primarily humoral or B cell responses against *T. gondii*, but weakly cell-mediated responses (Johnson, Lanthier et al. 2004).

On the other hand, vaccination using the live attenuated S48 *T. gondii* strain, a tissue cyst defective strain, proved to efficiently reduce toxoplasmosis-induced abortions and neonatal mortality in sheep (Buxton, Thomson et al. 1991), to elicit $CD4^+$ and $CD8^+$ T cell-mediated immunity and IFNγ production, and to limit parasite dissemination to the lymphatic system (Innes, Panton et al. 1995). Eventually, this vaccine was commercialized under the name Toxovax (Innes, Bartley et al. 2009). Unfortunately, the use of a live vaccine in humans poses potential risks given the zoonotic nature of this pathogen and the possibility of revertant parasites causing breakthrough infections, while its short shelf-life hinders considerably its mass marketing.

DNA plasmid for coding parasite antigens have been investigated as a possible vaccine alternative especially since this method is able to induce both $CD4^+$ and $CD8^+$ T cell responses (Jongert, Roberts et al. 2009). For instance, vaccination with a plasmid coding for SAG1 has been shown to provide complete protection to a lethal challenge and reduce cyst numbers (Nielsen, Lauemoller et al. 1999), but it failed to provide sterile immunity or prevent transplancental transmission (Angus, Klivington-Evans et al. 2000) (Couper, Nielsen et al. 2003). Similar vaccination trials have been carried out with plasmids coding for secretory proteins including MIC2, MIC3, MIC4, M2AP, AMA1, ROP1, ROP2, GRA1, GRA2, GRA4, and GRA7 (Beghetto, Nielsen et al. 2005) (Jongert, Melkebeek et al. 2008) (Quan, Chu et al. 2012).

The difficulties in developing an efficient vaccine against an intracellular pathogen such as *Toxoplasma gondii* highlight the need to better understand the interactions between host and pathogen. Since cell-mediated immunity is critical in controlling these infections, deciphering the basic biological mechanisms required to mount such a response is pivotal. Cellular immune responses are deeply affected by the route and effectiveness of antigen presentation (Kaufmann and Hess 1999), and it is of great interest to understand how *T. gondii* deals with antigen presentation and how it modulates the host's immune system. Ultimately, understanding these processes could contribute not only to the knowledge of

intracellular parasitism and host-parasite interactions, but aid in the design of efficient T cell-based vaccines.

1.4. Immune response and antigen presentation against *T. gondii*

In immunocompetent hosts, resistance to toxoplasmosis is characterized by a robust Th1-type response that elicits the cellular arm of the immune system, specifically the $CD4^+$ and $CD8^+$ T cells which ensure protective immunity mainly be producing interferon gamma (IFNγ) (Suzuki, Orellana et al. 1988) (Gazzinelli, Hakim et al. 1991) (Denkers and Gazzinelli 1998). Initially, this Th1-type response involves nuclear factor kappa B (NF-κB)- and mitogen-activated protein kinase (MAPK)-driven production of interleukin-12 (IL-12) by macrophages, dendritic cells, and neutrophils (Gazzinelli, Wysocka et al. 1994). In turn, IL-12 stimulates T lymphocytes to produce IFNγ (Figure 1.3). This cytokine, in combination with tumor necrosis factor alpha (TNFα), activates hematopoietic and non-hematopoietic effector cells to restrict replication and kill parasites by producing potent antimicrobicidal reactive oxygen intermediates (O_2^-, H_2O_2) and nitric oxide (NO), by inducing tryptophan starvation, and by activating p47 GTPases and leukotrienes (Adams, Hibbs et al. 1990) (Yong, Chi et al. 1994) (Butcher, Greene et al. 2005). The pivotal roles of these different cytokines (IFNγ, TNFα, IL-12) in the response against toxoplasmosis was highlighted by different studies that clearly showed that depletion *in vivo* of these molecules by injecting depleting antibodies increased susceptibility to the infection (Araujo 1992) (Johnson 1992) (Hunter, Candolfi et al. 1995).

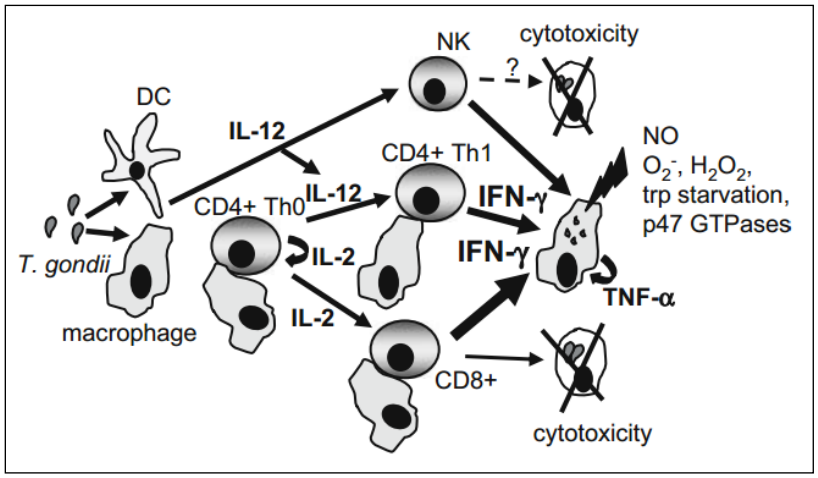

Figure 1.3: Regulatory and anti-parasitic effector mechanisms during acute infection with *T. gondii* (Lang, Gross et al. 2007).

One of the critical steps in the generation of pathogen-specific $CD8^+$ and $CD4^+$ T cells is the presentation of peptide antigens in the context of major histocompatibility complex (MHC) class I and II, respectively (Janeway 2001). A third pathway relying on CD1 molecules, MHC-I-like molecules, can present lipid and glycolipid antigens to invariant natural killer T (iNKT) cells (Cohen, Garg et al. 2009). Virtually all nucleated cells express MHC-I on their surface, while only professional antigen presenting cells (pAPCs), including dendritic cells (DCs), macrophages, and B cells, can readily present antigens on MHC-II molecules (Hudson and Ploegh 2002). The expression of the different CD1 isoforms display tissue and cell-type variations; group 1 CD1 molecules (a, b, c, and e in humans) are exclusively found on pAPCs and thymocytes while group 2 (d in humans and mice) can be expressed by both hematopoietic and non-hematopoietic cells (Dougan, Kaser et al. 2007).

Endogenous or intracellular antigens are proteolytically degraded, enter the ER through the transporter associated with antigen processing (TAP) complex, and are loaded onto MHC-I to be presented on cell surface to cytotoxic $CD8^+$ T lymphocytes (CTL) bearing a cognate T cell receptor (TCR) specific to the peptide-MHC-I (pMHC-I) complex (Hudson and Ploegh 2002).

On the other hand, exogenous or extracellular antigens are internalized by pAPCs through endocytosis/phagocytosis mechanisms (Guermonprez, Valladeau

et al. 2002), enter the endocytic pathway, are degraded within endolysosomes, and peptides are loaded onto MHC-II molecules to be presented at the surface to $CD4^+$ T cells (Hudson and Ploegh 2002). This latter subset of T cells is required to provide help, hence referred to as T helper (Th) cells, by secreting cytokines such as IL-2 and IFNγ to effector cells of the immune system (Schepers, Arens et al. 2005). MHC-II molecules can also present endogenous antigens through a process known as autophagy (Sant 1994) (Nimmerjahn, Milosevic et al. 2003) (Li, Gregg et al. 2005). Portions of the cytoplasm or even whole organelles can be enveloped by bi-layered membranes of unknown origin and contained within what is referred to as autophagosomes. These autophagosomes can then fuse with endolysosomes and deliver their content to be processed and loaded on MHC-II molecules. Alternatively, heat-shock chaperones and proteins, including HSC70, HSP40, and HSP90, recognize and bind target proteins to be imported into endocytic compartments to be processed for presentation.

In addition, exogenously acquired antigens can also be presented by MHC-I molecules by a process called cross-presentation (Kasturi and Pulendran 2008). Exogenous antigens, as opposed to endogenous, are internalized, degraded, and translocated into the cytosol by a mechanism that is still unclear. They are degraded into antigenic peptides by the proteasome, transported into the ER lumen in a TAP-dependent manner, and loaded onto MHC-I molecules. Alternatively, antigens may be internalized and processed by a TAP-independent mechanism for MHC-I presentation through a non-cytosolic pathway whereby antigens are processed within acidified endocytic compartments (Pfeifer, Wick et al. 1993).

CD1 proteins survey the endocytic pathway until they intersect with lipid and glycolipid antigens (Barral and Brenner 2007). With the help of molecules involved in lipid metabolism, notably saposins, these lipid antigens are loaded onto CD1 molecules. Group 1 CD1 molecules (a, b, c, and e) present antigens to clonally diverse T cells, while those from group 2 (d) present lipid antigens to invariant natural killer T cells (*i*NKT). Specific lipid antigens from different

pathogens have been reported to be presented by these molecules, such as *M. tuberculosis* mycolic acids (Beckman, Porcelli et al. 1994), lipoglycan lipoarabinomannan, phosphatidylinositol mannosides (Sieling, Chatterjee et al. 1995), and *L. donovani* lipophosphoglycan (Amprey, Im et al. 2004).

With regard to *Toxoplasma gondii*, parasite antigens are presented by both MHC-I and MHC-II complexes, as revealed by the generation of parasite-specific $CD8^+$ and $CD4^+$ T cells (Denkers and Gazzinelli 1998). Gubbels and colleagues provided one of the first indications that parasite material could exit the PV and seep into host cell cytoplasm and nucleus (Gubbels, Striepen et al. 2005). They engineered a parasite strain to secrete Cre recombinase, a type I topoisomerase, via secretory organelles (secCre) and GFP-STOP host cells in which a silent GFP (green fluorescent protein) gene is activated upon Cre-mediated deletion of a transcriptional stop signal. Their group was able to detect some GFP expression in a few infected cells (1.7%), suggesting that secCre was able to escape the PV into host cell compartments. Presumably, other parasite molecules could escape the PV in similar fashion.

Using a parasite strain that secrete ovalbumin (secOVA) into its PV, Dzierszinski and associates showed that actively infected host cells, as opposed to bystander cells, can process and present *Toxoplasma*-derived antigens via the endogenous MHC-I pathway, and activate OVA-specific B3Z $CD8^+$ T cell hybridoma (Dzierszinski, Pepper et al. 2007). This hybridoma was generated by fusing a T cell to a lymphoma cell that expresses a β-galactosidase (*lacZ*) reporter enzyme upon activation to cleave the substrate X-gal yielding a colored substrate that can be measured by colorimetric assays (Karttunen, Sanderson et al. 1992). Exploiting this system and using different host cell types (DCs, macrophages, fibroblasts, and astrocytes), their group showed that active invasion by OVA-expressing parasites could lead to priming and activation of OVA-specific $CD8^+$ T cells (Dzierszinski, Pepper et al. 2007).

Another group concluded that cross-priming of $CD8^+$ T cells directly correlates to the recruitment of host endoplasmic reticulum (hER) to the PV in *T.*

gondii-infected DCs (Goldszmid, Coppens et al. 2009). According to this study, DCs actively invaded by OVA-secreting transgenic parasites were able to induce a strong proliferation of and IFNγ production by OT-I cells, which are $CD8^+$ T cells specific for the OVA-derived SIINFEKL peptide presented by MHC-I molecules (Hogquist, Jameson et al. 1994). Conversely, DCs that had phagocytozed dead parasites were able to process and present the parasite-derived OVA peptide to OT-II $CD4^+$ T cells, which are specific for SIINFEKL peptide but presented by MHC-II molecules (Barnden, Allison et al. 1998), but were unable to present the antigen to OT-I $CD8^+$ T cells by cross-presentation. Furthermore, using immunofluorescence microscopy, immunogold labeling, and immunocytochemical staining for an ER-specific marker, this group observed host-derived luminal ER content within the parasite's PV which suggests that direct communication between these two compartments can occur.

In contrast, conventional phagosomes containing live or dead parasites did not fuse with the hER, judging by the lack of hER material within phagosomes. Furthermore, OT-I $CD8^+$ T cells proliferation was markedly abrogated when the infected DCs with pretreated with exotoxin A (ExoA), a toxin that inhibits the Sec61 translocon, which is required for the translocation of proteins from the ER to the cytoplasm. Taking into account all of these observations, it appears that active invasion leads to the association of the parasite's PV and the host cell's ER, to the exchange of luminal material, to the translocation of parasite proteins from the hER to the cytoplasm, and finally to the processing and presentation of parasite proteins onto MHC-I molecules.

Evidence is scarce about the contribution of CD1 and presentation of *Toxoplasma*-derived lipid antigens to the resistance against the infection. At the present time, only one report has shown that lack of CD1d in knock-out mice exacerbates susceptibility to acute oral infection (Smiley, Lanthier et al. 2005). Other reports have postulated that CD1-restricted NKT cells are involved in resistance (Denkers, Scharton-Kersten et al. 1996) (Denkers and Sher 1997).

Generation of pathogen-specific $CD8^+$ T cells and their functional activity are greatly enhanced by $CD4^+$ T helper cells, and it has been demonstrated that this latter lymphocyte subset are essential for the maintenance of $CD8^+$ T cell effector immunity against *T. gondii* (Casciotti, Ely et al. 2002). In fact, removal of $CD4^+$ T cells by using a depleting monoclonal antibody led to the failure of the generation of protective effector $CD8^+$ T cells in the mouse model (Gazzinelli, Hakim et al. 1991).

Another study has shown that the frequency of splenic and intracerebral *T. gondii*-specific effector and memory $CD8^+$ T cells is independent of CD4+ T helper cells (Lutjen, Soltek et al. 2006). Indeed, depletion of the latter subset either prior to the infection or during the chronic phase did not alter the frequency of the $CD8^+$ T cell population. The persistence of *Toxoplasma* antigens in the brain and the contribution of natural killer (NK) cells may have compensated for the absence of $CD4^+$ T cells (Combe, Curiel et al. 2005) and led to the generation of $CD44^+$ $CD62L^-$ effector $CD8^+$ T cells. Generation of $CD44^+$ $CD62L^+$ memory $CD8^+$ T cells was also observed in the spleen, an organ without parasite persistence, in the absence of $CD4^+$ T cells (Lutjen, Soltek et al. 2006). In striking contrast to the frequency, the functional activity of intracerebral $CD8^+$ T cells is partially dependent on $CD4^+$ T cells. Depletion of the latter during the acute phase reduced the frequency of intracerebral, but not splenic IFNγ-producing and cytotoxic *T. gondii*-specific $CD8^+$ T cells. These variations in the organs reflect the different cellular compositions. For instance, dendritic cell subpopulations absent in the brain, may have partially compensated for the absence of $CD4^+$ T cells in the spleen, while $CD4^+$ T cells may be required to overcome the immunosuppressive environment within the brain to ensure optimal $CD8^+$ T cell activity. In fact, depletion of $CD4^+$ T cells in chronically infected mice led to a fourfold reduction of intracerebral IFNγ-producing $CD8^+$ T cells, strongly suggesting that continuous support by T helper cells is required to maintain an optimal functional activity by effector $CD8^+$ T cells. In addition to a defective antibody response (Dao, Fortier et al. 2001) (Johnson and Sayles 2002), the functional impairment observed in intracerebral, but not splenic $CD8^+$ T cells

directly contributed to the death of $CD4^+$ T cell-depleted mice from toxoplasmic encephalitis, arguing that $CD4^+$ T cell play a pivotal role in the protection against the infection. As mentioned above, generation of parasite-specific $CD4^+$ T cells requires antigen presentation to occur in a MHC class II-restricted fashion.

1.5. Class-II gene transcription and regulation

The expression of MHC-II is predominantly controlled at the level of transcription by a highly conserved regulatory module located 150-300 base pairs (bp) upstream of the transcription initiation site in all MHC-II genes (Reith and Mach 2001) (Ting and Trowsdale 2002) (Boss and Jensen 2003). The SXY module, the MHC-II-specific regulatory module, consists of four sequences, namely the S, X, X2, and Y boxes (Figure 1.4). This module is found in the promoters of the genes encoding for both the α and β-chains of all MHC-II molecules, including the three human MHC-II isotypes (HLA-DP, -DQ, and -DR) as well as the two murine isotypes (H2-A and -E). The same module is found upstream of genes encoding for accessory proteins, specifically the MHC-II associated invariant chain (Ii or CD74), H2-DM and H2-DO (or HLA-DM and HLA-DO in humans, respectively) (Reith, LeibundGut-Landmann et al. 2005). It is noteworthy to mention that the Ii gene is located on a separate chromosome from the rest of the MHC-II genes (Glimcher and Kara 1992), and although both basal and cytokine-induced class-II and Ii expression is typically concerted, uncoordinated expression has been reported (Momburg, Koch et al. 1986) and could be due to the presence of additional promoter and enhancer elements unique to Ii (Zhu and Jones 1990) (Figure 1.5).

There are four key *trans*-acting regulatory factors that interact with the SXY module and dictate transcription: the class-II major histocompatibility complex transactivator (CIITA), a non-DNA binding factor known as the "master regulator", the regulatory factor X5 (RFX5), the RFX-associated protein (RFXAP), and the RFX-associated ankyrin-containing protein (RFXANK)

(Steimle, Otten et al. 1993) (Steimle, Durand et al. 1995) (Durand, Sperisen et al. 1997). The RFX complex, composed of RFX5, RFXAP, and RFXANK, interacts with X2-box-specific cyclic-AMP-responsive-element-binding protein (CREB), the Y-box-specific nuclear transcription factor Y (NFY), and an unidentified S-box-specific factor to form the MHC-II enhanceosome (Moreno, Beresford et al. 1999) (Mantovani 1999) (Muhlethaler-Mottet, Krawczyk et al. 2004). In turn, CIITA interacts with the enhanceosome complex to recruit additional chromatin modification and remodeling factors, namely the CREB-binding protein (CBP), p300, p300/CBP-associated factor (PCAF), brahma-related gene 1 (BRG1) and co-activator-associated arginine methyltransferase 1 (CARM1), and to engage transcription by recruiting the RNA polymerase II (Ting and Trowsdale 2002) (Reith, LeibundGut-Landmann et al. 2005).

While the components of the enhanceosome are expressed in most cell types regardless of their MHC-II expression status, the synthesis of CIITA is tightly controlled and its activation is the determining factor for MHC-II expression in pAPCs. Furthermore, stimuli that inhibit or down-regulate IFNγ-induced MHC-II expression, such as cytokines like tumor growth factor beta (TGFβ), IL-1, IL-4, and IL-10, various pathogens, and certain drugs, typically target CIITA by interfering with its expression (Kanazawa, Okamoto et al. 2000) (O'Keefe, Nguyen et al. 1999) (Le Roy, Muhlethaler-Mottet et al. 1999) (Gao, De et al. 2001) (Zhong, Fan et al. 1999) (Luder, Lang et al. 2003) (Pai, Convery et al. 2003) (Kwak, Mulhaupt et al. 2000) (Youssef, Stuve et al. 2002).

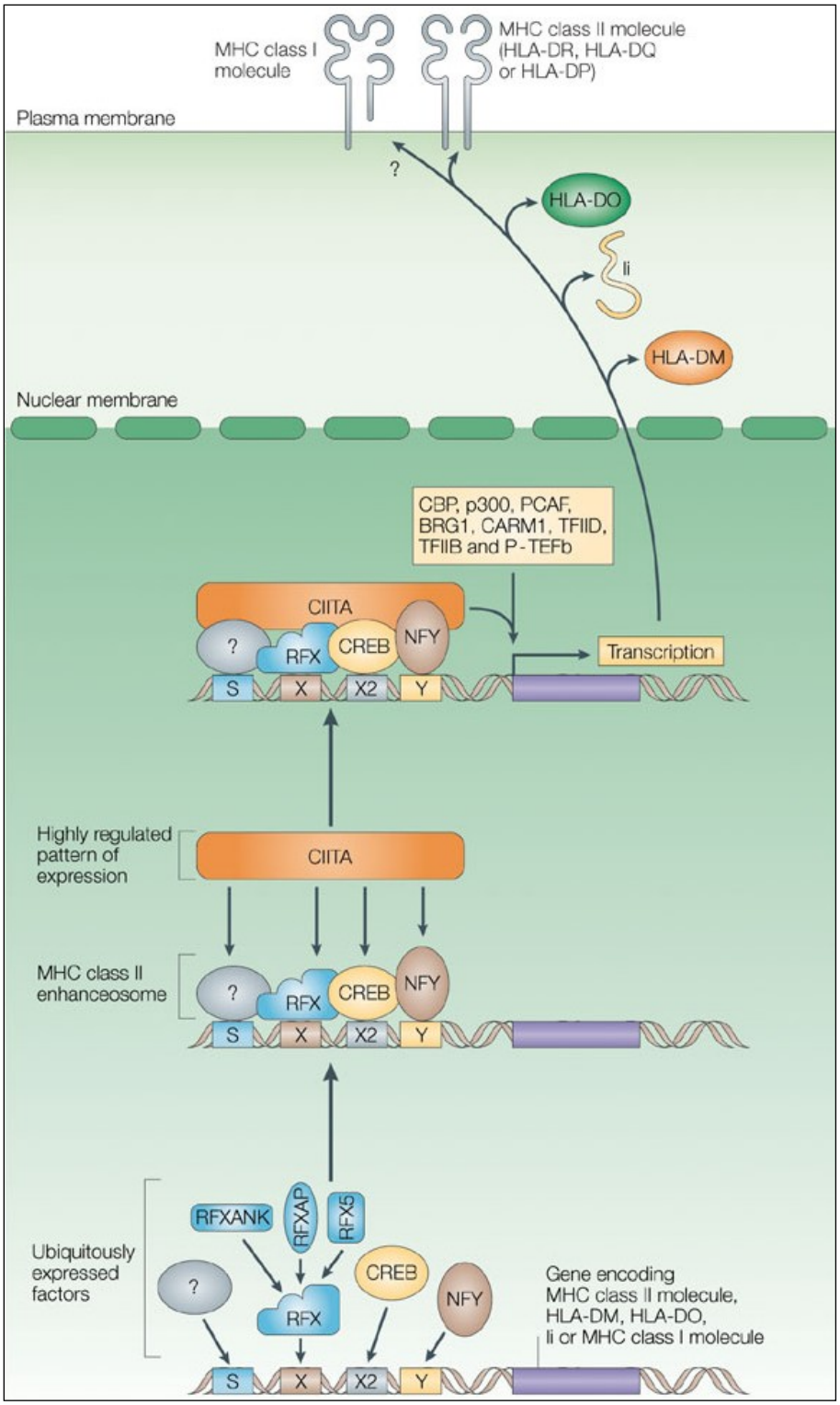

Figure 1.4: Regulation of the transcription of MHC class II genes (Reith, LeibundGut-Landmann et al. 2005).

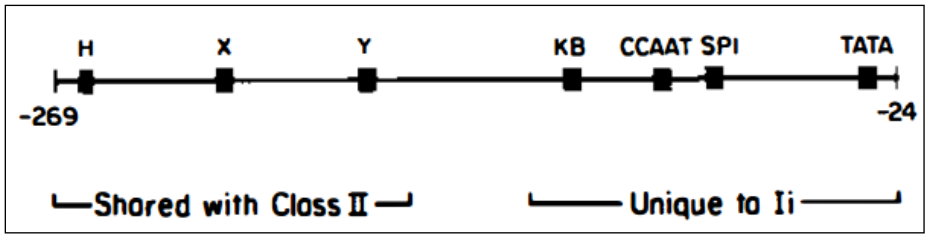

Figure 1.5: The invariant chain promoter (Glimcher and Kara 1992).

Transcription of CIITA is controlled by four distinct promoters known as pI, pII, pIII, and pIV in humans (Muhlethaler-Mottet, Otten et al. 1997). Promoters pI, pIII, and pIV are highly conserved, while the mouse pII has yet to be identified and its function in humans remains elusive. Cell-type-specific, cytokine-induced, and developmentally modulated MHC-II expression is dictated by the use of these promoters and the three CIITA isoforms they give rise to. For instance, pI is utilized by myeloid cells, such as conventional DCs, and macrophages, pIII is used by cells of lymphoid origin namely B and T cells, as well as plasmacytoid dendritic cells (pDCs), while pIV mainly drives IFNγ-induced MHC-II expression in myeloid cells, but also in thymic epithelial cells (TECs) and non-hematopoietic cells (Reith, LeibundGut-Landmann et al. 2005). Studies have focused primarily on pIV for numerous reasons. First, pIV-deficient mice display a severe reduction in $CD4^+$ T cell numbers (Waldburger, Suter et al. 2001) (Waldburger, Rossi et al. 2003) due to a defect in the positive selection in the thymus which relies on MHC-II expression by TECs (Starr, Jameson et al. 2003). Second, IFNγ-driven MHC-II expression in non-haematopoietic cells like respiratory and intestinal epithelial cells, endothelial cells, astrocytes, and fibroblasts depends on the pIV promoter. The induced expression of MHC-II in these cells have been suggested to play a tolerogenic role by contributing to the generation of peripheral $CD4^+$ $Foxp3^+$ regulatory T (T_{reg}) cells (Krupnick, Gelman et al. 2005) (Jiang, Yang et al. 2008), and lost of MHC-II expression can lead to a local inflammatory response (Kreisel, Richardson et al. 2010). Lastly, several pathogens have elaborated ways of interfering with CIITA by targeting activation

of pIV following IFNγ stimulation (Reith, LeibundGut-Landmann et al. 2005), as seen with *Toxoplasma gondii* infection (Luder, Lang et al. 2003).

Interferon gamma is a soluble cytokine of the type II class of interferons (Gray and Goeddel 1982) that dimerizes to bind to its heterodimeric receptor consisting of the ligand-binding interferon gamma receptor alpha chain (IFNγRα) and the non-binding interferon gamma receptor beta chain (IFNγRβ) (Hemmi, Bohni et al. 1994). Binding of IFNγ to its receptor leads to its phosphorylation by Janus kinase 1 (JAK1) and 2 which then allows signal transducer and activator of transcription 1 (STAT1) to bind, come into close proximity to the JAK kinases and be phosphorylated (Reith, LeibundGut-Landmann et al. 2005) (Figure 1.6). Phosphorylated STAT1 homodimerizes and translocated into the nucleus. Along with another factor called the upstream transcription factor 1 (USF1), STAT1 dimers bind to a IFNγ-activated site (GAS)-E-box motif found in the pIV promoter region, while two other factors, IFN-regulatory factor 1 (IRF1) and 2 (IRF2), bind to the IRF-element (IRF-E). The concerted binding of these factors initiates the transcription of CIITA which eventually leads to MHC-II synthesis.

1.6. MHC-II protein synthesis, trafficking, and loading

MHC-II molecules are synthesized in the ER where they associate with the MHC-II associated invariant chain (Ii or CD74) chaperone (Hudson and Ploegh 2002) to form a pentameric complex, whereby one α and one β MHC-II chain associate with Ii trimers (Koch, Zacharias et al. 2011) (Figure 1.7).

The invariant chain is a non-polymorphic type II membrane protein expressed as four different isoforms in humans, p33, p35, p41, and p43, while there are only two in mice, p31 and p41, all of which can bind to nascent MHC-II molecules (Landsverk, Bakke et al. 2009). Alternative splicing of the transcript gives rise to either p33, or p31 in mice, and the p41 isoforms, where the latter has an extra exon (O'Sullivan, Noonan et al. 1987). In humans, an alternative translation initiation site adds an extension of 16 residues at the cytoplasmic N-

terminus (Strubin, Long et al. 1986). With regards to MHC-II, the importance of Ii is threefold. First, it chaperones correctly assembly of the different MHC-II chains. Second, it prevents non-specific loading of self-peptides onto nascent MHC-II molecules by occupying the MHC-II groove. Third, Ii guides MHC-II trafficking until its complete maturation. Indeed, Ii contains di-leucine-based sorting motifs within its cytoplasmic tail (Pieters, Bakke et al. 1993) (Odorizzi, Trowbridge et al. 1994) that are recognized by either AP1 and AP3, or AP2 adaptor proteins that will send Ii/MHC-II complexes to the cell surface as immature complexes, or directly to the endocytic pathway for maturation from the trans-Golgi network (TGN), respectively (Kongsvik, Honing et al. 2002) (Bonifacino and Traub 2003).

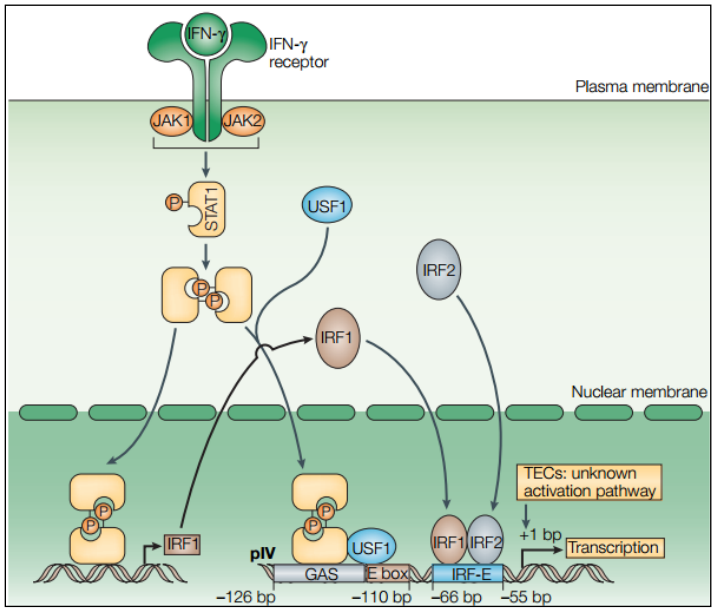

Figure 1.6: IFNγ signaling and the molecular regulation of pIV (adapted from (Reith, LeibundGut-Landmann et al. 2005)).

The starting point for Ii/MHC-II complexes in the endocytic pathway is within early endosomes (EEs). These highly dynamic compartments can receive endocytic cargo from different sources either from the extracellular milieu following internalization events, the TGN, or the cytosol (Huotari and Helenius 2011), including antigens. Maturation of EEs to late endosomes (LEs), and subsequent fusion with lysosomes to form endolysosomes leads to an acidification and a significant drop in the lumenal pH. Acidification is required for the self-

activation of aspartic and cysteine proteases, namely legumain (or asparaginyl endopeptidase, AEP) and cathepsins (Hsing and Rudensky 2005). These activated enzymes will break down antigens into small antigenic peptides. These same proteases will cleave in a sequential manner the invariant chain, proceeding directionally from the N- to the C-terminus, giving rise to intermediate degradation products p22 and p10, and finally leaving the Class II-associated invariant chain peptide (CLIP) in the MHC-II groove (Sercarz and Maverakis 2003).

The exchange of CLIP for a higher-affinity antigenic peptide, typically 13 to 18 residues-long, is facilitated by HLA-DM (H2-DM in mice), an MHC-II-like molecule, by inducing conformational changes in the peptide binding groove, a process referred to as MHC-II loading (Busch, Rinderknecht et al. 2005). This process occurs in the MHC-II compartment (MIIC), which is enriched for MHC-II, Ii and HLA-DM. It was shown that HLA-DM also performs peptide editing whereby it will preferentially remove peptides that contain a suboptimal side chain with lower affinity to the MHC-II groove or peptides shorter than 11 residues thereby selecting the most stable peptide/MHC-II complex (Kropshofer, Vogt et al. 1996), shaping the antigen repertoire presented to T cells, and establishing immunodominance (Nanda and Sant 2000). Interestingly, CLIP binds with various affinities due to the highly polymorphic nature of the MHC-II groove (Schulze and Wucherpfennig 2012). In fact, CLIP can spontaneously dissociate from low-affinity MHC-II molecules, while the activity of HLA-DM is essential for the removal of CLIP tightly bound with high-affinity to MHC-II molecules (Stebbins, Loss et al. 1995). Peptide-loaded MHC-II complexes (pMHC-II) are finally brought to the cell surface to be presented to $CD4^+$ T cell bearing a cognate TCR.

Given the intricacy of the MHC-II pathway and the levels regulation, it becomes evident that pathogens have multiple targets to choose from to interfere with antigen presentation and subvert the immune response.

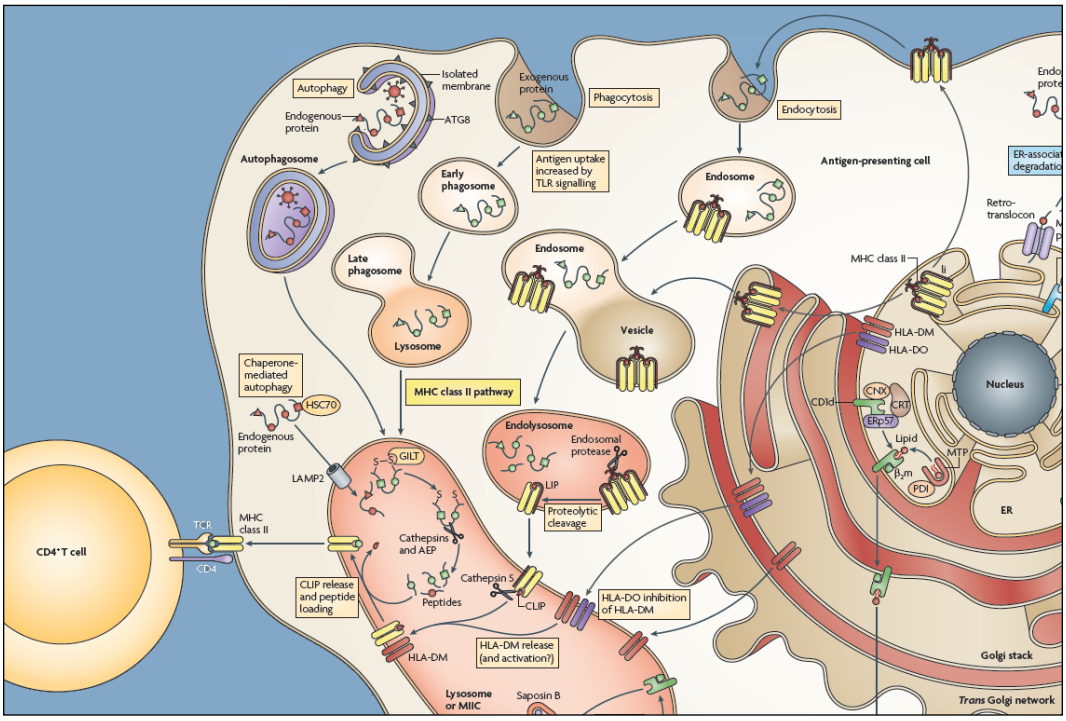

Figure 1.7: The MHC-II antigen presentation pathway (adapted from (Wearsch and Cresswell 2009)).

1.7. Immune subversion and interference with MHC-II antigen presentation

Many pathogens, whether viral, bacterial, protozoan, or filarial, have devised ways to subvert immune functions with a propensity to target antigen presentation. Alike other pathogens, *Toxoplasma gondii* has evolved numerous ways to subvert immune functions of its host to gain an advantageous edge over the immune system and to establish a chronic infection9gag. Different groups were able to show that the parasite can lower NO production by inhibiting the inducible nitric oxide synthase (iNOS) transcription (Seabra, de Souza et al. 2002) (Luder, Algner et al. 2003), inhibit transcription of interferon-inducible p47 GTPases (IRG) (Butcher, Greene et al. 2005), inhibit production of pro-inflammatory cytokines like IL-12 and TNFα (Aliberti, Serhan et al. 2002) (Butcher, Kim et al. 2005), and induce anti-inflammatory cytokines like IL-10 (Khan, Matsuura et al. 1995) via the STAT3/6 pathway (Butcher, Kim et al.

2005), TGFβ (Bermudez, Covaro et al. 1993), and IFNα and β (Diez, Galdeano et al. 1989). By interfering with pro-inflammatory signaling pathways that promote antigen presentation by inducing MHC-II gene transcription and targeting their components such as NF-κB (Shapira, Harb et al. 2005), MAPK (Kim, Butcher et al. 2004), and STAT1 (Zimmermann, Murray et al. 2006), *T. gondii* modulates MHC-II expression during infection.

Work by Zimmermann and associates have shown that active invasion by the parasite blocks phosphorylation and hence activation of STAT1 (Zimmermann, Murray et al. 2006). This inhibition is accomplished by inducing suppressor of cytokine signaling 1 (SOCS1), which inhibits JAK kinases (Alexander and Hilton 2004) and leads to the proteasomal degradation of bound STAT1 (Zhang, Farley et al. 1999). Therefore, by blocking the activation of STAT1 despite IFNγ stimulation, *T. gondii* impedes MHC-II expression at the level of transcription. In fact, mRNA levels of MHC-II have been reported to be lower in cells infected with live parasites (Luder, Lang et al. 2003) (Lang, Algner et al. 2006). However, it was recently shown that the induction of SOCS1 is a strain-specific effect, whereby type I parasites induce SOCS1 expression, while type II parasites fail to do so (Stutz, Kessler et al. 2012). This induced expression is mediated by the p38 MAPK-dependent activation of early growth response 2 (egr2), a transcription factor previously reported to regulate SOCS1 expression (Mostecki, Showalter et al. 2005) and to be activated following rhoptry discharge (Phelps, Sweeney et al. 2008). The strain dependency effect explains why nuclear translocation and accumulation of STAT1 following IFNγ stimulation is not disturbed in type II-infected cells (Lang, Algner et al. 2006). Rather, binding of STAT1 to IFNγ-regulated promoters is impeded due to a defective recruitment of chromatin remodelling components, notably BRG1, to the failed formation of the remodelling complex, and thus to an inhibited acetylation of histones (Lang, Hildebrandt et al. 2012). Also, active invasion into the host cell is required to induce SOCS1, since MIC8 knock-outs, which are unable to invade (Kessler, Herm-Gotz et al. 2008), did not up-regulate the expression of this molecule (Stutz,

Kessler et al. 2012). In contrast, MHC-II inhibition does not require active invasion, and is observed with all parasite types. In fact, non-infected bystander cells within an infected culture are also slightly inhibited following IFNγ treatment in comparison to non-infected control cultures. These observations suggest that *T. gondii* utilizes multiple strategies to block MHC-II expression not limited to STAT1 interference.

Moreover, it was shown that *T. gondii* tachyzoites preferentially invade immature DCs, and block maturation of these cells even when stimulated with pro-inflammatory stimuli known to up-regulate surface MHC-II such as IFNγ, bacterial lipopolysaccharide (LPS), CD40L, and TNFα (McKee, Dzierszinski et al. 2004). As previously mentioned, impaired chromatin remodelling at STAT1-regulated promoters partly explains the global unresponsiveness of *Toxoplasma*-infected cells to maturation signals, at least with regards to IFNγ (Lang, Hildebrandt et al. 2012). Transcriptional inhibition of MHC-II genes leads to lower MHC-II protein levels (Luder, Lang et al. 1998) (Luder, Lang et al. 2003) (Lang, Algner et al. 2006) and consequently impedes MHC-II-restricted antigen presentation and $CD4^+$ T cell activation (Luder, Walter et al. 2001) (McKee, Dzierszinski et al. 2004). Obviously, impairing the ability of pAPCs to present parasite-associated antigens to T cells constitutes a momentary advantage for *Toxoplasma* to gain a head start on the host's immune response.

Molecules that inhibit MHC-II expression and maturation have been successfully identified in some pathogenic bacteria, viruses, and other protozoan and filarial parasites. Some of these molecules have been shown to interfere with MHC-II transcription by either directly degrading transcription factors, such as the *Chlamydia* CPAF which degrades RFX5 and USF1 (Zhong, Fan et al. 1999) (Zhong, Fan et al. 2001) (Fan, Dong et al. 2002) and the *Leishmania* CPB cysteine peptidases that degrades IκB and NF-κB (Cameron, McGachy et al. 2004), or by interfering with upstream signaling pathways and chromatin remodeling like the *Mycobacterium tuberculosis* 19-kDa LpqH lipoprotein which blocks TLR2-induced MAPK activation and decreases histone acetylation of the

pIV CIITA promoter (Pennini, Pai et al. 2006). On the other hand, other inhibitory molecules target MHC-II trafficking through the endocytic pathway, such as the *Salmonella enterica* SifA (Mitchell, Mastroeni et al. 2004) and the *Helicobacter pylori* VacA (Molinari, Salio et al. 1998), antigen processing, alike the *Brugia malayi* Bm-CPI-1 and -2 cystatins which inhibit lysosomal cysteine proteases (Manoury, Gregory et al. 2001), or even directly degrade MHC-II molecules, as seen with the *Leishmania* CPB (De Souza Leao, Lang et al. 1995). The HIV-1 Nef protein has been shown to modify trafficking of MHC-II molecules specifically, promoting the surface expression Ii-associated immature MHC-II molecules while reducing up to two-fold surface expression of peptide-loaded MHC-II molecules (Stumptner-Cuvelette, Morchoisne et al. 2001). Although several host factors have been identified as being affected during active invasion and some parasite factors have been linked to virulence, *T. gondii* molecules that interfere with antigen presentation via the MHC-II pathway have yet to be identified. Since many different steps of the MHC-II pathway could be targeted (ex: signaling, transcription, translation, trafficking, etc.), as seen with the different pathogens and their inhibitory molecules, a broad approach has to be considered in order to identify these molecules without limiting our focus to one particular step. In the following chapter, we discuss the details of a forward genetic screening strategy elaborated to this end.

Chapter 2

2.1. Elaboration of a forward genetic screening strategy to identify *T. gondii* genes coding molecules inhibiting MHC-II expression

Since other pathogens express molecules that have been shown to directly inhibit MHC-II antigen presentation, we hypothesized that *T. gondii* also expresses molecules whose function is to directly inhibit MHC-II molecules. In an attempt to identify these parasite molecules, the first approach considered was a classical forward genetic screening. Forward genetics consist of identifying the genotype responsible for a given phenotype (Hartwell 2008). The feasibility of genetic manipulation in *T. gondii* is facilitated by its haploid genome during most of its life stages, including the tachyzoite stage which is used in our laboratory setting, and the accessibility to its completely sequenced genome within a dedicated database (i.e. http://toxodb.org) (Roos, Donald et al. 1994) (Donald and Roos 1995) (Kissinger, Gajria et al. 2003) (Kim and Weiss 2004) (Gajria, Bahl et al. 2008). For instance, a successful forward genetic screen was accomplished by one group using a chemical mutagen, N-nitroso-N-ethylurea (ENU), to generate genome-wide mutations. By isolating temperature-sensitive mutants, they were able to identify genes involved in the parasite's cell cycle (Gubbels, Lehmann et al. 2008). Alternatively, insertional mutagenesis using plasmid constructs has been proven to be a highly efficacious method to disrupt genes throughout the genome in *T. gondii* (Donald and Roos 1995) (Roos, Sullivan et al. 1997). Considering this latter method, we elaborated a forward genetic screening strategy in an attempt to identify the genes of interest with regard to our hypothesis. In other words, we wished to identify mutated genes that cause a phenotypic abnormality in *T. gondii* parasites characterized by the incapacity to block host cell IFNγ-induced MHC-II expression, activation and maturation.

2.2. Rationale overview

Our initial hypothesis proposed that by disrupting the *T. gondii* genes coding for the inhibitory molecules, an altered phenotype would be observed, specifically an inability of the parasite to block IFNγ-induced MHC-II expression in infected pAPCs, which could eventually lead to the identification of inhibitory molecules. To avoid any bias and to ensure no gene is omitted *a priori*, random mutations would be generated throughout the parasite's genome. Insertional mutagenesis has proven to be a very effective method to disrupt genes in *T. gondii*; it is estimated that in a single electroporation cuvette containing 10^7 parasites, every single gene can be disrupted by non-homologous recombination using a highly efficient plasmid such as bifunctional dihydrofolate reductase-thymydylate synthase (DHFR*-TS)-based plasmids (Roos, Sullivan et al. 1997).

The rationale behind this assumption resides in the fact that between 70 and 90% (depending on the strain) of the starting 10^7 electroporated parasites, or 7 to 9 x 10^6, are viable when using an Amaxa Nucleofector electroporator, of which 5% are stably transfected (3.5 to 4.5 x 10^5). The *T. gondii* genome spans 8 x 10^7 base pairs (bp) and the DHFR*-TS plasmid integrates randomly throughout the genome; this yields an average of one insertion in one of the stable transgenic parasite for any 178- to 229-nucleotide (nt) segment of DNA:

$$8 \times 10^7 \div 4.5 \times 10^5 = 178 \text{ nt or } 8 \times 10^7 \div 3.5 \times 10^5 = 229 \text{ nt}$$

There are about 8,000 genes in its genome, contained in 14 chromosomes, and most of these genes are larger than 229 bases, and the insertional plasmid spans 8 kb. Therefore, it is achievable to hit every single gene within the genome. In addition, since tachyzoites (form used for this study) are haploid, a single insertion is sufficient to disrupt a single-copy gene (Donald and Roos 1995), simplifying the mutagenesis process, but limiting to non-essential genes in this stage *in vitro*.

This technique allows for a very broad approach, but it also requires the screening of a great number of parasites. To this end, fluorescence activated cell

sorting (FACS), a flow cytometry technique used to separate and collect cells according to parameters defined by the user, allows for high throughput screening of these numerous mutants. First, three stable parental lines of parasites with different genetic backgrounds are engineered to express a yellow fluorescent protein (YFP) in frame with the P30 signal peptide under the control of the constitutively expressed α-tubulin promoter. The P30 gene contains a signal peptide that allows the YFP reporter to be secreted into the PV via the default secretory pathway (from ER to Golgi, to dense granules, and to PV lumen). This fluorescent reporter allows tracking of the parasites by flow cytometry, but also allows the distinction between a PV formed upon active invasion from a phagosome formed during phagocytosis by microscopy. Upon active invasion, parasite proteins are secreted and accumulate within the PV, but not within phagosomes.

Once the parental lines are generated, they are mutagenized by insertional mutagenesis using a plasmid that randomly integrates via non-homologous recombination to create a library of random mutants (Donald and Roos 1995) (Roos, Sullivan et al. 1997). The library of mutant parasites is used to infect professional antigen presenting cells (pAPCs), and a cell-autonomous marker is chosen to monitor parasite phenotype. Since we are looking for mutant parasites unable to inhibit IFNγ-induced MHC-II expression, surface MHC-II molecules are used as a marker. Staining with antibodies conjugated with two different fluorochromes against surface MHC-II allows to monitor surface expression of this marker before and after infection and the addition of the maturation signal (i.e. IFNγ). The combination of two fluorochromes and the parasite fluorescent reporter, the flow cytometer enables sorting of cells displaying the phenotype of interest. In this case, infected cells expressing high levels of MHC-II labeled with the antibody used to stain after infection and IFNγ stimulation, but not with the antibody used to stain prior to infection, are sorted. Multiple rounds of sorting are carried out to validate the phenotype observed, but also to enrich for the mutants of interest (Figure 2.1).

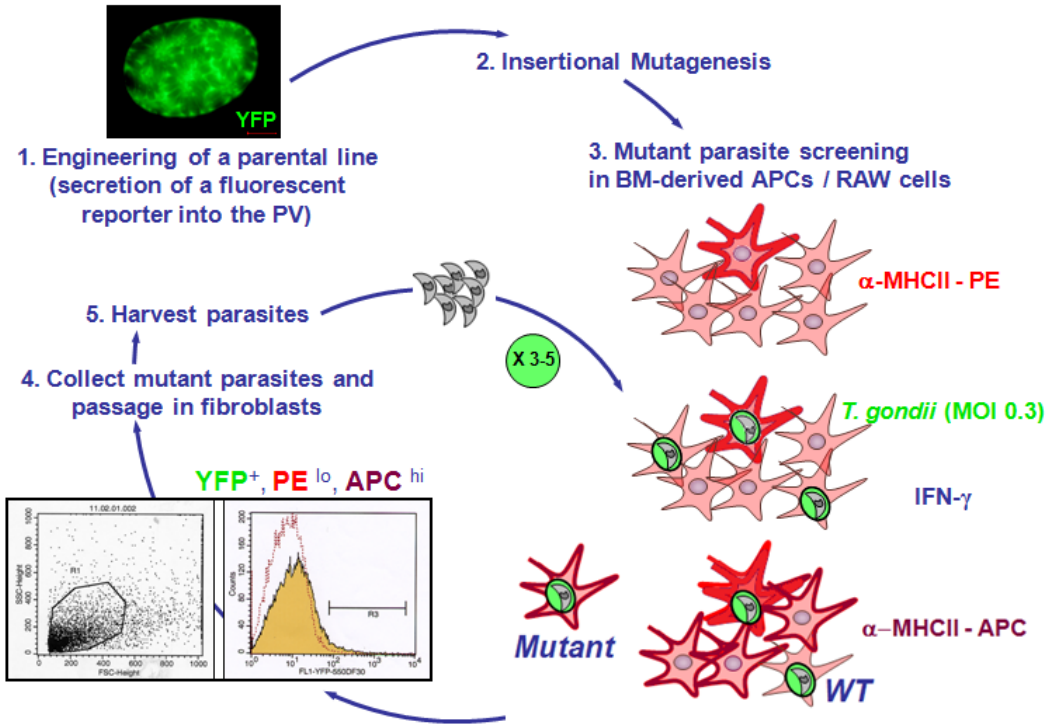

Figure 2.1: Flow chart of the forward genetic screening strategy. Generally speaking, there are five steps to the genetic screen. The parental lines are first engineered to express and secret YFP in the PV. Then, these parasites are mutagenized by insertional mutagenesis. Either cell-line or bone-marrow derived pAPCs are infected with the mutant population, stimulated with IFNγ, and analyzed by flow cytometry for their MHC-II expression patterns. The infected host cells displaying the sought phenotype (i.e. YFP^{+}, PE^{lo}, APC^{hi}) are sorted by FACS, and the mutant parasites they harbor are passaged in fibroblasts. Once the parasites recover, replicate, and lyse out, they are used for subsequent rounds of infection/sorting to enrich for the desired phenotype.

At this point, the sorted parasites represent a heterogeneous population that harbors different mutations. Therefore, mutant parasites are cloned and their mutated gene loci are identified. Two techniques can be used, either inverse PCR or plasmid rescue (Donald and Roos 1995) (Roos, Sullivan et al. 1997). When the mutated sequences are known, they can be analyzed by database mining utilizing the numerous computational tools available on the *Toxoplasma* database website (http://toxodb.org). Here, the isolated loci can be associated to known, putative, or novel genes. Finally, the identified gene can be linked to a parasite protein, and ultimately to its mechanism of action in the host cell.

2.3. Parasite and host cell culture

Three different strains were cultured: two of these strains were type I or virulent strains, RHΔ*HXGPRT*-Δ*UPRT* (henceforth referred to as RHΔΔ) and RHΔ*cpsII*, a uracil auxotroph that lacks a functional carbamoyl phosphate synthetase II, an enzyme required for *de novo* pyrimidine synthesis, and that cannot replicate without an exogenous source of uracil (Fox and Bzik 2002). The third strain was a type II or avirulent cyst-forming strain, PrugniaudΔ*HXGPRT* (henceforth referred to as PruΔ). All strains were cultured in human foreskin fibroblast (HFF) cell monolayers in culture-treated 25 cm^2 T-flasks with the appropriate medium (for RH strains: EMEM, 1% FBS, 2 mM L-glutamate, 1,000 U/ml penicillin, 1,000 µg/ml streptomycin, 50 µg/ml gentamicin, and for PruΔ: DMEM, 10% FBS, 2 mM L-glutamate, 1,000 U/ml penicillin, 1,000 µg/ml streptomycin, 50 µg/ml gentamicin) at 37°C, 5% CO_2, as previously described (Roos, Donald et al. 1994). These cells are primary fibroblasts that can be maintained for weeks as confluent monolayers, and their relative large size allow a high parasite yield. Upon lysis of monolayers due to parasite replication and egress, parasites were passaged to new HFF flasks. Stocks for each strain were kept frozen at -80°C and liquid nitrogen (N_2) in a cryoprotectant medium consisting of fetal bovine serum (FBS) and 10% dimethyl sulfoxide (DMSO).

Three different host cell types were tested for the MHC-II inhibition assay: RAW 264.7, bone marrow-derived macrophages (BMMΦ), and bone marrow-derived dendritic cells (BMDCs). RAW 264.7 cells (ATCC TIB-71) are an Abelson virus-transformed murine macrophage cell line (Raschke, Baird et al. 1978). This cell line was propagated indefinitely in culture without additional growth factors in the medium (DMEM, 10% FBS, 2 mM L-glutamate, 1,000 U/ml penicillin, 1,000 µg/ml streptomycin, 50 µg/ml gentamicin). BMMΦ and BMDCs were obtained by differentiating precursor cells from murine bone marrow, as previously described (Weischenfeldt and Porse 2008), (Lutz, Suri et al. 2000). Briefly, mice were euthanized by CO_2 asphyxiation, and hind legs were collected in Dulbecco's modified Eagle's medium (DMEM). The marrow was

flushed out of the bones, and live precursor cells were counted using trypan blue exclusion staining. For BMMΦ, 5 x 10^6 precursor cells were resuspended in culture medium (DMEM, 10% FBS, 2 mM L-glutamate, 1,000 U/ml penicillin, 1,000 µg/ml streptomycin, 50 µg/ml gentamicin, 2.5% HEPES, 55µM beta-mercaptoethanol, 1 mM sodium pyruvate (Wisent, St-Bruno, Quebec, Canada)) supplemented with 30% L929 fibroblast supernatant (containing M-CSF), and cells were seeded in tissue culture-treated Petri dishes. The differentiation medium was changed three days after seeding. Differentiated macrophages were used after 8 days for the assays. As for bone marrow-derived dendritic cells (BMDCs), 2 x 10^6 precursor cells were resuspended in culture medium (RPMI, 10% FBS, 2 mM L-glutamate, 1,000 U/ml penicillin, 1,000 µg/ml streptomycin, 50 µg/ml gentamicin, 2.5% HEPES, 55µM beta-mercaptoethanol) supplemented with 40 ng/ml of rGM-CSF and 10 ng/ml rIL-4 (Peprotech, Rocky Hill, NJ) in Petri dishes. Fresh medium was added on day 3 and changed on day 6 after seeding, and cells were used on day 7 for the assays.

2.4. Generation of the parasite parental lines

Tachyzoites were transfected with a p*tub1* P30 YFP *sag1*-CAT-*sag1* plasmid (Figure 2.2). This plasmid encoded a yellow fluorescent protein (YFP) reporter in frame with the *T. gondii* P30 signal peptide under the control of the constitutively expressed α-tubulin promoter. The P30 gene has a signal peptide that allows the YFP reporter to be secreted into the PV via the default secretory pathway (from ER to Golgi, to dense granules, and to PV). Secretion of the reporter protein allows the distinction between a PV formed upon active invasion from a phagosome formed during phagocytosis by microscopy. Upon active invasion, parasite proteins are secreted and accumulate within the PV, but not within phagosomes. The plasmid also encoded a drug selectable marker, the chloramphenicol acetyl transferase (CAT) gene, regulated by the surface antigen 1 (*sag1*) promoter, conferring resistance to chloramphenicol (an antibiotic) to the parasites in which the plasmid has successfully integrated into the genome (Kim,

Soldati et al. 1993). In addition, the plasmid contained an ampicillin resistance gene (*Amp*^{R}) to ensure the replication of successfully transformed DH5α *Escherichia coli* bacteria only and amplification of the plasmid. Briefly, bacteria were transformed by heat-shock with the plasmid and incubated overnight in a 37°C shaker in ampicillin-containing LB broth. Then, the plasmid was purified using a QIAGEN Tip 500 Plasmid DNA Purification Maxi-Kit (Hilden, Germany), as described by the manufacturer. The purified plasmid was then precipitated with ethanol.

The three parental parasite lines were transfected with the plasmid using an Amaxa Nucleofector electroporator (Basel, Switzerland) and its U-33 program. Briefly, 2 x 10^7 and 5 x 10^7 parasites, from the RH and Pru strains respectively, were harvested from the HFF cultures and resuspended in nucleofector solution supplemented with supplement 1 (electroporation buffer), placed into an electroporation cuvette, and the plasmid, also resuspended in the same electroporation buffer, was added to the cuvette. A higher number of parasites was needed for the Prugniaud strain since efficiency drops significantly compared to the RH strain, for reasons yet to be determined (Weiss and Kim 2007). After electroporation, parasites were inoculated onto fresh HFF flasks. The following day, chloramphenicol was added to the culture at a concentration of 20 μM to initiate selection (Kim, Soldati et al. 1993). Selection using chloramphenicol typically requires several *in vitro* passages since the drug has a delayed action; it targets the prokaryotic translation machinery within the mitochondrion in *T. gondii*, but it does not affect the first round of division, and acts upon the second cycle of host cell lysis.

At this point, the parasite lines consisted of heterogeneous populations. Therefore, populations were cloned by fluorescence activated cell sorting (FACS), sorting YFP-expressing or "bright" parasites into 96-well plates previously cultured with HFF monolayers (Figure 2.3A). Monitoring lysis plaques to ensure a single parasite was sorted into the well, the clones were observed by epifluorescence (Figure 2.3B). The brightest clones were kept and were

henceforth considered as the parental lines (RHΔΔ p*tub1* P30 YFP *sag1*-CAT-*sag1*, RHΔ*cpsII* p*tub1* P30 YFP *sag1*-CAT-*sag1*, and PruΔ p*tub1* P30 YFP *sag1*-CAT-*sag1*), to be used for insertional mutagenesis.

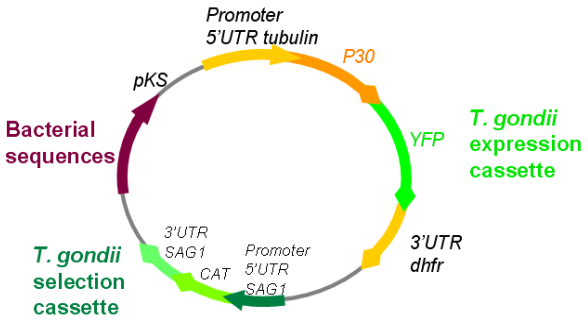

Figure 2.2: The p*tub1* P30 YFP *sag1*-CAT-*sag1* plasmid. This schematic representation of the p*tub1* P30 YFP *sag1*-CAT-*sag1* plasmid used to engineer the three parental lines depicts key features. The YFP reporter protein gene is in frame with the signal peptide from the P30 gene, which is under the control of 5'UTR (untranslated region) tubulin-α promoter. The CAT gene, flanked by the 5'UTR promoter and 3'UTR sequences from the *sag1* gene, confers resistance to chloramphenicol (CAP). The RHΔΔ, RHΔ*cpsII*, and PruΔ were all transfected with this plasmid by electroporation.

2.5. Host cell evaluation for the screen

Before proceeding to the mutagenesis and the phenotypic screening, the appropriate cell type had to be evaluated for its IFNγ-induced MHC-II surface expression. As mentioned before, three cell types were considered: RAW 264.7, BMMΦ, and BMDCs. These cell types were evaluated for their ability to expression surface MHC-II molecules upon IFNγ stimulation, a strong stimulation signal that has been shown to induce cell maturation in RAW 264.7 cells (St-Denis, Chano et al. 1998) (Lang, Algner et al. 2006) and bone marrow-derived pAPCs (McKee, Dzierszinski et al. 2004) (Hardy, Diallo et al. 2009). Of significant importance, the ability of parasites to infect each cell type without being phagocytosed and killed was also assessed.

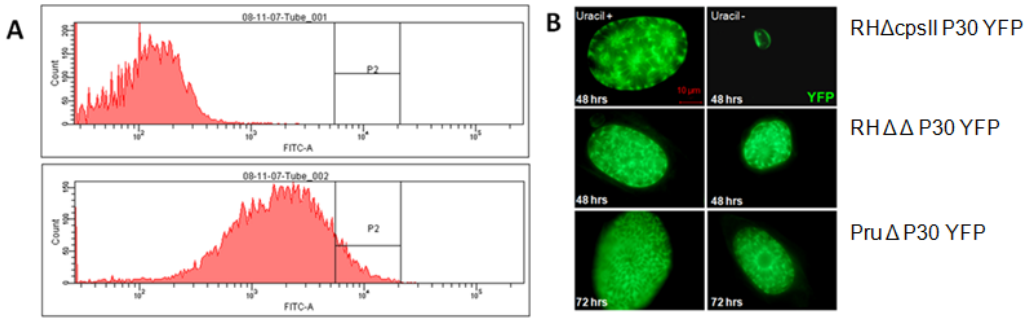

Figure 2.3: Cloning of the YFP-expressing parental lines. (A) Fluorescence profiles of negative control and transfected YFP-expressing parasites (top and bottom histograms, respectively) were assessed by flow cytometry. Parasites found within the defined gate (P2 box) were sorted into 96-well plates (one cell per well) in order to obtain clonal populations. The process was repeated for RHΔΔ P30 YFP and PruΔ P30 YFP parasites. Sorting of YFP^+ parasites was accomplished by utilizing a BD FACSAria cell sorter equipped with a 488-nm laser and a 515-545-nm filter (FITC); YFP is excited at 488 nm and emits at 535 nm. X axis represents fluorescence intensity, and Y axis represents cell count. (B) Transfected YFP^+ parasite clones were observed by epifluorescence. Cells were inoculated into 6-well plates containing confluent HFF cells on glass coverslips. Cells were incubated for 48 or 72 hours, as indicated, fixed with PFA 3.7%, and then observed under 100X oil-immersion with a FITC filter using a Nikon Eclipse E800. The panels show PVs filled with replicating parasites and secreting YFP into the PV. On the top left panel, the RH*ΔcpsII* P30 YFP parasites were grown in the presence of uracil in the medium, while parasites on the top right panel were deprived of uracil. This last feature was only carried out to make sure the strain was indeed uracil auxotroph. The three brightest clones were selected for RH*ΔcpsII* P30 YFP and Pru*Δ* P30 YFP, and six for the RH*ΔΔ* P30 YFP.

First, RAW 264.7 cells were considered and were stimulated with varying concentrations of IFNγ (10, 100, or 1000 U/ml), and fixed with 3.7% paraformaldehyde (PFA) every 2 hours from 2 to 12 hours, and every 4 hours from 12 to 24 hours after induction. Then, an immunofluorescent assay (IFA) was performed and the MHC-II molecules were immunolabeled using a primary rat anti-mouse-MHC-II (IA/IE) phycoerythrin (PE)-conjugated antibody (eBioscience, San Diego, CA), and a secondary donkey anti-rat IgG Alexa Fluor 594-conjugated antibody (Molecular Probes, Carlsbad, CA). Once labeled, the cells were observed by epifluorescence, and the time point and the stimulation factor concentration for which MHC-II labeling was the highest were determined (Figure 2.4). In addition, IFNγ-stimulated RAW 264.7 macrophages were labeled with an anti-MHC-II-PE antibody and analyzed by flow cytometry (data not shown). Repeated results obtained from the latter two experiments suggests that

stimulation with 100 U/ml IFNγ for 16 hours gave the strongest labeling, however only a fraction of the cell population (≤ 30%; data not shown), too low for the screen, was able to up-regulate surface MHC-II expression upon stimulation.

Hence, bone marrow-derived macrophages (BMMΦ) were tested similarly. MHC-II labeling upon IFNγ stimulation was greater and consistent (Figure 2.5), therefore this cell type was used to proceed onward to determine the ideal multiplicity of infection (MOI).

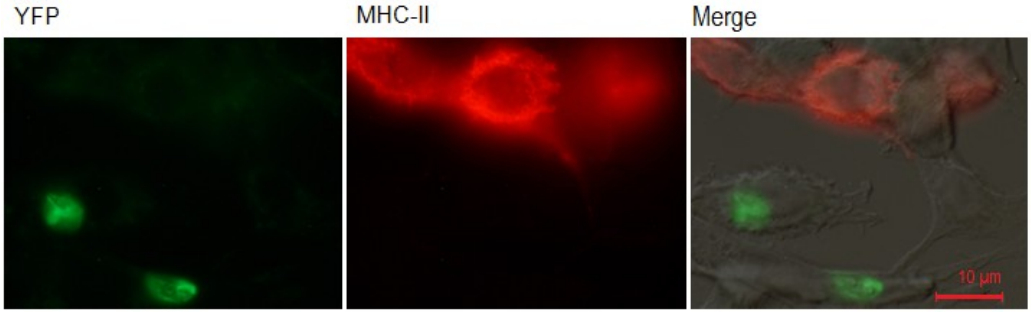

Figure 2.4: Inhibition of IFNγ-induced MHC-II expression in infected RAW 264.7 cells. RAW 264.7 macrophages were cultured on coverslips in 24-well plates (2 x 10^5 cells/well). Cells were infected with live RH*ΔcpsII P30 YFP* tachyzoites for 16 hours at an MOI of 1:1. Then, the cells were stimulated with 100 U/ml IFNγ for 24 hours, and fixed with 3.7% PFA. An IFA was performed; Fc receptors were blocked using mouse IgG antibodies, and MHC-II antibodies were labeled with a rat anti-mouse-IA/IE PE-conjugated antibody (primary) and a donkey anti-rat-IgG Alexa Fluor 594-conjugated antibody (secondary). Cells at the bottom of the above pictures (100X) were infected with YFP^+ parasites (one parasite per cell), while the top cells remained uninfected, the MHC-II molecules were labeled by the antibodies (PE + Alexa Fluor 594). Note that these uracil-auxotroph parasites were deprived from uracil and could not replicate. These observations confirm the fact that active invasion leads to an impaired MHC-II expression even upon stimulation, and also that parasite replication is not required.

As shown in Table 2.1, an MOI of 0.3 was suitable for the screen since infection rates were high enough and numbers of multiple infections were lower than at MOI 0.5 or 1. However, flow cytometry analysis revealed, as expected, that BMMΦ effector functions had a tendency to deteriorate PVs, and a small fraction of infected cells could still express MHC-II (data not shown). Thus, bone marrow-derived BMDCs were planned to be evaluated as host cells, since they are less phagocytic than macrophages and have less potent killing mechanisms.

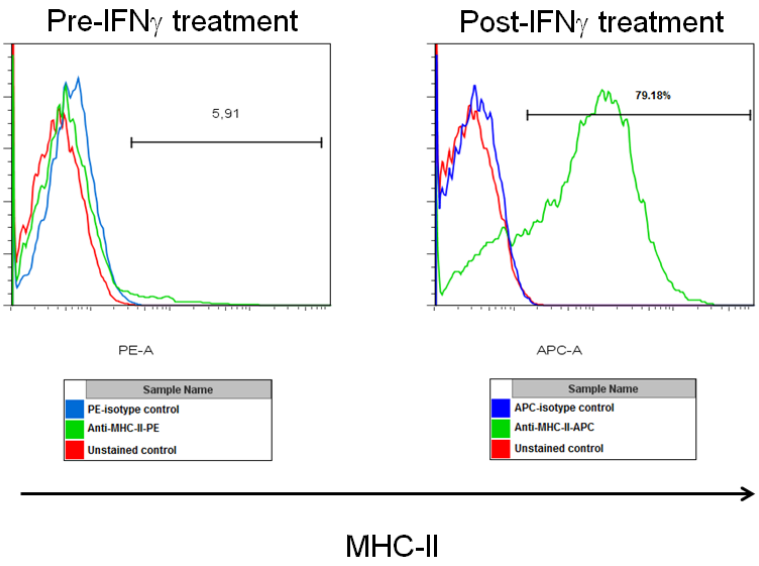

Figure 2.5: Flow cytometry analysis of IFNγ-induced MHC-II expression of BMMΦ. Cells were seeded in 6-well plates (5 x 10^6/well), stained with a rat anti-mouse-MHC-II-PE antibody (1 µl of 0.2 mg/ml stock solution per 10^6 cells) for 1 hour, then washed. Macrophages were stimulated with 100 U/ml IFNγ for 16 hours, and subsequently stained with a rat anti-mouse-MHC-II-APC antibody (1 µl of 0.2 mg/ml stock solution per 10^6 cells), fixed with PFA 3.7%, and analyzed by flow cytometry. Note that Fc receptors were blocked using mouse IgG antibodies and anti-mouse-CD16/32 antibodies before each staining. Results above indicate that around 6% of cells were already matured and their surface MHC-II molecules were stained with the PE-conjugated antibody. On the other hand, ~79% of cells were labeled for MHC-II following stimulation.

2.6. Insertional mutagenesis

Parasites from each clonal parental line would have been transfected with a second plasmid, pDHFR*-TSc3ABP-Kan/m2m3 (Figure 2.6A). This dihydrofolate reductase-thymidylate synthase (DHFR*-TS)-based plasmid was previously shown to integrate randomly into the genome by heterologous recombination at a very high frequency (Donald and Roos 1995) (Roos, Sullivan et al. 1997). It contains a kanamycin resistance gene (*Kan*^{R}) and a rare ABP (*Asc*I – *Bss*HII – *Pac*I) restriction enzyme site. These two key features would be extremely useful for subsequent steps, namely inverse PCR and plasmid rescue (see section 2.9 for details). Also, the DHFR*-TS plasmid contains two mutations, m2 (Ser^{36} → Arg) and m3 (Thr^{83} → Asn), that confer resistance to pyrimethamine (Reynolds and Roos 1998), which can be used as a drug selectable marker to select for successfully mutagenized clones (Donald and Roos 1995).

The plasmid was grown in DH5α *E. coli* bacteria, purified, and precipitated following the same protocol as previously described for the p*tub1* P30 YFP *sag1*-CAT-*sag1* plasmid (see section 2.4). However, the DHFR*-TS plasmid was linearized with *NotI* restriction enzyme to increase integration efficiency (Roos, Sullivan et al. 1997) (Figure 2.6B) before being stored until needed. Note that the genetic screen was not carried out beyond this point because we obtained parallel results that indicated the existence of a layer of interference with MHC-II at the post-translational level (as discussed in section 2.11); the subsequent steps that would have followed are nonetheless detailed in the following sections. Up to 2 x 10^7 parasites were to be transfected with 50 μg of linearized plasmid using an Amaxa electroporator. After the transfection, parasites would have been transferred to fresh HFF flasks containing culture media supplemented with 1 μM pyrimethamine and dialyzed FBS to initiate the selection process.

Strain	MOI	1 PV/cell (%)	2 PV/cell (%)	> 2 PV/cell (%)	Infected cells (%)
RHΔΔ P30 YFP	0.3	5.6	0.5	0	6.1
	0.5	12.9	1.4	0.5	14.8
	1	13	3	7	23
RHΔcpsII P30 YFP (+ uracil)	0.3	6.4	0	0	6.4
	0.5	11.2	1.1	0.5	12.8
	1	17.4	7.3	2.8	27.5
PruΔ P30 YFP	0.3	2.1	0.4	0	2.5
	0.5	3	2	1	6
	1	5.3	2.4	1.8	9.5

Table 2.1: Multiplicity of infection and number of parasitophorous vacuole per infected cell *in vitro*. BMMΦ were seeded in 24-well plates (5 x 10^5/well), and infected with either strain of parasites, RHΔΔ P30 YFP, RHΔcpsII P30 YFP, or PruΔ P30 YFP, at an MOI of either 0.3, 0.5, or 1 for 6 hours. Cells were then stimulated with 100 U/ml IFNγ for 16 hours. Cells were then fixed and mounted onto microscope slides. 200 cells were counted in different fields of each slide, and the number of PVs per infected cell was determined. An MOI of 0.3 seemed to give the fewest multiple-infected cells.

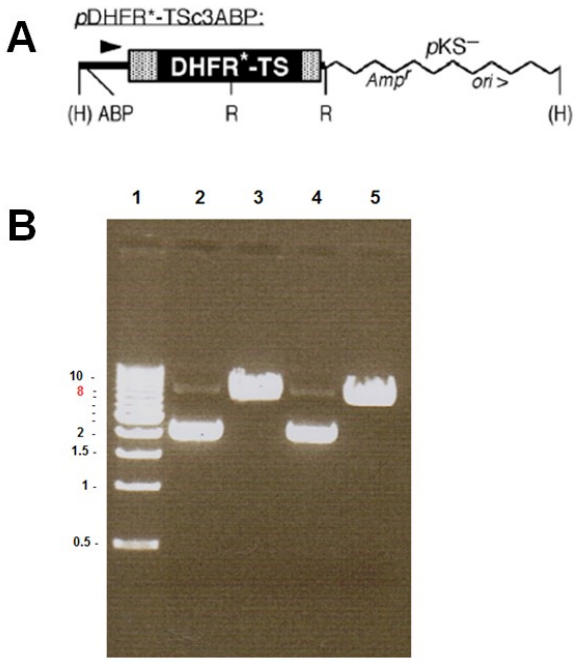

Figure 2.6: The pDHFR*-TSc3ABP-Kan/m2m3 plasmid. (A) The pDHFR*-TSc3ABP-Kan/m2m3 plasmid was planned to be used for the mutagenesis of the parental lines. Features include the DHFR-TS minigenes with two mutations (m2 and m3) that confers resistance to pyrimethamine, restriction sites H (*Hin*dIII), ABP (*Asc*I – *Bss*HII - *Pac*I polylinker), and R (*Eco*RI), and the bacterial vector sequence (*p*KS$^-$) that includes an ampicilin resistance gene (*Amp*^{r}) and a bacterial origin of replication (*ori*>) (Adapted from (Roos, Sullivan et al. 1997)). (B) The pDHFR*-TS plasmid was digested by adding the *Not*I restriction enzyme 1:20 (v/v) (supplemented with NEB3 buffer), and incubating overnight at 37°C. A small sample was taken from the mixture and ran on a 0.8% agarose gel. Lane 1 shows the 1 kb molecular weight maker, lane 2 the undigested plasmid (0.5 µg of DNA), and lane 3 the *Not*I-digested plasmid (1µg of DNA). The band in lane 2 represents super-coiled plasmid, and migrates further on the gel than the linearized plasmid in lane 3. Lanes 4 and 5 are duplicates of lanes 2 and 3.

2.7. Mutant library screening and flow cytometry

After the pyrimethamine-resistance selection process in HFF cells, mutant parasite would have been screened for the phenotype of interest, i.e. those that are unable to inhibit IFNγ-induced MHC-II expression. First, host cells (pAPCs) were to be stained with a rat anti-mouse-MHC-II (IA/IE) phycoerythrin (PE)-conjugated antibody before inoculation with the parasites. Phycoerythrin is a fluorochrome that absorbs and emits an orange-yellowish fluorescence at 488 and 575 nm, respectively, upon excitation typically with a He-Ne laser which can be used to sort cells using a fluorescence-activated cell sorter (FACS). After the first staining, cells were to be infected with the mutant library at a multiplicity of

infection (MOI) of 0.3, in other words three parasites for every ten host cells. As previously determined, this ratio would have minimized the frequency of multiple infections in a single cell. This latter scenario could have potentially complicated the screening process if multiple parasites harboring different mutations or mutants and wild-type parasites were to be found within the same cell, especially if one parasite has a dominant phenotype over the other mutants, some of which could have been of interest. Six hours post-infection, cells were to be treated with IFNγ and incubated for 16 hours. Following stimulation, cells were to be stained with a rat anti-mouse-MHC-II (IA/IE) antibody conjugated to allophycocyanin (APC). Allophycocyanin is another fluorochrome that has an absorption wavelength of 650 nm and an emission maximum of approximately 660 nm, emitting far-red light. The use of two different fluorochromes or colors is crucial for this sort. The first PE-conjugated antibody would monitor MHC-II expression before infection and detect cells that have already matured before the infection and stimulation. On the other hand, the second APC-conjugated antibody would bind to newly expressed surface MHC-II molecules. Once stained, cells were to be sorted by FACS; several phenotypes would have been expected.

- Cells stained with both PE- and APC-conjugated antibodies which would have corresponded to cells that would have matured before the infection (PE-high) and synthesized new MHC-II molecules (APC-high). These cells could either be infected (YFP-positive) or uninfected (YFP-negative); infection after maturation does not cause a down-regulation of surface MHC-II (McKee, Dzierszinski et al. 2004). Therefore, these cells could not be used to screen for the desired phenotype, i.e. parasites that inhibit maturation, and would have been discarded.

- Cells stained with APC-conjugated antibodies (APC-high), but PE-low and YFP-negative would consist of immature cells that were not infected and were able to mature upon IFNγ stimulation. These cells would also have been discarded.

- YFP-positive, but APC-low cells would have represented cells that were infected with a wild-type parasites or mutants behaving like wild-type parasites with regard to their inhibitory abilities. The parasites would have been rejected.

- YFP-positive (infected), APC-high, but PE-low cells would have been the phenotype sought after. These cells would have been infected by mutant parasites (YFP-positive) that had invaded immature cells (PE-low), and that were unable to block IFNγ-induced maturation and newly expression of MHC-II (APC-high). Parasites from these cells would be sorted and cultured.

Parasites found inside cells displaying the desired phenotype (YFP-positive, PE-low, APC-high) would have been sorted, passaged into HFF fibroblast cells, and incubated for 2-3 days. Then, these parasites were to be harvested, and used for a second round of FACS, following the aforementioned protocol. Actually, several rounds of FACS sorting were planned to be performed to enrich for the desired mutants, and to avoid the possibility of missing the phenotype if it had turned out to be a rare event.

2.8. Cloning

Once mutant parasites exhibiting the desired phenotype would have been enriched, they would have been cloned by sorting one infected cell (YFP-positive) per well in a 96-well plate containing a confluent layer of HFF cells, similarly to the way the original YFP-expressing parental lines were cloned.

2.9. Plasmid rescue and inverse polymerase chain reaction (PCR)

At this point, clones exhibiting the sought phenotype would have been individually isolated, and the mutations they harbored would have needed to be

isolated. Two molecular techniques could have been used, namely plasmid rescue and/or inverse PCR (Roos, Sullivan et al. 1997).

Plasmid rescue consist of transforming bacteria with a restriction enzyme-digested parasite genomic DNA construct. Briefly, genomic DNA (gDNA) from each clone would be digested using a restriction enzyme that cuts once within the bacterial vector sequence (zigzag line in Figure 2.7) and once in the flanking genomic DNA (sites X). Several different restriction enzymes would have been tested, specifically *Eco*RI, *Hin*dIII, and *Asc*I – *Bss*HII – *Pac*I restriction enzymes, in order to obtain restriction fragments of appropriate sizes. Genomic material from both the parental lines and the mutants would have been collected and digested with each of these enzymes in parallel and would have been ran on Southern blot using a radiolabeled-DHFR*-TS cDNA as the hybridizing probe. Fragments of 3.5 to 15 kb on Southern blots are suitable for plasmid rescue in *E. coli*, therefore the restriction enzyme that would have yielded a band within these lengths corresponding to the insertion would have been chosen for genomic digestion. Once the gDNA would have been digested with the chosen restriction enzyme, it would have been ligated and circularized overnight. Since the bacterial vector sequence contains a kanamycin resistance gene (Kan^R), successfully transformed bacteria would have been selected by virtue of kanamycin selection. Also, the vector sequence contains a bacterial origin of replication sequence (*ori*) which allows bacteria to generate numerous copies of the plasmid. Using primers specific for the bacterial vector, the gDNA sequence could have been amplified and sequenced.

Inverse PCR is an alternative technique that also uses restriction enzymes (Roos, Sullivan et al. 1997). Here, the restriction enzyme is chosen to cut once within the mutagenesis plasmid and once in the flanking gDNA (sites Y in Figure 2.7). Similarly, Southern blot analysis would have helped determining which restriction enzyme to use. The resulting fragments would have been ligated and circularized. Subsequently, PCR would have been carried out using primers of

opposite directions, indicated by the two arrows in Figure 2.7. The PCR products would have then been sequenced.

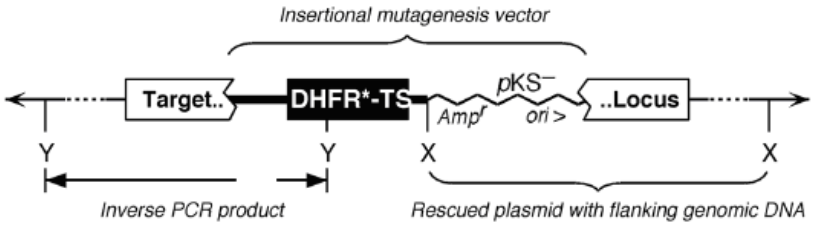

Figure 2.7: Schematic of a single-copy insertion of the DHFR*-TS plasmid within a gene. Upon insertion, the insertional mutagenesis vector may disrupt a gene or a regulatory sequence within the *T. gondii* genome. To obtain information on the disrupted gene locus and its flanking genomic sequence, two techniques can be performed, inverse PCR and plasmid rescue. In both cases, restriction enzymes are used to cut once in the flanking genomic sequence, and once in the DHFR*-TS minigenes (inverse PCR; sites Y) or at the linkage site between the DHFR*-TS minigenes and the bacterial vector (plasmid rescue; sites X) (adapted from (Donald and Roos 1995)).

2.10. Database mining

Once the disrupted genomic loci would have been identified and sequenced after rescue, a thorough analysis was to be carried out by referring to the different databases available. One of the most powerful tools currently available is the *Toxoplasma gondii* database (ToxoDB; http://toxodb.org) (Kissinger, Gajria et al. 2003) (Gajria, Bahl et al. 2008). ToxoDB offers the full genome sequence and annotations on the *T. gondii* ME49 strain, the genomic sequence of the GT1, VEF, and RH strains, as well as the apicoplast genome. One can browse annotations on ESTs, TIGR Gene Indices clustered ESTs, SAGE tags, SNPs, cosmid and BAC ends, microarray and proteomics studies, and use more than 40 query tools to analyze data (Gajria, Bahl et al. 2008). Furthermore, this database provides predictions according to various algorithms for open reading frames (ORFs), protein predictions, Gene Ontology function predictions, and BLAST similarities to the NCBI non-redundant protein database. With these numerous features, computational analysis of our findings would have certainly yield interesting information on *T. gondii* genes. Moreover, it would have been possible to extent these findings to other species by using such algorithms as

OrthoMCL based on orthology. Using OrthoMCL, genes from *T. gondii* were grouped with orthologous genes from 86 other eukaryotic and prokaryotic genomes (Chen, Mackey et al. 2006).

2.11. Discussion

Although powerful, the forward genetic screen elaborated above could have presented some shortcomings. For instance, *T. gondii* tachyzoites are haploid. Therefore, insertional mutagenesis could have potentially disrupted essential non-redundant genes, which would have led to a deleterious phenotype. If the genes involved in the inhibition of antigen presentation are somehow linked to essential functions within the conditions of the screen, they would not have been detected. Alternatively, a reverse genetics approach could have been better suited to study this type of genes, whereby genes suspected to be involved in antigen presentation inhibition would be disrupted by targeted insertional mutagenesis by homologous recombination. Targeted homologous recombination can be successfully achieved in *Toxoplasma*; it has been demonstrated with the use of vectors derived from the dihydrofolate reductase-thymidylate synthase (DHFR*-TS) (Donald and Roos 1994) and the uracil phosphoribosyltransferase (UPRT) (Donald and Roos 1995) cDNA with over 8 kb of contiguous genomic sequence. However, such an approach would require knowledge as to which genes, or at the very least a set of predetermined candidate genes, to target for disruption.

Recently, a system exploiting the use of the KU80 knock-out strain, which lacks the KU80 protein involved in nonhomologous end-joining DNA repair pathway, has rendered targeted gene deletion through homologous recombination highly efficient (greater than 97%) (Fox, Ristuccia et al. 2009). This last system was exploited to generate specific knock-out strains lacking various secreted proteins and enzymes which were tested, as detailed in the following chapters.

Regardless, if the MHC-II inhibition phenotype is due to a multi-gene effect, two possibilities could have arisen from this screen. First, gene products could act as a complex, in which case disruption of one gene would have deprived the complex from one subunit, and plausibly have led to an altered phenotype. Second, proteins encoded by these genes could be part of a cascade where they act sequentially. Hence, deletion of one gene could have blocked one of the steps and have disrupted the entire pathway, unless redundant gene functions are present and could have rescued the phenotype.

The genetic screen was not carried out beyond the linearization of the mutagenesis plasmid due to several reasons. First, biochemical analyses were being carried out in parallel to the screen giving promising results at a faster pace, and given the time frame of my doctoral thesis, this alternative approach was pursued further. Ultimately, this second approach allowed our group to conceive the first manuscript, described in Chapter 3. Second, subsequent observations revealed that *T. gondii* interferes with MHC-II antigen presentation at multiple levels, both transcriptional and post-translational, as discussed in the following chapters. It is foreseeable that although a mutant that would be unable to inhibit MHC-II expression could be isolated, the presentation of parasite-derived antigens in an MHC-II-restricted fashion could still be blocked by a post-translational mechanism involving host immune effectors of the endocytic pathway, thoroughly detailed in Chapter 4. Furthermore, intracellular MHC-II molecules could not have been detected by flow cytometry since only surface molecules could have been analyzed on live cells during the screening process of the mutants since fixation and permeabilization are required to stained for intracellular molecules with fluorescently-labelled antibodies. One could imagine that although being able to block surface expression of MHC-II molecules, some mutants might have been unable to inhibit synthesis of MHC-II, while interfering with trafficking of the molecules to the surface. Hence, potentially interesting mutants might have been overlooked given this experimental limitation.

Connecting Statement 1

Although the forward genetic screening was initially a legitimate strategy to identify the genes encoding for the inhibitory parasite molecules, an alternative approach exploiting various biochemical techniques was successfully undertaken to further characterize the nature of the inhibitory activity on MHC-II expression. A previous study had shown that PBS-soluble *Toxoplasma* lysates could inhibit IFNγ-induced MHC-II up-regulation in RAW264.7 macrophages upon IFN-γ stimulation (Lang, Algner et al. 2006). Also, pre-treatment of these parasite lysates with pronase, a non-specific protease mixture comprised of various endopeptidases and exopeptidases, abrogated almost entirely the inhibitory activity, suggesting that the *T. gondii* molecules involved in MHC-II inhibition is of proteinaceous nature. However, in this study pronase was inactivated by boiling, and it is possible that parasite molecules were denatured. Therefore, it could not be definitively concluded that the molecules sought were proteins; they could also be lipids, lipoproteins, or glycoproteins. Another study showed that co-treatment of THP-1 cells, a human myelomonocytic cell line, with *T. gondii* lysates inhibited LPS-induced production of pro-inflammatory cytokines such as IL-12, IL-8 and TNFα (Lee, Heo et al. 2008). These studies demonstrated that parasite molecules can have some effect on MHC-II expression and the release of pro-inflammatory cytokines, thereby mimicking the inhibitory effects of live *T. gondii* infection to some extent. Keeping these observations in mind, it seemed possible to carry out biochemical methodologies to tease out, isolate, and then identify the inhibitory molecules.

The first step to this approach was to separate the lysate fraction that displayed inhibitory activity from the one that does not (i.e. PBS-soluble vs. insoluble). To determine the nature of the inhibitory molecules, a protease digestion using proteinase K, a broad-spectrum serine endopeptidase (Kraus, Kiltz et al. 1976), was performed on the lysate fraction that contains the MHC-II inhibitory activity. Instead of boiling the samples to inactivate the protease, Pefablock (4-(2-aminoethyl) benzenesulfonyl fluoride hydrochloride or AEBSF),

an irreversible serine protease inhibitor, was added to stop proteolysis. This method ensured that the lost of inhibitory activity was not due to heat-induced denaturing, but specifically to the degradation of proteins. Subsequent analyses revealed that proteins are likely candidates for the inhibitory activity.

Subcellular fractionation methods using continuous isopycnic Percoll density gradient centrifugation (PDG) followed by a sucrose gradient have been elaborated to isolate *Toxoplasma* apical organelles, namely micronemes, rhoptries, and dense granules (Leriche and Dubremetz 1991) (Foussard, Leriche et al. 1991) (Hehl, Lekutis et al. 2000) (Bradley, Ward et al. 2005). Isolation of rhoptries only is possible with this technique, but dense granules cannot be collected free of rhoptry contamination (Bradley, Ward et al. 2005). Isolation of whole organelles such as peroxisomes (Luers, Hartig et al. 1998) and immature secretory organelles (ISG) (Dittie, Klumperman et al. 1999) from animal tissues, and amyloplasts, chloroplasts and nuclei from plant cells (Kausch, Owen et al. 1999) by immunoprecipitation has been achieved. Unfortunately, this technique has yet to be successful in isolating whole organelles in apicomplexan parasites (Blackman and Bannister 2001). Fortunately, testing different fractions obtained from PDG gave important clues as to the subcellular origin of the inhibitory activity, most likely from rhoptries and/or dense granules.

As another source of parasite material, excreted-secreted antigens (ESA) were found to have inhibitory activity on MHC-II expression. Parasite ESA were initially recovered from culture supernatants of infected host cells *in vitro*, and were also found to be highly immunogenic during human and experimental toxoplasmosis (Darcy, Deslee et al. 1988). Active secretion of proteins by tachyzoites in host cell free media has been described by incubating freshly egressed parasites in media containing 10% mammalian serum at 37^{o}C. It was shown that ESA contain at least dense granule proteins (Coppens, Andries et al. 1999), yet the exact composition of ESA remains uncertain given the fact that this protocol includes mammalian proteins as well, complicating the proteomic analysis. However, our results show that serum does not appear to be required to

trigger release of some ESA into the medium by extracellular tachyzoites. Since we hypothesized that the inhibitory molecules may originate from secreted organelles and that ESA displayed inhibitory activity, we used this source of parasite material to perform a two-step fractionation using ion exchange chromatography followed by size-exclusion chromatography. The fractions having the highest inhibitory effect on BMMΦ were analyzed by tandem mass spectrometry and database mining, ultimately allowing us to draw a list of possible inhibitory molecule candidates originating from secretory organelles.

In the following chapter, we discuss these biochemical analyses that were carried out in an attempt to identify these elusive *Toxoplasma gondii* molecules and list a number of potential candidates.

Chapter 3. Manuscript I

Title:

Excreted-secreted antigens from *Toxoplasma gondii* secretory organelles inhibit interferon gamma-mediated MHC-II up-regulation in bone marrow-derived macrophages

Authors and Affiliations:

Louis-Philippe Leroux*, Dayal Dasanayake*, Manami Nishi[¶], Barbara A. Fox[#], David J. Bzik[#], Armando Jardim*[§], Florence S. Dzierszinski*[¤§]

*Institute of Parasitology, McGill University, Sainte-Anne-de-Bellevue, Québec, Canada

[¶]Indiana University, Indianapolis, Indiana, USA

[#]Dartmouth Medical School, Lebanon, New Hampshire, USA

[¤]Carleton University, Ottawa, Ontario, Canada

[§]Corresponding authors

3.1. Abstract

The obligate intracellular protozoan parasite *Toxoplasma gondii* interferes with MHC-II antigen presentation to dampen the $CD4^+$ T cell response in order to gain a head start on the host adaptive immune response. Although it was clearly established that *T. gondii* inhibits MHC-II gene transcription and that MHC-II molecule levels remain low in infected host cells, the causative inhibitory molecule(s) has (have) yet to be identified. In this present study, we show that the inhibitory activity segregated to the high-speed supernatant (HSS) prepared from sonicated parasite lysates, and was enriched with increasing centrifugal speeds. The inhibitory activity was found to be of proteinaceous nature since it was protein dose-dependent and was completely lost after treating the HSS with a broad-spectrum protease. Subcellular fractionation using a Percoll gradient revealed that the inhibitory activity is likely found in rhoptries (ROP) and/or dense granules (GRA), even though several ROP and GRA knock-out strains were still able to inhibit MHC-II expression during live infection. In addition, excreted-secreted antigens (ESA) from extracellular tachyzoites displayed inhibitory activity, and the proteins obtained from a two-step fractionation of the ESA material using ion exchange chromatography followed by size-exclusion chromatography were analyzed by tandem mass spectrometry generating a list of possible inhibitory molecule candidates originating from secretory organelles.

3.2. Introduction

Toxoplasma gondii is a highly ubiquitous obligate intracellular protozoan parasite that is able to infect virtually any warm-blooded vertebrate, including humans and mice (Frenkel, Dubey et al. 1970), (Dubey, Miller et al. 1970). During the acute phase of the infection, rapidly-dividing tachyzoites can actively invade any nucleated cell, including cells of the immune system, while disseminating throughout the host (Dubey 2004). Within the infected host cell, the parasite resides and replicates asexually in a non-fusogenic parasitophorous

vacuole (PV). As the adaptive immune response retaliates soon after the start of the infection, tachyzoites convert to slowly-dividing bradyzoites and eventually, these latter will encyst in immune privileged sites such as the brain and muscle tissues as early as 6 to 9 days post-infection (Dubey, Speer et al. 1997). In a healthy individual with an intact immune system, toxoplasmosis is generally asymptomatic and encysted parasites can remain dormant for the remainder of the host's life. However, congenital toxoplasmosis poses serious threats to the fetus of pregnant women, and can have deleterious effects such as blindness, chorioretinitis, hydrocephaly, and even mental retardation (Montoya and Remington 2008). In addition, spontaneous reactivation of encysted parasites can occur in immunosuppressed individuals such as in the case of AIDS patients, individuals receiving chemotherapy against cancer or immunosuppressive drugs during organ transplant, or elderly people with an aging immune system (Dubey 2004), (Luft and Remington 1992).

The immune response mounted against toxoplasmosis is characterized by a strong Th1-type response, eliciting both parasite-specific $CD4^+$ and $CD8^+$ T lymphocyte populations to produce IFNγ, the key inflammatory cytokine that provides protective immunity (Gazzinelli, Hakim et al. 1991), (Suzuki, Orellana et al. 1988), (Denkers and Gazzinelli 1998). Despite the robust immune response mounted against *T. gondii*, the parasite is still able to encyst and thereby establish a chronic infection, partly by subverting some of the immune mechanisms early on in the infection, such as inhibition of pro-inflammatory signaling cascades (NF-κB (Shapira, Harb et al. 2005) (Rosowski, Lu et al. 2011), MAPK (Kim, Butcher et al. 2004), STAT1 (Zimmermann, Murray et al. 2006) (Lang, Hildebrandt et al. 2012) (Stutz, Kessler et al. 2012), CIITA (Luder, Lang et al. 2003)), and induction of the anti-inflammatory STAT3/6-mediated transcription (Butcher, Kim et al. 2005) (Ong, Reese et al. 2010) (Jensen, Wang et al. 2011). Notably, the parasite is able to delay and dampen the development of $CD4^+$ T helper cell response, which is required to generate protective $CD8^+$ T cell effector activity (Gazzinelli, Hakim et al. 1991), (Gazzinelli, Xu et al. 1992).

Priming and activation of $CD4^+$ T cells require antigens to be processed and presented in the context of major histocompatibility complex class II (MHC-II) molecules (Janeway 2001). MHC-II molecules are synthesized in the endoplasmic reticulum (ER) and associate with the associated invariant chain (Ii or CD74) chaperone to form a pentameric complex, guiding correct assembly of MHC-II α and β chains and preventing non-specific binding of self-peptides to nascent MHC-II molecules (Koch, Zacharias et al. 2011). Professional antigen presenting cells (pAPCs), which include macrophages, dendritic cells, and B cells, readily express these proteins following pro-inflammatory stimulation (Hudson and Ploegh 2002). With the help of the invariant chain's di-leucine sorting motifs, Ii-MHC-II complexes traffic either to the cell surface as immature complexes or directly to the endocytic pathway (Pieters, Bakke et al. 1993), (Odorizzi, Trowbridge et al. 1994). Within maturing and acidifying endosomal compartments, resident proteases, namely legumain and cathepsins, cleave antigens to yield small antigenic peptides. These proteases also cleave the invariant chain until only the class II-associated invariant chain peptide (CLIP) is left in the MHC-II groove (Hsing and Rudensky 2005). This short peptide is displaced by an MHC-II-like molecule called H2-DM (or HLA-DM in humans) and replaced by a higher affinity antigenic peptide, a process referred to as the loading of MHC-II molecules. Ultimately, these mature peptide-loaded MHC-II molecules (pMHC-II) make their way to the cell surface to be presented to $CD4^+$ T cell bearing a cognate receptor (TCR).

Previous studies have clearly demonstrated that *Toxoplasma gondii* interferes with antigen presentation in the context of MHC-II (Luder, Lang et al. 1998) (Luder, Walter et al. 2001) (McKee, Dzierszinski et al. 2004), partly by inhibiting transcription of MHC-II and other related genes in infected cells (Luder, Lang et al. 2003) (Lang, Algner et al. 2006). Furthermore, it was shown that lysates can partially mimic the inhibitory effects of live parasites on the expression of MHC-II (Lang, Algner et al. 2006); however, the molecule(s) that directly inhibit MHC-II expression has (have) yet to be identified. On the other hand, molecules that inhibit MHC-II expression and maturation have been

successfully identified in some protozoan and filarial parasites, as well as pathogenic bacteria. Some of these molecules interfere with MHC-II transcription by either directly degrading transcription factors, such as the *Chlamydia* CPAF (Zhong, Fan et al. 1999), (Zhong, Fan et al. 2001), (Fan, Dong et al. 2002) and the *Leishmania* CPB cysteine proteases (Cameron, McGachy et al. 2004), or by interfering with upstream signaling pathways and chromatin remodeling like the *Mycobacterium tuberculosis* LpqH lipoprotein (Pennini, Pai et al. 2006). Alternatively, other inhibitory molecules target MHC-II trafficking through the endocytic pathway, antigen processing and loading onto MHC-II molecules, while others even degrade MHC-II molecules themselves. Such molecules include the *Brugia malayi* Bm-CPI-1 and 2 cystatins (Manoury, Gregory et al. 2001), the *Helicobacter pylori* VacA (Molinari, Salio et al. 1998) and *Salmonella enterica* SifA (Mitchell, Mastroeni et al. 2004) secreted effector proteins, and the *Leishmania* CPB proteases (De Souza Leao, Lang et al. 1995), (Courret, Frehel et al. 2001).

In the case of *T. gondii*, no such molecule with MHC-II inhibitory activity has been clearly identified, even though several secreted molecules have been shown to have immunomodulatory properties in infected cells, such as ROP16 (Saeij, Coller et al. 2007) and 18 (Fentress, Behnke et al. 2010) (Steinfeldt, Konen-Waisman et al. 2010) (Niedelman, Gold et al. 2012), and GRA15 (Rosowski, Lu et al. 2011). In this present study, we show that the inhibitory activity is caused by a protein(s) originating from the parasite's secretory organelles, most likely the rhoptries or dense granules. Furthermore, by using several different protein fractionation techniques, we were able to narrow down the possibilities to a short list of protein candidates, adding to the plethora of molecules the parasite utilizes to subvert host functions to its own advantage.

3.3. Materials and Methods

3.3.1. Mice

Four to 6-week old wild-type C57BL/6 mice were purchased from Charles River Laboratory (Wilmington, MA) or alternatively bred in-house, and housed and maintained according to the McGill University Animal Care Committee (Permit AUC #5380).

3.3.2. Parasites and Host Cell Cultures

Type I virulent *T. gondii* tachyzoite cultures of the RH strain, wild-type (WT) and transgenic lines, were maintained by serial passage in human foreskin fibroblasts (HFF) (ATCC, Manassas, VA), as previously described (Roos, Donald et al. 1994). Transgenic parasite clonal lines were engineered to express yellow fluorescent protein (YFP) secreted in the parasitophorous vacuole (PV). The *ptub*P30-YFP/*sag*CAT plasmid was previously described (McKee, Dzierszinski et al. 2004). The various rhoptry (ROP1, 4/7, 14, 16, and 18) and dense granule (GRA2, 3, 5, 6, 7, 8, 9, and 12) *T. gondii* knock-out strains were generated using the KU80 system as previously described (Fox, Ristuccia et al. 2009).

Bone marrow-derived macrophages (BMMΦ), were obtained by differentiating precursor cells from murine bone marrow (Weischenfeldt and Porse 2008). Briefly, mice were euthanized by CO_2 asphyxiation, and hind legs were collected in DMEM. Marrow was flushed out of bones, and live precursor cells were counted using trypan blue exclusion staining. To generate macrophages, 5 x 10^6 precursor cells were resuspended in culture medium (Dulbecco's modified Eagle's medium, 10% FBS, 2 mM L-glutamate, 1,000 U/ml penicillin, 1,000 µg/ml streptomycin, 50 µg/ml gentamicin, 2.5% HEPES, 55µM beta-mercaptoethanol, 1 mM sodium pyruvate (Wisent, St-Bruno, Quebec, Canada)) supplemented with 30% L929 fibroblast supernatant (containing G-CSF), and cells were seeded in tissue culture-treated Petri dishes. Medium was

changed three days later. Differentiated macrophages were used after 8 days for the assays.

3.3.3. Parasite whole and high-speed supernatant (HSS) lysates, and bicinchoninic acid (BCA) assay for protein quantification

T. gondii whole lysates were prepared from 2-5 x 10^9 freshly lysed-out tachyzoites. Parasites were resuspended in ice-cold phosphate buffered saline (PBS), and subjected to three 5 minute-cycles of freeze-thaw from liquid nitrogen (N_2) to a 37°C water bath. Then, parasites were sonicated on ice for 10 minutes, with one-second pulses at 30% duty cycle using a Sonic Dismembrator 500 (Fisher, Pittsburgh, PA). Protein concentrations were determined by the bicinchoninic acid (BCA) assay (Pierce, Rockford, IL), according to the manufacturer's specification, with Triton X-100 0.1% added to the working reagents. Protein concentration was adjusted to 2.5 mg/ml and aliquots were stored at -80°C. High-speed supernatant (HSS) lysates were prepared similarly, but following sonication, the lysates were sequentially centrifuged at 20,000, 40,000, 60,000, and 100,000 *x g* for 30 minutes at 4°C using a fixed angle TLA-100.3 rotor (Beckman Coulter, Brea, CA). The supernatant fraction was removed and the pellet fraction was resuspended in an equal volume of PBS. Protein concentrations were determined as described above for both fractions, and aliquots were stored at -80°C.

3.3.4. Subcellular fractionation

Subcellular fractionation was carried out as essentially described (Leriche and Dubremetz 1991) (Hehl, Lekutis et al. 2000) (Bradley, Ward et al. 2005). Fractionation was performed using 5 x 10^9-10^{10} freshly lysed out *T. gondii* RHΔΔ *ptub*P30-YFP tachyzoites. Parasites were resuspended in ice cold SMDE buffer (250 mM sucrose, 10 mM 3-(N-morpholino)propanesulfonic acid (MOPS), 2 mM

dithiothreitol (DTT), 1 mM ethylenediaminetetraacetic acid (EDTA), pH 7.2-7.4) at a concentration of 5 x 10^8 parasites/ml. Parasites were disrupted at 7,000 psi using a Stansted cell homogenizer (Harlow, Essex, UK). Homogenates was clarifiedat 1,300 *x g* for 20 minutes at 4°C to pellet intact parasites. The supernatant fraction was spun at 25,000 *x g* for 24 minutes at 4°C in an SW 28 Ti rotor (Beckman Coulter) to obtain a high speed organellar pellet. The pellet was resuspended in 30% Percoll in SMDE buffer and spun at 61,500 *x g* for 25 minutes at 4°C using a fixed angle 70.1 Ti rotor (Beckman Coulter) to generate a gradient. Fourteen fractions of about 0.7 ml were collected from the bottom and labelled from the bottom up. Each fraction was spun at 100,000 *x g* for 90 minutes to remove Percoll, and organellar material was collected, transferred to a new tube, resuspended in PBS, and sonicated on ice at 30% duty cycle for 5 min, with one second pulses. Protein concentration was determined, and fractions were stored at -80°C.

3.3.5. Excreted-secreted antigens (ESA) production

Large scale ESA production was performed using freshly egressed RH WT tachyzoites, filtered using 3 µm-pore polycarbonate filters (Millipore, Billerica, MA) washed in PBS. Parasites were resuspended in DMEM at a concentration of 1 x 10^9 tachyzoites/ml in 50 ml conical tube and incubated at 37°C with shaking (150 RPM) for 3 h. Cultures were cooled to 20°C and parasites removed by centrifugation at 2,000 *x g* for 15 min at 4°C. The supernatant was removed and centrifuged at 10,000 *x g* for 10 min to remove residual cells. This supernatant containing parasite-free ESA material was concentrated using 3 kDa MWCO centrifugal filters (Millipore) at 14,000 *x g* and used immediately or stored at -80°C.

3.3.6. Testing parasite viability

Tachyzoites were resuspended as described for ESA production. A 10 µl sample of cell suspension was mixed with a 500 µL solution of DMEM containing 10 µg/ml propidium iodide (PI) (EMD Chemicals, Gibbstown, NJ) and after a 5 minute incubation at 20°C the sample was analyzed by flow cytometry to quantify dead parasites. A similar 10 µl aliquot of parasites was taken after ESA production (3 h later), treated and analyzed to assess parasite viability during ESA production.

3.3.7. MHC-II inhibition assay

Day 7 bone marrow-derived macrophages (BMMΦ) were plated at 3 x 10^5 cells per well in 24 well-plates, and incubated overnight to allow cells to adhere. On the following day, cells were inoculated with freshly harvested *T. gondii* tachyzoites at a multiplicity of infection (MOI) of 3:1. When required for flow cytometry analysis, parasites were stained with 20 µM CellTracker Green CMFDA (5-chloromethylfluorescein diacetate) or CellTrace Far Red DDAO-SE (Molecular Probes, Carlsbad, CA) in DMEM for 30 min at 20°C before inoculating the macrophages. *T. gondii* lysates were diluted to a final concentration of 200 µg/ml or as otherwise indicated in culture medium, while subcellular fractions were diluted to 150 µg/ml, while crude ESA, and ESA fractions were tested at constant volumes. After inoculation and addition of lysates or subcellular fractions, cells were incubated for 2-6 h, then interferon gamma (IFNγ) was added to a final concentration of 100 U/ml (BioSource, Carlsbad, CA) and cultures were incubated for 18-20 h.

3.3.8 Flow cytometry analysis

MHC-II expression by BMMΦ was determined by flow cytometry using a BD FACSAria and analyzed with FACSDiva software (BD Biosciences, Franklin

Lakers, NJ). First, Fc receptors were blocked by adding rat IgG and rat anti-mouse CD16/32 (Fcγ III/II) (clone 2.4G2) (BD Biosciences) for 15 min on ice. After blocking, cells were stained with allophycocyanin (APC)- or phycoerythrin (PE)-conjugated anti-IA/IE (MHC-II) antibodies (clone M5/114.15.2) (eBioscience, San Diego, CA). For intracellular staining, cells were first fixed in 1% paraformaldehyde (PFA) for 10 min on ice, and then the fixative agent was quenched by adding 0.1 M glycine PBS, and the cells were resuspended in permeabilization buffer (0.05% saponin, 0.1% BSA in PBS) for 20 min on ice. After permeabilization, cells were stained using the above mentioned antibodies, washed then fixed again with 1% PFA and analyzed by flow cytometry. Flow cytometry data was analyzed using FlowJo software (Tree Star, Ashland, OR).

3.3.9. Western blotting and silver staining

Subcellular fractions were precipitated in acetone at -20°C for 1 h and the protein pellet was resuspended in SDS-PAGE buffer with or without beta-mercaptoethanol (reducing and non-reducing conditions, respectively). Samples were boiled for 5 min, and then loaded onto a 10% resolving SDS-PAGE gel. Proteins were transferred to nitrocellulose membranes and blocked in 5% dry skim milk in TTBS (Tris-HCl 15 mM, NaCl 140 mM, Tween 20 0.05%) overnight at 4°C. Reduced samples were probed with a rabbit anti-GFP, followed by a goat anti-rabbit-HRP antibody (Bio-Rad, Hercules, CA), while non-reduced samples were probed with a mouse anti-ROP2,3,4 and a mouse anti-SAG1 antibodies (kind gifts from Jean-François Dubremetz, University of Montpellier, France), followed by a rabbit anti-mouse IgG-HRP (Bio-Rad). Membranes were developed using the Amersham ECL kit (GE Healthcare, Fairfield, CT). ESA and lysates samples were resolved by SDS-PAGE under reducing conditions as described above. Membranes were probed with murine anti-MIC2, GRA3, and ROP2,3,4 primary antibodies (1:200) and a rabbit anti-mouse secondary antibody (1:8000).

Proteins on an SDS-PAGE gel were visualized using a modified version of Blum's silver staining protocol (Blum, Beier et al. 1987). Briefly, the gel was fixed overnight in a fixative solution (10% v/v acetic acid, 30% v/v ethanol), rinsed in 20% v/v ethanol for 20 min, and then in deionized water for 10 minutes, soaked in sensitizer solution (0.02% w/v sodium thiosulfate) for 1 minute, and rinsed in deionized water for 20 seconds and repeated three times. The gel was then soaked in 0.02% w/v silver nitrate for 45 min followed by a rinse with deionized water for 10 seconds. The bands were developed in developer solution (0.3% w/v sodium carbonate, 0.025% v/v formaldehyde, 0.001% w/v sodium thiosulfate) until they were sufficiently visible. Finally, the gel was soaked in stop solution (0.4 M Tris, 2.5% v/v acetic acid) for 5 min and stored in deionized water.

3.3.10. Size-exclusion chromatography

The sample to be injected was in Dulbecco's PBS (DPBS) pH 7.5. 200-250 µl of concentrated soluble material was injected onto a Superose-12 column (Amersham Pharmacia, Pittsburgh, PA) equilibrated with DPBS pH 7.5. The column was developed using a Beckmann Coulter System Gold solvent module with a flow rate of 0.5 ml/min. Fractions of 1 ml were collected every 2 min unless otherwise stated.

3.3.11. Ion-exchange chromatography

The sample to be injected was concentrated and washed multiple times with 50 mM Tris-HCl buffer pH 7.5. The sample was then injected onto a MonoQ (Pharmacia) column pre-equilibrated against the same buffer. Up to 2 ml of concentrated material was injected depending on necessity and the unbound material was collected. A linear gradient from 0 to 1 M NaCl in 50 mM Tris-HCl

pH 7.5 over a period of 1 h was used for anion exchange. The flow rate was set at 0.5 ml/min and fractions were collected every 2 min (1 ml each).

3.3.12. Mass spectrometry (LC-MS/MS) and identification of candidate proteins

Tris(2-carboxyethyl)phosphine (TCEP) was added to the protein samples in PBS to reach a final concentration of 5 mM. Samples were incubated at 37°C at 650 rpm for 30 minutes. 1 µg of trypsin was added and the samples were digested overnight at 37°C. The following day, the samples were dried down in a Speed Vac and resolubilized in 50 µl of 5% acetonitrile (ACN) and 0.2% formic acid (FA). 20 µl of each sample was injected onto a C18 pre-column (0.3 mm i.d. x 5 mm) and peptides were separated on a C18 analytical column (150 µm i.d. x 100 mm) using an Eksigent nanoLC-2D system. A 76-min gradient from 10–60% A/B (A: 0.2% formic acid, B: acetonitrile and 0.2% formic acid) was used to elute peptides with a flow rate set at 600 nl/min.

The liquid chromatography (LC) system was coupled to an LTQ-Orbitrap mass spectrometer (Thermo Fisher). Each full MS spectrum was followed by three MS/MS spectra (four scan events), where the three most abundant multiply charged ions were selected for MS/MS sequencing. Tandem MS experiments were performed using collision-induced dissociation in the linear ion trap. The data were processed using the Mascot 2.2 search engine (Matrix Science). The selected variable modifications were carbamidomethyl, deamidation, oxidation and phosphorylation. Database mining was carried out with the tandem mass spectra against the *Toxoplasma gondii* GT1 protein database (v7.2) available on toxodb (http://toxodb.org) to obtain candidates.

3.4. Results

3.4.1. The MHC-II inhibitory activity is found in the high-speed supernatant prepared from sonicated whole-parasite lysates, and is enriched with increasing centrifugal speeds

In an attempt to isolate the inhibitory molecules, we first needed to characterize the general biochemical properties of the inhibitory activity. As previously mentioned and shown here (Figure 3.1), lysates prepared from sonicated parasites mimicked the MHC-II inhibition observed with live parasites. Subjecting the lysates to different centrifugal speeds, from 20,000 to 100,000 *x g*, to separate insoluble material (i.e. pellet) from soluble and organelle associated molecules (i.e. high-speed supernatant or HSS), revealed that the inhibitory activity was enriched in the latter fraction, especially with higher centrifugal speeds (60,000 and 100,000 *x g*). Although the inhibition levels were not as high as those seen with live parasites, the lysates were still able to significantly inhibit IFNγ-induced MHC-II expression in bone marrow-derived macrophages, indicating that biochemically isolating the inhibitory molecules and observing a similar phenotype is possible.

3.4.2. The inhibition of MHC-II expression is dose-dependent and is protease-sensitive

Treating BMMΦ cultures with increasing protein doses of HSS lysates led to increased MHC-II inhibition (Figure 3.2A). However, the inhibition levels at the different protein concentration tested did not reach those observed in cells infected with live parasites. Considering the fact that HSS lysates also contained other biological molecules such as lipids from microbodies and nucleic acids, when macrophages were treated with increased concentration of proteins, as measured by the BCA assay, these cells were potentially exposed to increased doses of the former molecules. Therefore, the HSS lysates were treated with proteinase K, a broad-spectrum endopeptidase (Kraus, Kiltz et al. 1976), to digest

all proteins (Figure 3.2B). The inhibitory activity on MHC-II expression by proteinase K-treated HSS lysates was then compared to that observed using undigested lysates. Macrophages treated with undigested lysates displayed significantly lower MHC-II levels as well as cells infected with live parasites (Figure 3.2C). On the other hand, this inhibitory activity was completely lost in HSS lysates that were first treated with proteinase K prior to testing on macrophages. In fact, MHC-II levels in cells treated with digested lysates were almost identical to those of untreated control cultures. These observations strongly suggested that the inhibitory activity was associated with a molecule of a proteinaceous nature and correlates with previous reports (Lang, Algner et al. 2006) (Lee, Heo et al. 2008).

3.4.3. The inhibitory activity segregates to the rhoptry/dense granule-enriched subcellular fractions

Since several proteins originating from the secretory organelles have been shown to directly affect different immune-related pathways (Saeij, Coller et al. 2007) (Fentress, Behnke et al. 2010) (Steinfeldt, Konen-Waisman et al. 2010), (Rosowski, Lu et al. 2011) (Niedelman, Gold et al. 2012), we performed subcellular fractionation (Hehl, Lekutis et al. 2000), (Leriche and Dubremetz 1991), to isolate different organelles and to test these for MHC-II inhibitory activity. The inhibitory activity was greatest in the bottom three fractions, especially fraction 1 (F1) (Figure 3.3). Although the technique used to separate organelles and other cell structures yielded fractions with slightly mixed compositions, these experimental results revealed that fractions containing both rhoptries and dense granules had the highest inhibitory activity, lending credence to the possibility that molecules from the secretory organelles inhibit MHC-II expression. Also, the top-most fraction (F14) displayed more inhibition than the middle fractions (from F4 to F13). The matching Western blots suggest that this top fraction contained rhoptries, but also dense granules that could have floated to

the top of the gradient along with ghost parasites or remained attached to cellular membranes.

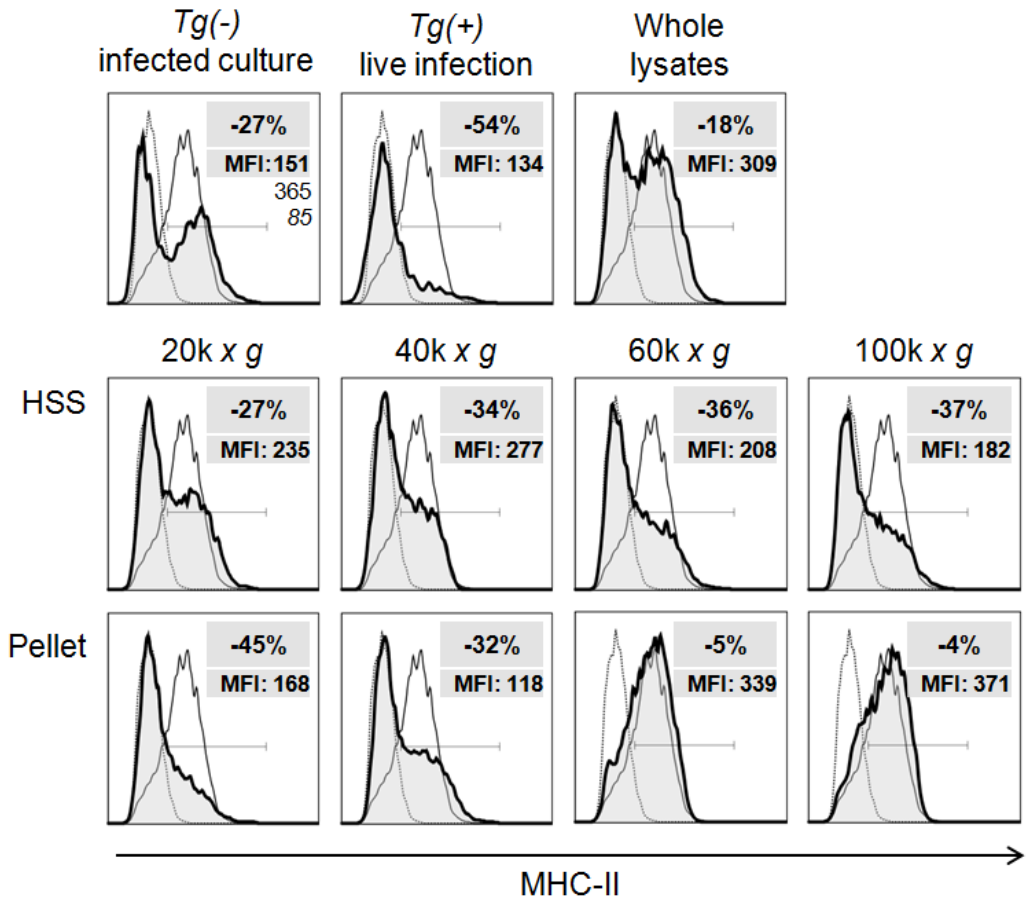

Figure 3.1: The MHC-II inhibitory activity is found in the high-speed supernatant prepared from sonicated whole-parasite lysates, and is enriched with increasing centrifugal speeds. BMMΦ cultures were treated with 200 μg/ml of either the high-speed supernatant (HSS) or the pellet obtained from centrifugation of sonicated parasites at different centrifugal speeds, ranging from 20k to 100k *x g* as indicated, incubated for 4 hours, stimulated with 100 U/ml IFNγ, and analyzed by flow cytometry for MHC-II expression. Alternatively, cells were infected with live parasites or treated with unseparated whole lysates (i.e not centrifugated). The analysis revealed that higher centrifugal speeds enriched the inhibitory activity in the HSS fraction. In fact, inhibitory activity was almost nil in the pellet fractions at 60k and 100k *x g*. These observations suggest that the inhibitory activity derives from soluble factors or maybe molecules associated to inclusion bodies not pelleted. MHC-II ^{high} populations were gated in each sample and the proportion of cells (%) within this gate was subtracted from the untreated control culture to give a "% inhibition" value, indicated in the gray box within each histogram. Experimental samples are indicated by solid shaded curves, the untreated control culture by the solid curve, and the isotype control by the dotted line. Mean fluorescence intensity (MFI) values are indicated for each population (i.e. italicized for isotype control, standard font for non-infected non-treated control cells, bold font for experimental samples. *Tg(-)* and *Tg(+)* refer to non-infected cells within infected cultures, and infected cells, respectively. Results are representative of four independent experiments.

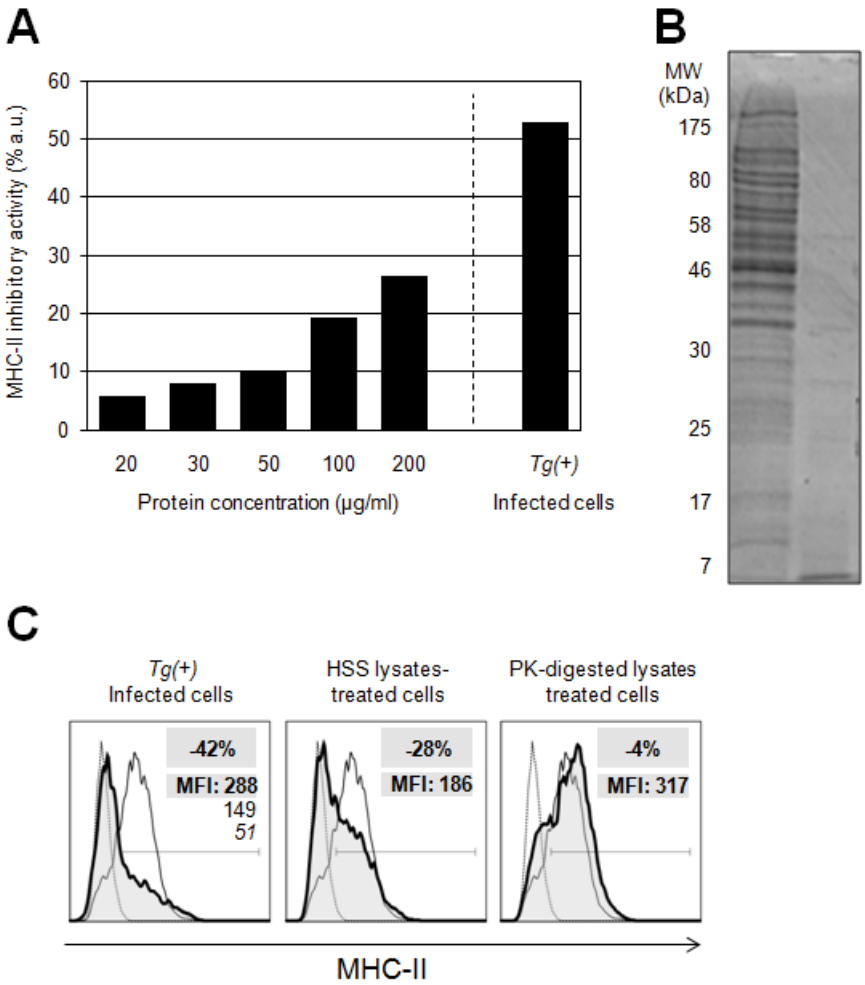

Figure 3.2: The inhibitory activity is protein dose-dependent and is completely lost after proteolysis. (A) BMMΦ cultures were treated with increasing protein concentrations of HSS lysates from 20 to 200 µg/ml for a few hours, and then stimulated with 100 U/ml IFNγ for 18 hours. Cells were then harvested and MHC-II expression was analyzed by flow cytometry. MHC-II ^{high} populations were gated in each sample and the proportion of cells (%) within this gate was subtracted from the untreated control culture to give a "% inhibition" value. As indicated by the histogram, increasing protein amounts led to greater inhibition or, in other words, to lower MHC-II expression. Cultures infected with live parasites were included in the analysis as a reference. (B) SDS-PAGE analysis revealed the complex protein contents of the undigested HSS lysates (lane 1) and the complete proteolysis of proteinase K-digested HSS lysates (lane 2). (C) BMMΦ were infected with live parasites, treated with 200 µg/ml of HSS lysates prepared from sonicated tachyzoites, or HSS lysates digested with proteinase K (PK, 5 µg/ml, 37°C, 1 hr) + pefabloc + protector solution. Cells were stimulated with 100 U/ml IFNγ for 18 hours, and then stained using PE-conjugated rat anti-mouse IA/IE (MHC-II) antibodies and analyzed by flow cytometry. Infection with live parasites led to the greatest MHC-II inhibition (42%), while undigested HSS lysates caused a somewhat lower but significant inhibition (28%). However, cells treated with the proteinase K–digested lysates showed normal MHC-II levels (only 4% inhibition) comparable to untreated control cultures (solid curve). Experimental samples are indicated by solid shaded curves and the isotype control is indicated by the dotted line. Mean fluorescence intensity (MFI) values are indicated for each population (i.e. italicized for isotype control, standard font for non-infected non-treated control cells, bold font for experimental samples. *Tg(+)* refers to infected cells. Results are representative of three independent experiments.

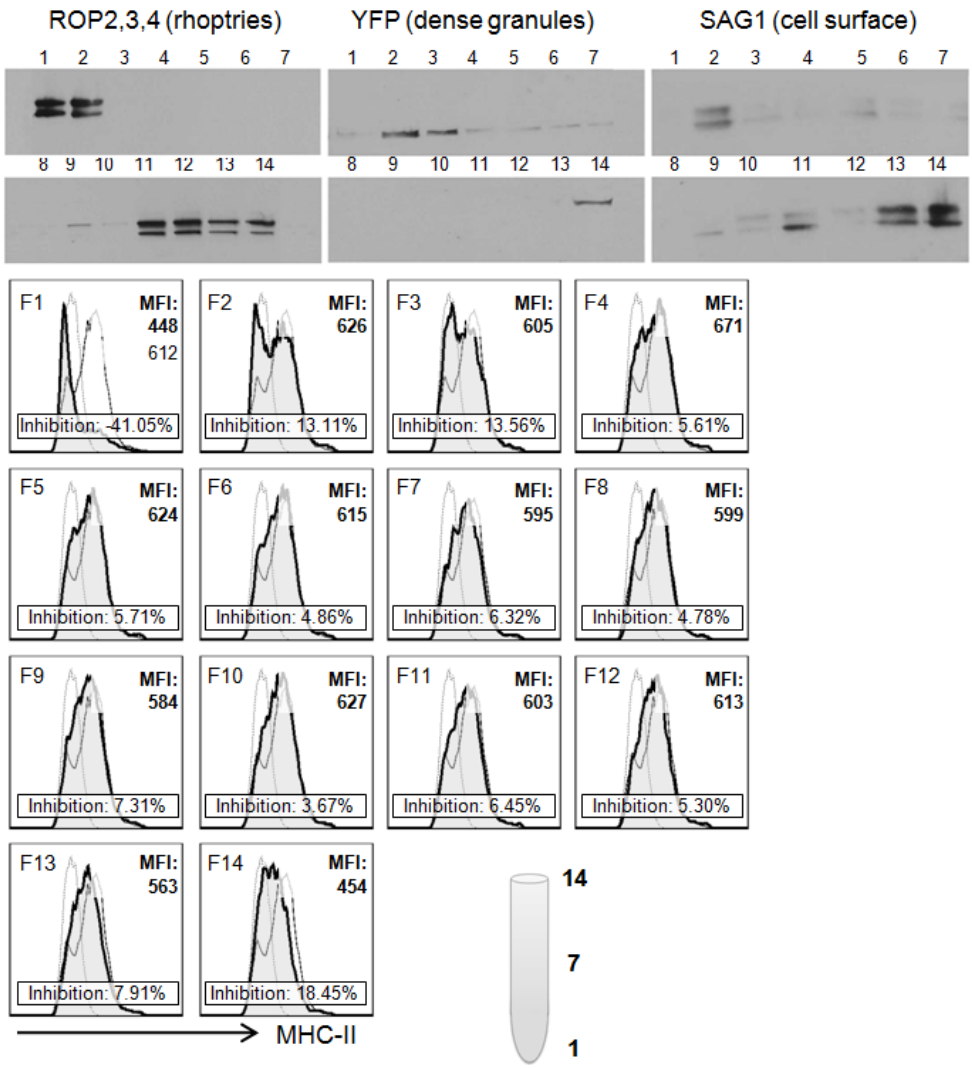

Figure 3.3: The inhibitory activity segregates to the rhoptry/dense granule-enriched fractions. BMMΦ cultures were treated with 150 µg/ml of each subcellular fraction collected from the Percoll gradient (solid shaded curve), and subsequently 100 U/ml IFNγ was added. Flow cytometry analysis of revealed that the bottom three fractions, especially fraction 1 (F1), had the greatest inhibitory activity. Western blots were performed in parallel to reveal the contents of each fractions, specifically probing for different secretory organelles (i.e. rhoptries, dense granules) and cell membrane (i.e. SAG1). Non-treated, IFNγ-stimulated control cultures (solid curve) were used as a reference, whereby MHC-II ^{high} populations were gated in each sample and the proportion of cells (%) within this gate was subtracted from the control culture to give a "% inhibition" value. Also, mean fluorescence intensity (MFI) values are indicated for each sample. The isotype control is indicated by the dotted line. Results are representative of three independent experiments.

3.4.4. Several rhoptry and dense granule knock-outs strains still inhibit MHC-II expression during active host cell invasion

Since subcellular fractionation experiments suggested that the inhibitory activity was found in fractions enriched in rhoptries and dense granules and that several secreted proteins from these organelles have been shown to have immunomodulatory properties, we tested several rhoptry (*Δrop1*, *4/7*, *14*, *16*, and *18*) and dense granule (*Δgra2*, *3*, *4*, *5*, *6*, *7*, *8*, *9*, *12*) knock-out parasites that were generated using the KU80 system. Flow cytometry analysis of BMMΦ cultures infected with these different knock-out cell lines revealed that all of these strains were still able to inhibit IFNγ-induced MHC-II expression (Figure 3.4). Although the inhibition levels varied slightly from one strain to another, they were all fairly similar to those seen with the control parental *Δku80* or WT strains (33 and 46%, respectively). The lowest inhibition levels were seen with *Δgra5* and *Δgra9* (both 28%), and the highest with *Δgra12* (46%). However, these results do not completely exclude the possibility that one of these molecules is directly involved in MHC-II inhibition. Rather, they might indicate either that redundant mechanisms are elicited by different molecules, which would compensate for the absence of one of these molecules (i.e. in the knock-out strains), or that multiple mechanisms are targeted by the parasite's arsenal of secretory molecules and that disrupting one of them by gene disruption is not enough to restore full MHC-II expression.

3.4.5. Excreted-secreted antigens (ESA) from extracellular parasites display inhibitory activity

At this point, we had determined that the inhibitory proteins were soluble and found in subcellular fractions enriched in rhoptries and dense granules. Another source of parasite material is excreted-secretory antigens (ESA). Parasite ESA were initially recovered from culture supernatants of infected host cells *in vitro*, and were also found to be highly immunogenic during human and

experimental toxoplasmosis (Darcy, Deslee et al. 1988). It had been shown that incubation of free parasites in media containing 10% mammalian serum at 37°C stimulated the release of parasite molecules. However, since the presence of serum would complicate downstream proteomic identification of inhibitory candidate molecules, we first sought to determine if ESA could be collected without the presence of FBS in the medium. Two separate extracellular tachyzoite suspensions, free of any host cell, were incubated in DMEM, with or without 10% FBS for 3 h at 37 °C. After removal of parasites, the supernatant was tested onto macrophages. The inhibitory activity on IFNγ-induced MHC-II expression was found with supernatants originating from both preparations of parasites, arguing that serum was not necessary for the release of MHC-II inhibitory molecules (Figure 3.5).

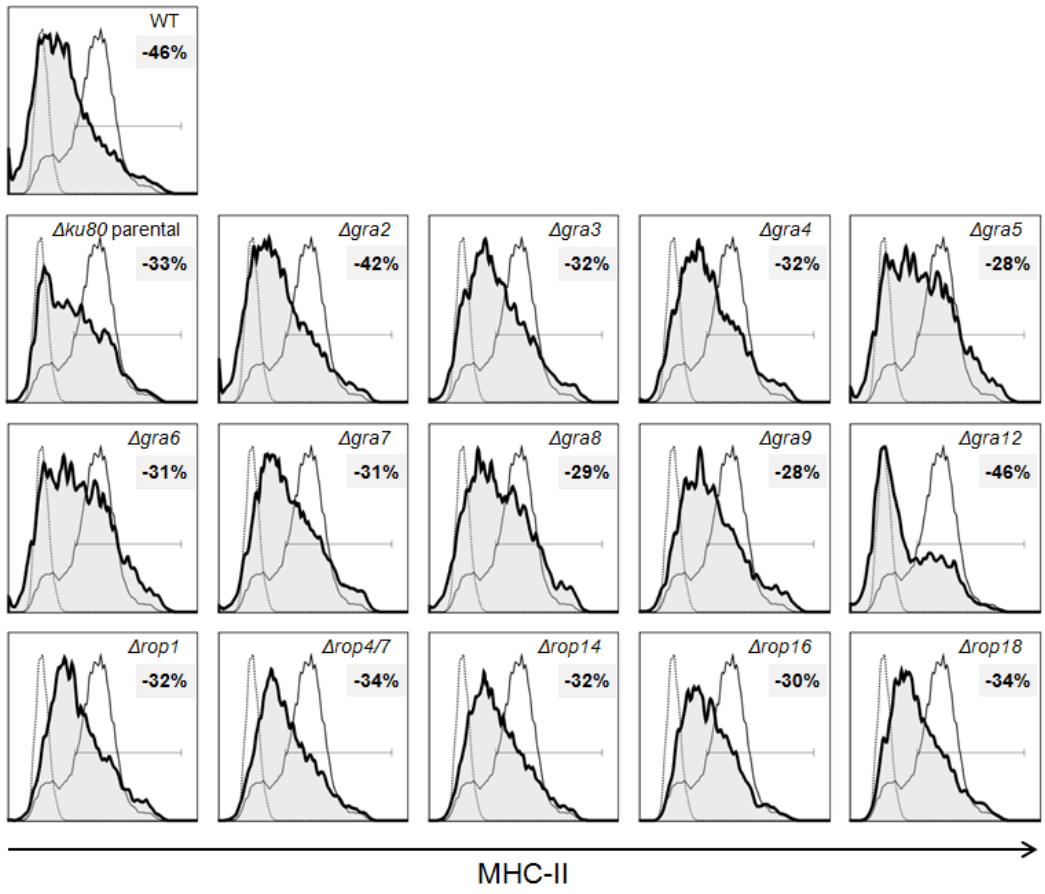

Figure 3.4: (see legend on page 71)

Figure 3.4: Several rhoptry (rop) and dense granule (gra) knock-out strains inhibit MHC-II expression during active host cell invasion. BMMΦ cultures were infected with different rhoptry (Δrop1, 4/7, 14, 16, and 18) and dense granule (Δgra2, 3, 4, 5, 6, 7, 8, 9, 12) knock-out parasites generated using the KU80 system, or WT and Δku80 parental strains as controls for 4 hours, then stimulated with 100 U/ml IFNγ for 18 hours. After incubating the culture with IFNγ, MHC-II expression was analyzed by flow cytometry. The analysis revealed that all knock-out strains tested were able to inhibit MHC-II expression in infected macrophages. MHC-II ^{high} populations were gated in each sample and the proportion of cells (%) within this gate was subtracted from the untreated control culture to give a "% inhibition" value, indicated in the gray box within each histogram. Experimental samples are indicated by solid shaded curves, the untreated control culture by the solid curve, and the isotype control by the dotted line. Results are representative of four independent experiments.

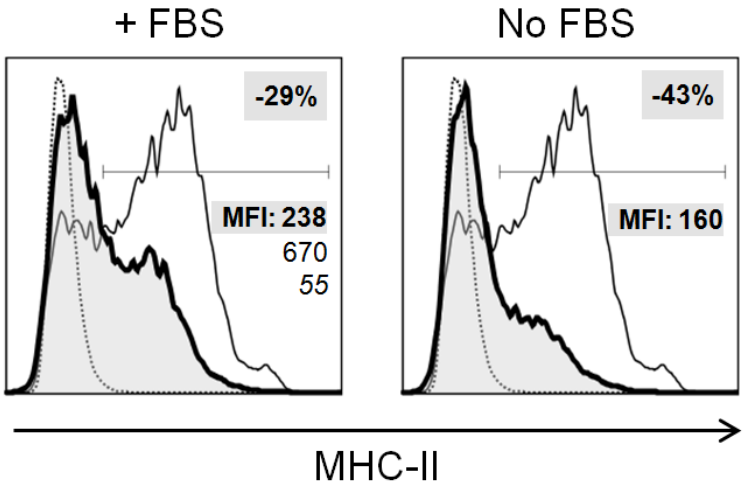

Figure 3.5: The release of MHC-II inhibitory molecules by extracellular tachyzoites does not require the presence of FBS in the incubation medium. Tachyzoites were separately incubated in DMEM with 10% FBS or without for 3 hours at 37°C with shaking. After 3 hours, parasites were removed by centrifugation and supernatants were added onto BMMΦ. MHC-II expression levels were quantified by flow cytometry. The analysis revealed that ESA material displayed inhibitory activity regardless of the presence or absence of FBS in the culture medium. In fact, ESA prepared without FBS caused higher inhibition. MHC-II ^{high} populations were gated in each sample and the proportion of cells (%) within this gate was subtracted from the untreated control culture to give a "% inhibition" value, indicated in the gray box within each histogram. Experimental samples are indicated by solid shaded curves, the untreated control culture by the solid curve, and the isotype control by the dotted line. Mean fluorescence intensity (MFI) values are indicated for each population (i.e. italicized for isotype control, standard font for non-infected non-treated control cells, bold font for experimental samples. Results are representative of two independent experiments.

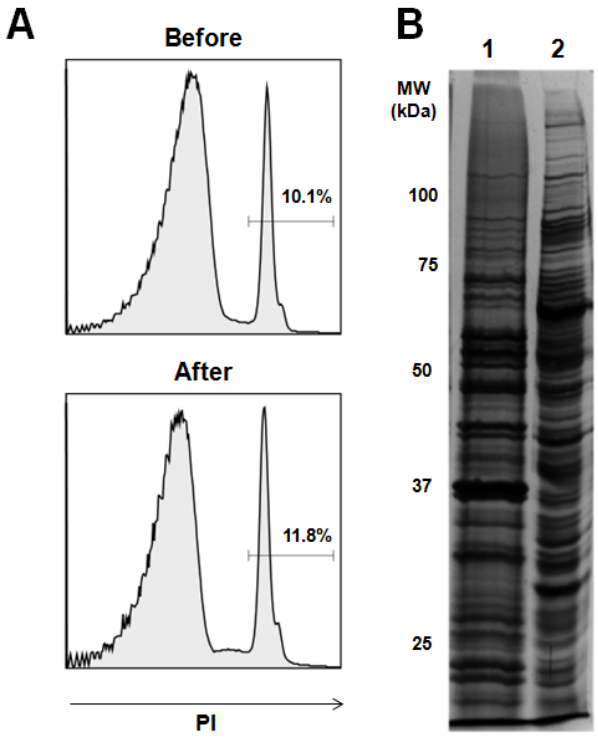

Figure 3.6: The release of MHC-II inhibitory molecules by extracellular tachyzoites is due to active secretion and not a result of parasite lysis. (A) A 10 µl sample of the parasite suspension was mixed with a 500 µl solution of DMEM containing 10 µg/ml propidium iodide (PI) both before and after ESA production. After 5 minutes at room temperature, the sample was analyzed by flow cytometry to quantify dead parasites. Analysis revealed that no significant death occurred during ESA production. Percentages of dead parasites are indicated on graph. (B) 3 µg of protein of soluble lysates (1) and ESA (2) were analyzed by SDS-PAGE. Bands were visualized by silver stain. The protein profiles, although very complex, proved to be slightly different.

A similar comparison between ESA and soluble lysates was carried out by Western blotting using antibodies specific for proteins originating from each secretory organelle (Figure 3.7). ESA material appeared to be highly enriched for MIC2, a marker for micronemes, compared to lysates. Note that this is due to the underrepresentation of this protein in the lysates as we have detected this protein using the same antibody with increasing amounts of lysates (data not shown). The signal for GRA3, a marker for dense granules, appeared to be quite similar between the two samples. The ROP markers, ROP2 and 4, although largely present in the lysates, were present in very low amounts in the ESA. Briefly, it appears that, although both having inhibitory activity, soluble lysates and ESA contained different protein profiles, but with some overlap.

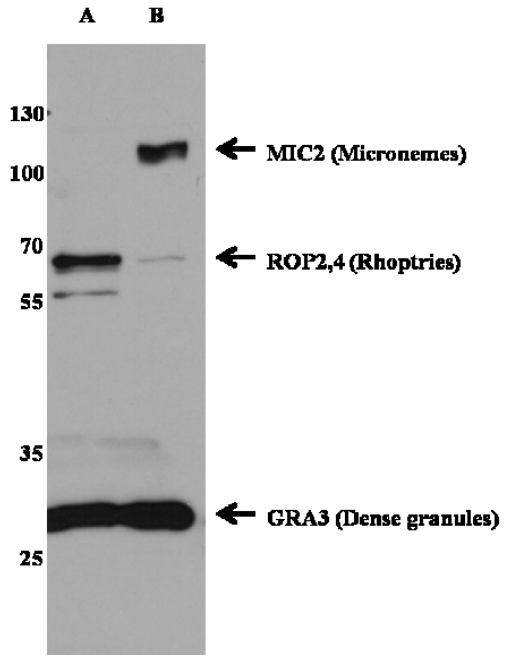

Figure 3.7: ESA is enriched for the microneme and dense granule markers MIC2 and GRA3 and not for the ROP2,4 rhoptry markers. Western blot using 3 µg of protein from soluble lysates and ESA probed with murine anti-MIC2, GRA3, and ROP2,4 primary antibodies (all at 1:200) and a rabbit anti-mouse secondary antibody (1:8000).

3.4.6. A two-step fractionation procedure narrows down the inhibitory activity to a few fractions, and tandem mass spectrometry reveals several protein candidates

To tease out the inhibitory molecules found in the ESA material, we devised an experiment consisting of two sequential fractionation steps. We first fractionated ESA proteins by ion-exchange chromatography (Figure 3.8A) and pooled the material eluted off the ion-exchange column into five fractions (A through E). SDS-PAGE analysis demonstrated the successful fractionation of proteins as the gel profiles differ significantly from each other (Figure 3.8B). Although MHC-II inhibition was found in all five fractions, Fraction E contained the most activity per amount of protein tested, suggesting a greater enrichment of activity (Figure 3.8C).

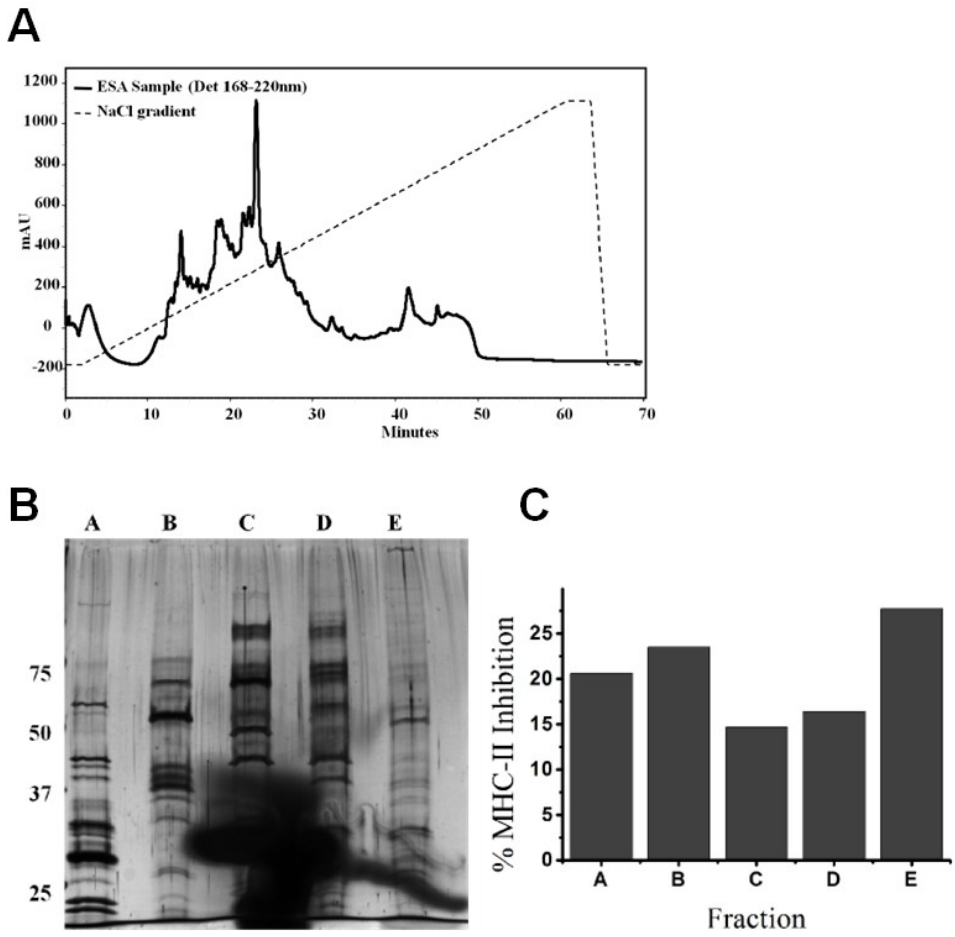

Figure 3.8: A fraction from 5 pooled ion-exchange fractions of ESA contained peak MHC-II inhibition. ESA samples were injected onto a MonoQ ion-exchange column. A NaCl gradient from 0 to 1M was used to elute proteins off the column. Fractions were collected every 2 minutes. (A) The HPLC detector output showing absorption values at 220 nm by eluting proteins. The solid and dashed graphs indicate the sample of interest and the salt gradient, respectively. Fractions were collected every 2 minutes, pooled and named Fraction A (mins 0-8), B (mins 10-16), C (mins 18-22), D (mins 24-28), and E (mins 30-40). The pools (A to E) were concentrated and washed in PBS. (B) 500 ng of each fraction was analyzed on an 8% SDS-PAGE gel and bands visualized by silver stain. (C) Each pool was tested on macrophages at 2.5 µg/ml, and % MHC-II inhibition per fraction was quantified.

Fraction E was then passed through a size-exclusion column to separate proteins based on their size. In order to simplify the MHC-II inhibition assay, 200 µl of each fraction were initially pooled and concentrated as Fractions 1 (1 to 18 min), 2 (19 to 30 min), 3 (31 to 39 min), 4 (40 to 51 min) and 5 (52 to 66 min), with the values in brackets corresponding to the elution time (Figure 3.9A). Pooled Fraction 2 had the highest MHC-II inhibition activity and upon re-testing each individual fraction (i.e. prior to pooling), minutes 22-27 were shown to contain the activity almost entirely (Figure 3.9B and C). These fractions were

concentrated, subject to in-solution tryptic digestion and candidates were identified by liquid chromatography coupled tandem mass spectrometry (LC-MS/MS). Database mining using the *Toxoplasma gondii* GT-1 genome identified 24 candidates (Table 2.1).

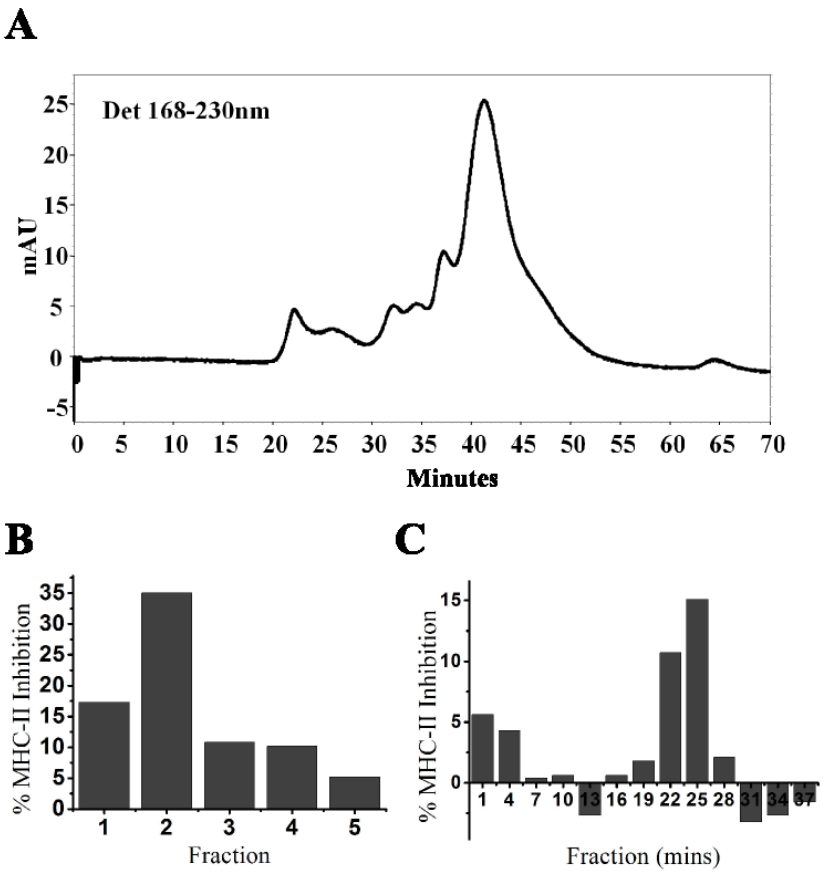

Figure 3.9: A size-exclusion fractionation step of Fraction E identified a few fractions with most MHC-II inhibition. Fraction E from the pooled ion-exchange fractions was injected onto a Superose-12 size-exclusion column. (A) The amount of protein eluting from the column as measured by the absorbance at 230 nm by the HPLC detector. Fractions were collected every 3 minutes. (B) 200 µl of each size-exclusion fraction was pooled and concentrated as Fractions 1 (mins 1 to 18), 2 (mins 19 to 30), 3 (mins 31 to 39), 4 (mins 40 to 51), and 5 (mins 52 to 66). 25 µL of each pool was tested on macrophages and MHC-II inhibition per fraction is indicated. (C) 25 µL of each original (not pooled) individual size-exclusion fraction constituting pooled fractions 1-3 was re-tested on macrophages to pinpoint MHC-II inhibition to a few fractions. % MHC-II inhibition per time fraction in minutes is graphically represented.

Protein ID	Protein Description	Mass (Da)	Protein Score	# of Peptides
TGGT1_024780	ATP-dependent DNA helicase II 70 kDa subunit putative	94432	73	1
TGGT1_075430	ATP-dependent helicase putative	175146	21	1
TGGT1_028940	casein kinase II alpha putative	34264	34	1
TGGT1_120520	conserved hypothetical protein	148383	37	1
TGGT1_040810	conserved hypothetical protein	50041	19	1
TGGT1_041870	conserved hypothetical protein	52624	18	1
TGGT1_055640	conserved hypothetical protein	102182	30	1
TGGT1_016150	conserved hypothetical protein	22419	29	2
TGGT1_056020	conserved hypothetical protein	118447	19	1
TGGT1_101530	conserved hypothetical protein	470616	27	1
TGGT1_052100	conserved hypothetical protein	142173	26	1
TGGT1_025460	conserved hypothetical protein	245738	32	1
TGGT1_017550	dense granule protein putative 7	25842	27	1
TGGT1_037870	dense granule protein 5 precursor putative	12969	35	1
TGGT1_124080	dihydroorotate dehydrogenase putative	65024	29	1
TGGT1_046120	flagellar WD-repeat protein PF20 putative	68221	22	1
TGGT1_068065	granule antigen protein GRA6 putative	24015	29	1
TGGT1_101070	NAD-specific glutamate dehydrogenase putative	135412	35	1
TGGT1_027510	origin recognition complex subunit putative	95374	48	1
TGGT1_045850	pre-mRNA splicing factor prp31 putative	59814	26	1
TGGT1_042710	rhoptry antigen putative	60916	54	2
TGGT1_026610	serine/threonine protein phosphatase 2A B56 delta subunit putative	71107	26	1
TGGT1_114010	SRS29B (= SAG1 P30)	32963	27	1
TGGT1_121080	WD-repeat protein putative	56045	18	1

Table 3.1: Database mining following MS/MS analysis of the ESA fraction displaying highest inhibitory activity listed 24 possible candidates. Database mining of the *T.* gondii GT-1 genome using the hits generated by LC-MS/MS analysis of the ESA fraction displaying highest inhibitory activity generated a list of possible candidates. Here the protein identification (ID), protein description as annotated in the database, the predicted mass in Daltons (Da), the protein score, and the number of peptides detected by MS/MS are listed.

3.5. Discussion

In recent years, there has been increasing evidence of the multiple mechanisms *Toxoplasma gondii* deploys to subvert the host immune system. Of particular interest is the parasite's ability to inhibit MHC-II expression in order to

interfere with antigen presentation and dampen $CD4^+$ T cell activation, and hence to gain a tactical advantage early in the infection. Although several studies detailed this phenotype (Luder, Lang et al. 1998) (Luder, Walter et al. 2001) (McKee, Dzierszinski et al. 2004), the causative inhibitory molecules had not yet been identified. In an attempt to identify these molecules, we considered parasite lysates as a starting point since they were shown to mimic the inhibitory effects of live parasites on MHC-II expression (Lang, Algner et al. 2006). We resorted to different biochemical techniques to fractionate and enrich for the inhibitory activity which allowed us to better characterize the nature of the molecules. The rationale behind these techniques was to either separate intact organelles and then test their content to determine the subcellular origin of the inhibitory activity, or to start with bulk material obtained from parasite lysates or unresolved ESA and to fractionate according to different biochemical properties such as solubility, size, and ionic charge in order to enrich for the inhibitory activity and to increase the likelihood of detecting and identifying the molecules of interest.

Treating lysates prepared from sonicated parasites with varying conditions revealed useful information. First, high-speed centrifugation allowed to remove insoluble material with little or no inhibitory activity (i.e. pellet) from the soluble MHC-II inhibitory fraction (i.e. supernatant) (Figure 3.1). The inhibitory activity within the latter fraction was enhanced with increasing centrifugal speeds suggesting that this activity is caused by soluble molecules. The protease-sensitivity and protein dose-dependence of the inhibitory activity clearly indicate that the inhibitory activity is mostly due to proteins (Figure 3.2).

Considering these last observations in the context of live infection, extracellular parasites could release soluble factors in their surroundings that would affect host immune cells prior to invasion in such a manner that would prevent the triggering of immune mechanisms, antigen presentation being one of these, upon entry and PV formation, and inhibit the local immune response. The manipulation of its environment could help *T. gondii* evade immune surveillance and establish a favourable niche for replication.

Such a scenario has been proposed to occur and was coined the "kiss-and-spit model" (Boothroyd and Dubremetz 2008), whereby the parasite would come into contact with host cell membrane, secrete the contents of its secretory organelles into the cytoplasm, but would fail to process to invade the cell and move along to the next host cell. The use of cytochalasin D (CytD), a actin polymerization inhibitor, was shown to mimic this event; although invasion was blocked, secretion of some microneme adhesins, formation of the tight junction, and secretion of rhoptry contents were accomplished by Cyt D-arrested parasites (Carruthers and Sibley 1997) (Hakansson, Charron et al. 2001). This secretion process led to the formation of empty vacuoles or "evacuoles" which, like parasite-containing PVs, associated with host cell mitochondria and ER, while avoiding fusion with endocytic compartments. Several ROP proteins have been detected in evacuoles, such as ROP1, ROP16, members of the ROP2 subfamily including ROP2 and ROP18, and a protein phosphatase 2C (PP2C-hn) (Nichols and O'Connor 1981) (Saffer, Mercereau-Puijalon et al. 1992) (Saeij, Boyle et al. 2006) (Gilbert, Ravindran et al. 2007) (Laliberte and Carruthers 2008).

If we take the phosphatase PP2C-hn as an example, it has been shown to localize to the host nucleus (hence the designation "-hn") (Gilbert, Ravindran et al. 2007) as well as ROP16 even during the formation of evacuoles (Saeij, Coller et al. 2007). Although these specific molecules may not have a direct role on MHC-II expression inhibition, the mere fact that molecules can find their way not only into the cytoplasm, but into the nucleus as well suggests that molecules from the secretory organelles could interfere with signaling pathways and transcription, and be linked to the inhibitory activity on MHC-II expression even before invasion. This possibility could explain, in part, why non-infected cells within an infected culture express lower levels of MHC-II molecules in comparison to non-infected cells from non-infected control cultures (Figure 3.1), as reported similarly (Stutz, Kessler et al. 2012).

The subcellular fractionation experiments corroborate in part this hypothesis. Indeed, the inhibitory activity seemed to parallel fractions enriched in

rhoptries and dense granules (Figure 3.3). Although the subcellular fractions presumably contained mixtures of these organelles as well as other contaminating material and that all ROP or GRA single KOs tested were able to inhibit MHC-II expression, assays using ESA supported the proposed hypothesis. ESA material collected in the culture medium revealed to contain mostly dense granule and microneme proteins, and displayed inhibitory activity on MHC-II expression by IFNγ-stimulated BMMΦ (Figures 3.5 and 3.7). Although rhoptry proteins seemed to be found in low amounts, we cannot discount the presence of other rhoptry proteins in the ESA since we only probed for two ROP antigens. The production of ESA required tachyzoites to be cultured extracellularly without host cells to avoid contamination from the latter, and without FBS to avoid masking the analysis of the parasite protein content. The incubation time was short enough minimize parasite death and lysis (Figure 3.6) arguing that the material collected in the culture supernatant originated from active excretion/secretion and not from cytoplasmic or other organelles not related to secretion, again adding credence to the idea that inhibitory activity originates from secretory organelles. In an early report demonstrating the requirement of FBS for optimal ESA secretion, the group had observed higher parasite survival in the presence of serum (Darcy, Deslee et al. 1988). They had reported >80% survival for parasites incubated with serum versus <60% for those that were not, based on an erythrosin B exclusion test. Our experiments showed an 88% survival rate, even in the absence of serum. Another study had shown that increasing the amount of serum in the incubation medium led to increased secretion of GRA1 (Coppens, Andries et al. 1999), suggesting that we may not have obtained optimal amounts of secretion in the absence of serum. Nonetheless we demonstrated the presence of a unique pool of proteins in comparison to soluble lysates in the absence of serum and that several secretory organelle proteins were enriched in our ESA preparations with inhibitory activity.

Since ESA could be prepared in the absence of FBS in the culture medium, subsequent fractionation procedures were successfully carried out. ESA proteins were fractionated first by ion-exchange chromatography, and the fraction

identified with the highest inhibitory activity was subjected to two rounds of size-exclusion chromatography, as detailed above (Figures 3.8 and 3.9). Subsequent database mining with the peptide hits obtained from LC-MS/MS revealed 24 candidates (Table 2.1). Only a single peptide was identified in the majority of these hits, and although not ideal, it was expected due to the lost of material following serial rounds of fractionation and the very low amount of proteins left. Nevertheless, we were able to identify several candidates.

A single microneme protein, MIC11, was identified in our analysis. MIC11 undergoes maturation by proteolytic removal an internal propeptide and lacks any recognizable adhesive sequence found in other microneme proteins (Harper, Zhou et al. 2004). Although this protein may have an alternate role to host cell attachment, its exact function has yet been confirmed.

RON9 and a putative ROP protein were the only two rhoptry candidates detected. RON9 has been found to be associate with RON10 in tachyzoites, and without its partner, RON9 is not targeted to rhoptries and is degraded (Lamarque, Papoin et al. 2012). Unlike several RON proteins that have been shown to interact with the microneme protein AMA1 to form the moving junction (Alexander, Mital et al. 2005; Besteiro, Michelin et al. 2009; Tonkin, Roques et al. 2011), RON9 and RON10 were not found to be a part of the moving junction and were not detected within the host cell after invasion (Lamarque, Papoin et al. 2012), and could potentially have an extracellular function making them interesting candidates for our study. However, RON10 was not detected in our study, but it should also be considered a candidate for future verifications. The other putative rhoptry protein detected is believed to be a pseudokinase belonging to the ROP5 family of proteins, a group of polymorphic pseudokinases that are important in virulence differences between parasite strains (Behnke, Khan et al. 2011; Reese, Zeiner et al. 2011). Since many *in silico* models predict kinase and phosphatase activities for several rhoptry proteins, the candidates listed could be secreted by rhoptries (Peixoto, Chen et al. 2010).

Among the dense granule proteins, a GRA5 precursor, GRA6, and GRA7 were identified. GRA5 has been shown to be secreted as a soluble protein as shown in FBS induced secretions and it associates with the PV membrane within the host cell (Lecordier, Mercier et al. 1993; Lecordier, Mercier et al. 1999). As for GRA6, it is stored in a soluble state within dense granules inside the parasite and within the PV, and associates with the PV network forming complexes with GRA2 and GRA4 (Lecordier, Moleon-Borodowsky et al. 1995; Labruyere, Lingnau et al. 1999). GRA7 has been detected in several locations within infected cells including the PV lumen, PVM, strands that extend from the PVM to the host cytosol, and in secretion by the infected cells (Fischer, Stachelhaus et al. 1998; Jacobs, Dubremetz et al. 1998). The above three dense granule proteins, along with GRA3, have been shown to form large complexes when secreted (Braun, Travier et al. 2008). The formation of high globular weight complexes could explain how these small dense granule proteins are present in size-exclusion fractions expected to contain large proteins. However, live infection with corresponding GRA KOs led to MHC-II inhibition (Figure 3.7). Therefore, either these proteins are irrelevant to the inhibitory activity, or other proteins can compensate and fulfill the same functions in a redundant matter.

Some of the other candidates identified only have assigned putative roles. Two helicases and other proteins involved in transcription and/or translation were present in our sample. These proteins could be either due to contamination in the preparation or inadvertently secreted along with other molecules. The majority of the largest proteins detected were hypothetical proteins with unknown functions, and without any structurally related proteins. If such large proteins were present in our samples, they were not likely visualized by SDS-PAGE analysis.

Since the hypothetical length is solely based on predicted translation of genes, it is unclear if these values represent the actual sizes of the translated proteins or if they are post-translationally cleaved to form smaller peptides in reality. In fact, many rhoptry and microneme proteins are proteolytically cleaved en route to their destination in the apical organelles, rendering the above

assumption realistic (Bradley and Boothroyd 1999; Bradley, Hsieh et al. 2002; Harper, Zhou et al. 2004). Also, the vast majority of the secretory organelle proteins still remain undiscovered, notably the dense granule proteins since their purification has not been possible yet.

In summary, we have shown that biochemical characterization, fractionation and enrichment of the MHC-II inhibitory activity is possible. We have narrowed down the list of possible candidates, which will be validated by KO strategy. Ultimately, the findings reported herein will guide future inquiries on the matter and may contribute to the understanding of underlying mechanisms engaged by secreted molecules.

Connecting Statement 2

In the previous chapter, biochemical analyses provided significant evidence as to the nature of the MHC-II inhibitory activity displayed by *Toxoplasma gondii*. This inhibitory activity appeared to originate from secretory organelles, most probably from dense granules, but possibly rhoptries as well. Although no single protein has been ruled as the definitive molecule responsible for this phenotype, a relatively short list of potential protein candidates has been generated, which partly fulfilled the goal of this project. Of all these molecules, none of them had been previously reported to contribute to the inhibition of IFNγ-induced MHC-II expression. In addition, the results obtained contribute to the description of the *T. gondii* secretome and may help characterize the functions of many hypothetical proteins found herein.

The aim of the previous project was to identify inhibitory molecules, yet an interesting phenotype still remained unaddressed. The current literature regarding *T. gondii* and its inhibition of MHC-II expression has focused strictly on the transcriptional interference. Interestingly, a few mature peptide- or CLIP-loaded MHC-II molecules were still observed in infected cells (Figure 4.1), but remained unable to efficiently present parasite-derived antigens to activate $CD4^+$ T helper cells. This seemingly counterintuitive conundrum needed to be addressed. In the following chapter, we provide evidence that a second, post-translational layer of regulation by the parasite was required to complement the transcriptional layer of inhibition to efficiently block antigen presentation. This second layer involves the MHC-II associated invariant chain (Ii). Furthermore, we assess the impact of the Ii and the peptide editor H2-DM, both critical players of the MHC-II pathway, during the course of infection in an animal model, detailing their contribution to the immune response and the outcome on cyst burden during chronic infection.

Chapter 4. Manuscript II

Title:

The invariant chain (Ii) and the peptide editor H2-DM modulate MHC-II antigen presentation and $CD4^+$ T cell effectors during infection by *Toxoplasma gondii*

Authors and Affiliations:

Louis-Philippe Leroux*, Manami Nishi[¶], Sandy El-Hage, Barbara A. Fox[#], David J. Bzik[#], Florence S. Dzierszinski*[¤§]

*Institute of Parasitology, McGill University, Sainte-Anne-de-Bellevue, Québec, Canada

[¶]Indiana University, Indianapolis, Indiana, USA

[#]Dartmouth Medical School, Lebanon, New Hampshire, USA

[¤]Carleton University, Ottawa, Ontario, Canada

[§]Corresponding author

4.1. Abstract

Toxoplasma gondii interferes with MHC-II antigen presentation to dampen $CD4^+$ T cell responses, and therefore gains a head start on the adaptive immune response. Transcriptional down-regulation of MHC-II genes by *T. gondii* is well known, but precise molecular mechanisms remain elusive. Here, we show that the first layer of transcriptional regulation is complemented by a second layer of interference in the host cell endocytic pathway involving the MHC-II associated invariant chain (Ii). Absence of Ii restored the ability of infected dendritic cells to present a parasite antigen in the context of MHC-II. Although the expression of MHC-II genes is typically coordinated, Ii mRNA and protein levels were surprisingly induced in infected bone marrow-derived murine macrophages (BMMΦ) and dendritic cells (BMDCs), while MHC-II and H2-DM expression was inhibited. The induced expression of Ii was not dependent on exogenous IFNγ, nor endogenous type I interferons and tumor necrosis factor alpha (TNFα). Ii accumulated in infected cells until host cell lysis, mainly in the ER, but not at the cell surface. This phenotype did not require active parasite replication, but was specific of live *T. gondii* infection. The Ii p10 cleavage product accumulated in infected BMMΦ while it was not observed in BMDCs, suggesting a cell-type specific bias in Ii proteolysis. Endosomal protease activities were indeed differentially modulated in infected BMDCs and BMMΦ. Moreover, acidification of endocytic compartments was compromised in infected cultures, pointing toward a wider manipulation of the host endocytic pathway. Opposing expression patterns of Ii and H2-DM had an effect *in vivo* on parasite dissemination towards lymphoid organs, $CD4^+$ T cells activation, IFNγ production during acute infection, and on cyst numbers and survival at the chronic phase of the infection, highlighting the importance of these components in MHC-II antigen presentation and the control of the infection.

4.2 Introduction

Toxoplasma gondii is an obligate intracellular protozoan parasite with a remarkable host range that consists of any warm-blooded vertebrate, including humans and mice (Frenkel, Dubey et al. 1970) (Dubey, Miller et al. 1970). During acute infection, rapidly-dividing tachyzoites primarily disseminate throughout the host and infect any nucleated cell, including cells of the immune system, in which it replicates within the parasitophorous vacuole (PV) (Dubey 2004). Shortly after infection, parasites reach immune privileged sites such as the brain and muscle tissues, and convert to more latent bradyzoites which will encyst to remain latent throughout the host's life. Encystation can occur as early as 6 to 9 days post-infection (Dubey, Speer et al. 1997), concomitant with the development of a parasite-specific adaptive immune response. Although toxoplasmosis is generally asymptomatic in healthy individuals, congenital toxoplasmosis can lead to serious birth defects such as hydrocephaly, mental retardation, blindness, and chorioretinitis (Montoya and Remington 2008). Furthermore, reactivation of encysted parasites is a serious threat to immunosuppressed individuals, such as AIDS patients, individuals receiving chemotherapy against cancer or immunosuppressive drugs during organ transplant, or to elderly people with an aging immune system (Dubey 2004) (Luft and Remington 1992).

In immunocompetent hosts, resistance against *T. gondii* is characterized by a robust Th1-type response that is mediated by the cellular arm of the immune system, namely $CD8^+$ and $CD4^+$ T cells, which provide protective immunity, mainly by producing IFNγ (Gazzinelli, Hakim et al. 1991) (Suzuki, Orellana et al. 1988) (Denkers and Gazzinelli 1998). Despite the induction of a strong immune response, the infection inevitably reaches the chronic stage as the parasite is able to encyst. It has been reported that *T. gondii* utilizes different mechanisms to subvert several immune functions, such as inhibition of pro-inflammatory signaling cascades, namely NF-κB (Shapira, Harb et al. 2005), MAPK (Kim, Butcher et al. 2004), STAT1 (Zimmermann, Murray et al. 2006) (Lang,

Hildebrandt et al. 2012) (Stutz, Kessler et al. 2012), CIITA (Luder, Lang et al. 2003), induction of the anti-inflammatory STAT3/6-mediated transcription (Butcher, Kim et al. 2005) (Ong, Reese et al. 2010) (Jensen, Wang et al. 2011), and inhibition of immunity-related GTPases (IRG)-mediated destruction of the PV (Fentress, Behnke et al. 2010) (Steinfeldt, Konen-Waisman et al. 2010) (Niedelman, Gold et al. 2012). Furthermore, it has been shown that *T. gondii* interferes with antigen presentation in the context of major histocompatibility (MHC) class II (Luder, Lang et al. 1998) (Luder, Walter et al. 2001) (McKee, Dzierszinski et al. 2004), which is required for priming and activation of $CD4^+$ T cells (Hudson and Ploegh 2002).

MHC-II glycoproteins are synthesized in the endoplasmic reticulum (ER), where they associate with the MHC-II associated invariant chain (Ii or CD74) chaperone to form a pentameric complex, whereby two MHC-II chains associate with Ii trimers (Koch, Zacharias et al. 2011). Professional antigen presenting cells (pAPCs), such as macrophages, dendritic cells, and B cells, readily express these molecules and their expression is up-regulated upon pro-inflammatory stimuli (Hudson and Ploegh 2002). The invariant chain, a non-polymorphic type II membrane protein, prevents non-specific loading of peptides onto MHC-II molecules by occupying the MHC-II groove. In addition, Ii contains di-leucine-based sorting motifs within its cytoplasmic region (Pieters, Bakke et al. 1993), (Odorizzi, Trowbridge et al. 1994) that are recognized by either AP1 and AP3, or AP2 adaptor proteins that will send Ii/MHC-II complexes to the cell surface as immature complexes, or directly to the endocytic pathway for maturation from the trans-Golgi network (TGN), respectively (Kongsvik, Honing et al. 2002) (Bonifacino and Traub 2003). Within acidified late endosomal compartments, resident aspartic and cysteine proteases (i.e. legumain and cathepsins) breakdown antigens into small antigenic peptides, and also cleave in a sequential manner Ii to yield the class II-associated invariant chain peptide (CLIP) found in the MHC-II groove (Hsing and Rudensky 2005). CLIP is displaced by the peptide editor H2-DM (or HLA-DM in humans), an MHC-II-like molecule, and a higher affinity antigenic peptide is loaded onto the mature MHC-II molecule. This complex is

then brought to the surface to be presented to $CD4^+$ T cells bearing a cognate receptor (TCR).

Previous studies have shown a transcriptional regulation by *T. gondii* of MHC-II and other related genes in infected cells, whereby interferon-gamma (IFNγ)-induced transcription is inhibited in infected cells (Luder, Lang et al. 2003) (Lang, Algner et al. 2006) (Kim, Fouts et al. 2007). Nevertheless, MHC-II proteins are still synthesized and detected in infected cells (Figure 4.1), yet antigen presentation is still impaired, and priming and activation of $CD4^+$ T cells is abrogated (Luder, Walter et al. 2001) (McKee, Dzierszinski et al. 2004). Therefore, our hypothesis was that the parasite might affect this process not only at the level of transcription, but also at a post-translational level in order to efficiently dampen antigen presentation in this context.

The aim of this study was to assess the impact of *T. gondii* infection on other key components of the MHC-II antigen presentation pathway, namely the invariant chain and H2-DM, and on the endocytic pathway in global way. Here, we show that Ii expression is discoordinated from that of MHC-II and H2-DM in *T. gondii*-infected pAPCs. Ii expression is induced by the parasite without exogenously added IFNγ or endogenous type IFNs and TNFα, and acts as a dominant negative on MHC-II presentation of endogenously-acquired, parasite-derived antigens. In addition, opposing expression patterns of Ii and H2-DM have an effect *in vivo* on parasite dissemination towards lymphoid organs, $CD4^+$ T cells activation, and IFNγ production during acute infection, but also on cyst numbers and survival at the chronic phase of the infection. Furthermore, we report a more general effect by *T. gondii* on the endocytic pathway during infection with effects on endosomal proteases, antigen processing and other functions.

4.3. Materials and Methods

4.3.1. Mice

Four to 6-week old wild-type C57BL/6 and Balb/c mice were purchased from Charles River Laboratory (Wilmington, MA), and Ii knock-out mice in the Balb/c (CAn.129S6(B6)-*Ii*^{tm1Liz}/J) and C57BL/6 (B6.129S6-*Ii*$^{tm1Liz/}$J) backgrounds (Bikoff, Huang et al. 1993), and H2-DM knock-out mice (B6.129S4-*H2-DMa*^{tm1Doi}/J) in the C57BL/6 background (Miyazaki, Wolf et al. 1996) were purchased from Jackson Laboratory (Bar Harbor, Maine) and bred in-house. Double knock-out animals were generated by cross-breeding Ii and H2-DM single knock-out lines, and cross-breeding the progeny for three generations. Genotype was confirmed by PCR. Type I IFN receptor knock-out in the C57BL/6 background (B6.129S2-*Ifnar1*^{tm1Agt}/Mmjax) (Muller, Steinhoff et al. 1994) were purchased from the Mutant Mouse Regional Resource Centers (MMRRC) (Bar Harbor, Maine). All animals were housed and maintained according to the McGill University Animal Care Committee (permit AUC #5380). Hind leg bones from Ii$^{-/-}$ and TNF$\alpha^{-/-}$ mice in the C57BL/6 background, to generate bone marrow-derived pAPCs, were kind gifts from Elizabeth Bikoff (University of Oxford) and Jörg Fritz (McGill University), respectively.

4.3.2. Parasites and Host Cell Cultures

Type I virulent *T.gondii* cultures of the RH strain, wild-type (WT), transgenic lines, and type II avirulent Prugniaud (Pru) *Δhgxprt* (hypoxanthine-guanine-xanthine phosphoribosyltransferase), kind gift from D. Soldati-Favre (University of Geneva) tachyzoites were maintained by serial passage in human foreskin fibroblasts (HFF) (ATCC, Manassas, VA), as previously described (Roos, Donald et al. 1994). The carbamoyl phosphate synthetase-II deletion mutant (*ΔcpsII*) (Fox and Bzik 2002) was maintained in culture in the presence of exogenous uracil 0.2 mM. Transgenic parasite clonal lines were engineered to express the fluorescent marker red fluorescent protein (RFP) (DsRed, BD

Clontech, Palo Alto, CA) in the cytosol, and the yellow fluorescent protein (YFP) secreted in the parasitophorous vacuole (PV), or, in the *ΔcpsII* background, the model antigen Eα (I-Eα peptide from Balb/c haplotype, (Itano, McSorley et al. 2003) fused to RFP in the cytosol, or secreted in the PV. The *ptub*-RFP/*sag*CAT and the *ptub*P30-YFP/*sag*CAT plasmids (Dzierszinski and Hunter 2008), and the *ptub*Eα-RFP/*sag*CAT and the *ptub*P30-Eα-RFP/*sag*CAT plasmids (Pepper, Dzierszinski et al. 2008) were previously described. Toxostatin 1 and 2 knock-outs, referred to as *Δcys1* and *Δcys2* respectively, were generated using the KU80 system as previously described (Fox, Ristuccia et al. 2009).

Bone marrow-derived macrophages and dendritic cells were obtained by differentiating precursor cells from murine bone marrow, as previously described (Weischenfeldt and Porse 2008), (Lutz, Suri et al. 2000). Briefly, mice were euthanized by CO_2 asphyxiation, and hind legs were collected in Dulbecco's modified Eagle's medium (DMEM). Marrow was flushed out of the bones, and live precursor cells were counted using trypan blue exclusion staining. For bone marrow-derived macrophages (BMMΦ), 5 x 10^6 precursor cells were resuspended in culture medium (DMEM, 10% FBS, 2 mM L-glutamate, 1,000 U/ml penicillin, 1,000 µg/ml streptomycin, 50 µg/ml gentamicin, 2.5% HEPES, 55µM beta-mercaptoethanol, 1 mM sodium pyruvate (Wisent, St-Bruno, Quebec, Canada)) supplemented with 30% L929 fibroblast supernatant (containing M-CSF), and cells were seeded in tissue culture-treated Petri dishes. Medium was changed three days later. Differentiated macrophages were used after 8 days for the assays. As for bone marrow-derived dendritic cells (BMDCs), 2 x 10^6 precursor cells were resuspended in culture medium (RPMI, 10% FBS, 2 mM L-glutamate, 1,000 U/ml penicillin, 1,000 µg/ml streptomycin, 50 µg/ml gentamicin, 2.5% HEPES, 55µM beta-mercaptoethanol) supplemented with 40 ng/ml of rGM-CSF and 10 ng/ml rIL-4 (Peprotech, Rocky Hill, NJ) in Petri dishes. Feeding medium was added on day 3 and replaced on day 6 after seeding. Cells were used on day 7.

4.3.3. Parasite whole and high speed supernatant (HS) lysates, and bicinchoninic acid (BCA) assay for protein quantification

T. gondii whole lysates were prepared from 2-5 x 10^9 freshly lysed-out RH WT tachyzoites. Parasites were resuspended in ice-cold phosphate buffered saline (PBS), and subjected to three 5 minute-cycles of freeze-thaw from liquid nitrogen (N_2) to a 37°C water bath. Then, parasites were sonicated on ice for 10 minutes, with one second-pulses at 30% duty cycle. Protein concentration was determined by the bicinchoninic acid (BCA) assay (Pierce, Rockford, IL), according to the manufacturer's specifications. Protein concentration was adjusted to 2,500 µg/ml and lysates aliquots were stored at -80°C until assay.

4.3.4. *In vitro* infection for invariant chain induction

Day 7 bone marrow-derived macrophages (BMMΦ) were plated at 3 x 10^5 cells per well in 24 well-plates, and incubated overnight to allow cells to adhere. On the following day, cells were inoculated with freshly harvested *T. gondii* tachyzoites at a multiplicity of infection (MOI) of 3:1. When required, parasites were stained with CellTrace Far Red DDAO-SE (Molecular Probes, Carlsbad, CA) at 20 µM in DMEM for 30 minutes at room temperature before inoculating the macrophages. After inoculation, cells were incubated for 4 hours, then extracellular parasites where rinsed away, and fresh medium was added with or without interferon gamma (IFNγ) at a final concentration of 100 U/ml (BioSource, Carlsbad, CA) and cultures were incubated for 20 hours, or at the indicated times.

4.3.5. Antigen presentation assay

Day 7 BMDCs were plated at 3 x 10^5 cells per well in 24 well-plates. Cells were then inoculated with freshly harvested *T. gondii* tachyzoites at an MOI of 3:1 for live parasites (RHΔΔ ptub RFP, RHΔcpsII ptub Eα-RFP, and RHΔcpsII ptub P30-Eα-RFP) or 8:1 for heat-killed parasites (RHΔcpsII ptub Eα-RFP).

After 4 hours of incubation, fresh medium was added supplemented or not with IFNγ at a final concentration of 100 U/ml, and pulsed or not with Eα peptide (ASFEAQGALANIAVDKA) at concentrations of 1, 5, or 10 µg/ml. Cells were incubated for 18-20 hours until harvested for flow cytometry analysis.

4.3.6. Flow cytometry and cell sorting

Ii (or CD74) expression by BMMΦ was assessed by flow cytometry using a BD FACSAria and analyzed with FACSDiva software (BD Biosciences, San Jose, CA). First, Fc receptors were blocked by adding rat IgG and rat anti-mouse CD16/32 (Fcγ III/II) (clone 2.4G2) (BD Biosciences) for 15 minutes on ice. After blocking, cells were stained with a fluorescein isothiocyanate (FITC)-conjugated rat anti-mouse CD74 (clone In-1) for 30 minutes on ice. For intracellular staining, cells were first fixed in 1% paraformaldehyde (PFA) for 10 minutes on ice, and then the fixative agent was quenched with 0.1 M glycine PBS, and the cells were resuspended in permeabilization buffer (0.05% saponin, 0.1% BSA in PBS) for 20 minutes on ice. After permeabilization, cells were stained using the above mentioned antibody. Isotype-matched antibody, rat IgG2b,κ-FITC, was used as a staining control (eBiosciences, San Diego, CA). After staining and washing, cells were fixed again in 1% PFA and analyzed by flow cytometry.

Presentation of the model antigen Eα in the context of MHC-II molecules by BMDCs was assess by flow cytometry after staining cells with a FITC-conjugated anti-Eα52-68 peptide bound to I-Aβ (clone YAe) antibody (eBioscience), as previously described (Murphy, Lo et al. 1989); live cells were analyzed. Flow cytometry data was analyzed using FlowJo software (Tree Star, Ashland, OR).

Sorting of macrophages and dendritic cells cultures was carried out using a BD FACSAria (BD Biosciences). Cultures were infected with RHΔΔ ptub P30-YFP tachyzoites at an MOI of 4:1 for 4 hours. Then, extracellular parasites were washed away, and fresh medium was added with or without 100 U/ml IFNγ.

Cells were incubated for 20 hours. After incubation, cells were harvested and stained with 50 μg/ml propidium iodide (PI) (EMD Chemicals, Gibbstown, NJ), prior to sorting; fluorescent cells labeled with PI were considered dead and excluded. Live cells were then gated according to infection state, whereas YFP-positive cells were infected and YFP-negative cells were not, and collected separately. Sorted samples were aliquoted and stored at -80°C.

4.3.7. *In vivo* infection and cell analysis

Four to 6-week old wild-type C57BL/6 mice were infected with 10^6 RHΔΔ *ptub*-RFP tachyzoites intraperitoneally (IP). Mesenteric lymph nodes (MLN) of infected animals were harvested 5 days post-infection, filtered through 70 μm-pore size nylon mesh cell strainers (BD Biosciences), and stained for flow cytometry. Staining protocol was performed as mentioned above, using the following antibodies: PerCP-Cy5.5-conjugated rat anti-mouse CD11b (M1/70), PE-Cy7-conjuagted Armenian hamster anti-mouse CD11c (N418), and FITC-rat anti-mouse CD74 (In-1). Isotype-matched controls were prepared in parallel (rat IgG2b,κ-FITC and –PerCP-Cy5.5, and Armenian hamster IgG-PE-Cy7).

T cell analysis was performed on cells collected from acutely infected, 4-6 week old wild-type, $Ii^{-/-}$, H2-$DM^{-/-}$, and $Ii^{-/-}$ H2-$DM^{-/-}$ mice. Briefly, mice were infected IP with 10^3 PruΔ tachyzoites. After 8 days of infection, MLN were collected, filtered through 70 μm-pore size nylon mesh cell strainers and stained for flow cytometry using the following antibodies: FITC-Armenian hamster-anti-mouse CD3ε (145-2C11), phycoerythirn (PE)-rat anti-mouse-CD4 (L3T4), allophycocyanin (APC)-rat anti-mouse CD25 (PC61.5), PE-Cy7-rat anti-mouse CD44 (IM7), and APC-eFluor780-rat anti-mouse CD62L (MEL-14) (eBioscience). Isotype-matched controls were prepared in parallel (Armenian hamster IgG-FITC, rat IgG2b,κ-PE and –PE-Cy7, rat IgG1,λ-APC, and rat Ig2a,κ-APC-eFluor780). Serum from these acutely infected mice and non-infected mice, as controls, was collected as well. Interferon-gamma levels were measured by

enzyme-linked immunosorbent assay (ELISA), using the eBioscience Mouse IFN-gamma ELISA Ready-SETGo! Kit according to the manufacturer's specifications.

For chronic infections, 10^3 PruΔ tachyzoites were injected intraperitoneally (I.P.). For RT-PCR analysis of brain cyst burden, brains were collected 20 days after post-infection. For histology, infected brains were collected 10, 15, 20, and 25 days post-infection.

4.3.8. Histology

Brains from WT, $Ii^{-/-}$, H2-$DM^{-/-}$, and double KO ($Ii^{-/-}$ H2-$DM^{-/-}$) mice 10, 15, 20, and 25 days after infection with 10^3 PruΔ I.P. were collected and fixed in neutral buffered formalin (10% v/v). Brains from non-infected control animals were collected as well. After fixation, 3-4 cross-sections were taken through the cerebrum and one representative section through the cerebellum. The sections were embedded in paraffin, and were placed onto glass microscopy slides. The slides were stained with hematoxylin and eosin. Pictures were taken using a Nikon Eclipse E800 microscope equipped with a Nikon digital camera DXM1200F and Nikon ACT-1 software.

4.3.9. Immunofluorescence and colocalization microscopy

Day 7 BMMΦ cultures were plated at 5 X 10^4 cells on glass coverslips in 24 well-plates, at incubated overnight at 37°C, 5% CO_2 to allow cells to firmly adhere to coverslips. The following day, cells were infected with freshly lysed out *T. gondii* RH WT tachyzoites at an MOI 2:1. Alternatively, cells were inoculated with heat-killed (HK) parasites, heated at 56°C for 10 minutes prior to inoculation, at an MOI of 10:1, treated with *T. gondii* lysates at a concentration of 200 μg/ml, infected with *Leishmania donovani* promastigotes (kind gift from Armando Jardim, Institute of Parasitology, Sainte-Anne-de-Bellevue, Canada) at an MOI of 15:1, or infected with *Salmonella enterica* Typhimurium 14028

bacteria (kind gift of Hervé Le Moual, McGill University, Montreal, Canada) at an MOI of 20:1 in the absence of antibiotics. After 4 hours extracellular parasites or bacteria were rinsed away, and fresh medium was added; antibiotics were re-supplemented to wells inoculated with bacteria. Cells were fixed after 24 hours or at the otherwise indicated times with 3.7% paraformaldehyde (PFA) in PBS for 10 minutes at room temperature. After fixation, coverslips were washed extensively with PBS, and permeabilized with Triton X-100 0.2% in PBS for 5 minutes, then blocked using 10 mg/ml bovine serum album fraction V (BSA), 10% FBS in PBS with mouse IgG (Sigma) for 15 minutes. Primary antibodies were incubated for 1 hour at room temperature: rat anti-mouse CD74 (clone In-1), rat anti-mouse IA/IE (MHC-II) (eBioscience), polyclonal rabbit anti-mouse Giantin (Golgi), polyclonal rabbit anti-mouse GRP78 BiP (ER), polyclonal rabbit anti-mouse EEA-1 (early endosomes), polyclonal rabbit anti-mouse LC3A/B (autophagosomes) (Abcam, Cambridge, MA), and polyclonal goat anti-mouse CD63 (M-13) (lysosomes) (Santa Cruz Biotechnology, Santa Cruz, CA). Fluorophore-conjugated secondary antibodies were incubated for 1 hour at room temperature: donkey anti-rat IgG (H+L) Alexa Fluor 488, and goat anti-rabbit IgG (H+L) Alexa Fluor 488 of 594 (Invitrogen, Carlsbad, CA). To stain the DNA and visualize the nuclei, samples were stained with 4',6-diamidino-2-phenylindole dilactate (DAPI). Coverslips were then mounted onto microscope slides with Fluoromount G (Southern Biotech, Birmingham, AL). Samples were visualized using a Nikon Eclipse TE2000-U microscope (Tokyo, Japan), images were deconvulved using AutoQuant X software (Media Cybermetrics, Phoenix, AZ), and images were processed with Adobe Photoshop (SanJose, CA), or, for colocalization experiments, a Zeiss LSM710 confocal microscope with Zen2010 software (Zeiss Canada, Toronto, Canada) were used to acquire images, and image processing and statistical calculations were performed with Fiji.

4.3.10. Western blotting

Sorted cells and extracellular tachyzoites were resuspended in lysis buffer (1% Triton X-100, 10 mM Tris, 150 NaCl), supplemented with protease inhibitor cocktail (Sigma-Aldrich) and DNase I (1 µg/mL). Protein material was precipitated in a methanol-ethanol-acetone mixture (50, 25, and 25% respectively) at -80°C overnight. After precipitation, protein material was resuspended in SDS-PAGE reducing buffer containing beta-mercaptoethanol, boiled for 5 minutes, and loaded onto a pre-cast 4-20% Tris-HCl minigel (Bio-Rad, Hercules, CA). Protein material equivalent to 2 x 10^6 BMMΦ or 10^6 for BMDCs, and 10^8 extracellular parasites were loaded per lane. Gels were ran at 20V using a Tetracell apparatus (Bio-Rad), and then transferred to nitrocellulose membranes. Membranes were blocked in 5% dry skim milk in TTBS (Tris-HCl 15 mM, NaCl 140 mM, Tween 20 0.05%) overnight at 4°C. Membranes were probed with a monoclonal rat anti-mouse CD74 clone In-1 (BD Pharmingen, San Jose, CA), followed by a goat-anti-rat IgG (H+L) antibody conjugated to horseradish peroxidase (HRP) (Santa Cruz Biotechnology). Bands were revealed using SuperSignal West Femto Substrate or ECL West Blotting Substrate (Pierce), according to manufacturer's specifications. Loading control was performed by probing with a rabbit anti-cytoskeletal actin antibody (Bethyl Laboratories, Montgomery, TX), followed by a goat-anti-rabbit IgG (H+L) antibody conjugated to HRP (Bio-Rad), and the presence of parasites was verified by probing with mouse anti-AcGFP-1 antibody, followed by a goat-anti-mouse IgG (H+L) antibody conjugated to HRP (Bio-Rad).

4.3.11. Reverse transcription (RT) and real time-PCR (RT-PCR)

Real time-PCR was performed using the Power SYBR Green Cells-to-Ct kit (Applied Biosystems, Carlsbad, CA), according to the manufacturer's instructions. Briefly, 10^5 sorted cells were lysed with the Lysis solution provided with the kit, followed by the reverse transcription (RT) using the Bio-Rad DNA Engine (Peltier Thermal Cycler) and the 20X RT Enzyme Mix with 2X SYBR RT

buffer. The concentration of the synthesized cDNA was determined using a NanoDrop ND-1000 (Wilmington, DE). PCR reactions were performed in a 7500 Real-Time PCR System (Applied Biosystems) using the Power SYBR Green PCR Master Mix, 400 nM final concentration of each designed PCR primer (19-25 nucleotides) (Appendix Table 1), and 3 µg of cDNA in a total volume of 20 µl. The β-actin primer provided in the SYBR Green Cells-to-Ct Control kit was used to amplify the endogenous control gene for normalization of the transcripts. The mRNA transcription level analysis was assessed using the $2^{-\Delta\Delta Ct}$ method compared to Δ the non-infected and non-stimulated BMMΦ sample used as a control (Livak and Schmittgen 2001).

4.3.12. Genomic DNA isolation and quantification of parasite burden by RT-PCR

Genomic DNA was isolated from MLN of acutely infected mice or brains of chronically infected animals using Roche High Pure PCR Template Preparation Kit, according to the manufacturer's specifications. To measure acute parasitemia or cyst burden, the 35-fold repetitive *T. gondii* B1 gene (Burg, Grover et al. 1989) was amplified by real-time PCR using Power SYBR Green PCR Master Mix (Applied Biosystems) with $MgCl_2$ concentration adjusted to 3.5 µM in a 50 µl reaction volume, 0.5 µg of template gDNA, and 0.5 µM of each forward primer (5'-TCCCCTCTGCTGGCGAAAAGT-3') and reverse primer (5'-AGCGTTCGTGGTCAACTATCGATTG-3') (Integrated DNA Technologies, Coralville, IO; (Lin, Chen et al. 2000). The B1 gene was amplified using an ABI 7500 RT-PCR System using a 10 minutes of initial denaturation at 95°C, followed by 35 cycles of 15 seconds of denaturation at 95°C, 30 seconds of annealing at 52°C, and 30 seconds of extension at 72°C. The threshold value was defined as 30 times the standard deviation of the baseline fluorescent signal, and cycle threshold values (Ct) were acquired during the annealing step. In order to normalize the Ct values, the mouse β-actin gene was amplified in the same conditions outlined above in separate tubes, but with 0.2 µM of each forward (5'-

CACCCACACTGTGCCCATCTACGA-3') and reverse (5'- CAGCGGAACCG-CTCATTGCCAATGG-3') primers (Jauregui, Higgins et al. 2001), 2.5 μM $MgCl_2$.

4.3.13. Cathepsins and legumain (AEP) enzymatic activities

Wild-type or $Ii^{-/-}$ day 7 BMDCs or day 8 BMMΦ cultures were plated at 2 x 10^6 cells per well in 6 well-plates, infected with RH WT tachyzoites (MOI 3:1) for 4 hours, extracellular parasites were rinsed away, fresh medium was added, and cultures were incubated for 20 hours. Cells were harvested and lysed using buffers of different depending on which enzyme was to be tested: 0.1 M KH_2PO_4, 0.5% Triton X-100, 1 mM EDTA, at pH 5.5 for cathepsin L and AEP, and pH 7.5 for cathepsin S. After lysis, material was spun and supernatant was collected. Protein concentration was measured by BCA, as described earlier. Material was added to an assay mixture at a final concentration of 100 μg/ml. Assay buffer compositions varied: 20 mM citric acid, 60 mM Na_2HPO_4, 0.1% CHAPS, 1 mM EDTA, 1 mM DTT, pH 4.3 for AEP, 340 mM sodium acetate (NaOAc), 60 mM acetic acid, 4 mM EDTA, 4 mM DTT, pH 5.5 for cathepsin L, and 50 mM NaOAc, 4 mM DTT, pH 5.5 for cathepsin L. For each enzyme to be tested, fluorogenic protease-specific substrates were added to each mix: Z-AAN-AMC for AEP, Z-FR-AMC for cathepsin L, and cathepsin S-substrate (EMD Chemicals, Gibbstown, NJ). Mixtures were incubated for 1 hour at 37°C, and reactions were stopped by adding 100 mM sodium monochloroacetate, 70 mM acetic acid, 30 mM sodium acetate, pH 4.3 to cathepsin L mixture, and trifluoroacetic acid final 0.5% for AEP and cathepsin S. Fluorescence values were obtained using a Varian Cary Eclipse spectrofluorometer (Agilent Technologies, Santa Clara, CA): 360 nm and 460 nm for AEP, 370 nm and 460 nm for cathepsin L, and 340 nm and 405 nm for cathepsin S, excitation and emission wavelengths, respectively for each substrate.

4.3.14. Endosomal pH measurement

Endosomal pH measurement was carried out as previously described (Savina, Vargas et al. 2010). Briefly, WT or $Ii^{-/-}$ day 8 BMMΦ were plated at 2 x 10^6 cells per well in 6 well-plates, infected with RHΔΔ *ptub*-RFP tachyzoites (MOI 3:1) for 4 hours, extracellular parasites were rinsed away, fresh medium was added, and cultures were incubated for 20 hours. Cells were harvested and pulsed with polybead amino 3.0 µm microspheres (Polysciences, Warrington, PA) labelled with fluorescein isothiocyanate (FITC) (Sigma) and FluoProbes647 (FP647) (Interchim, Montluçon, France) for 15 minutes at 37°C in CO_2-independent medium (Invitrogen). Cells were extensively washed with ice-cold PBS, resuspended in medium and incubated at 37°C, 5 % CO_2. Aliquots of the cell suspensions were taken at different time points (chase) and analyzed immediately by flow cytometry, gating on cells having internalized a single bead, and mean fluorescence intensity (MFI) values were obtained. Standard curves were generated by resuspending cells in CO_2-independent medium at different pH values, ranging from 3 to 8.5 with 0.5 increments, and adding lysomomotropic agents 40 mM final ammonium chloride and 0.1% final sodium azide to artificially impose the pH of medium in the endocytic pathway. Since the fluorescence intensities of FP647 is pH-insensitive and FITC is pH-sensitive, ratios FITC / FP647 were calculated and plotted against the known pH values of the standards.

4.4. Results

4.4.1. Although MHC-II expression is inhibited, MHC-II molecules are still detected in infected cells

It is well known that *T. gondii* inhibits MHC-II expression in infected pAPCs (Luder, Lang et al. 1998) (Luder, Walter et al. 2001) (McKee, Dzierszinski et al. 2004). However, upon closer inspection of these infected cells, MHC-II molecules were still detected. First, microscopy observations revealed

that MHC-II molecules were found in infected cells, although quite reduced compared to the non-infected cell counterparts, and appeared as small dots within the cells (Figure 4.1A). Second, flow cytometry analyses of surface and total (i.e. surface + intracellular) MHC-II molecules correlated with microscopy data, whereby MHC-II molecules were detected in IFNγ-stimulated infected cells (Figure 4.1B). Third, Western blot analyses of FACS-sorted murine BMMΦ cells revealed the presence of SDS-resistant, mature MHC-II molecules in infected cells (Figure 4.1C). Altogether, these observations suggest that despite inhibiting MHC-II expression, some molecules are still synthesized and mature in *T. gondii*-infected cells, yet MHC-II antigen presentation is impaired nonetheless (Luder, Walter et al. 2001) (McKee, Dzierszinski et al. 2004). Hence, another layer of inhibition beyond transcription and translation must be involved to ensure thorough inhibition of MHC-II presentation in infected cells. From this hypothesis, we turned to other major components of the MHC-II pathway and assessed how their expression was influenced during infection by *T. gondii*.

4.4.2. Invariant chain (Ii) molecules accumulate mostly in the endoplasmic reticulum (ER) of *T. gondii*-infected cells until egress of the parasite, even in the absence of IFNγ

Although MHC-II and Ii gene transcription and protein expression are typically coordinated (Glimcher and Kara 1992), not only was Ii transcription induced, Ii molecules actually accumulated in BMMΦ infected with *T. gondii* tachyzoites without IFNγ stimulation (Figure 4.2), while MHC-II expression was not induced. The accumulation of Ii proteins was detected in infected cells (full arrows) approximately 15 hours after parasite inoculation, and occurred until egress of the parasites. However, Ii accumulation was not observed in neighboring non-infected cells (empty arrows) of the same cultures, suggesting that the induction was cell autonomous.

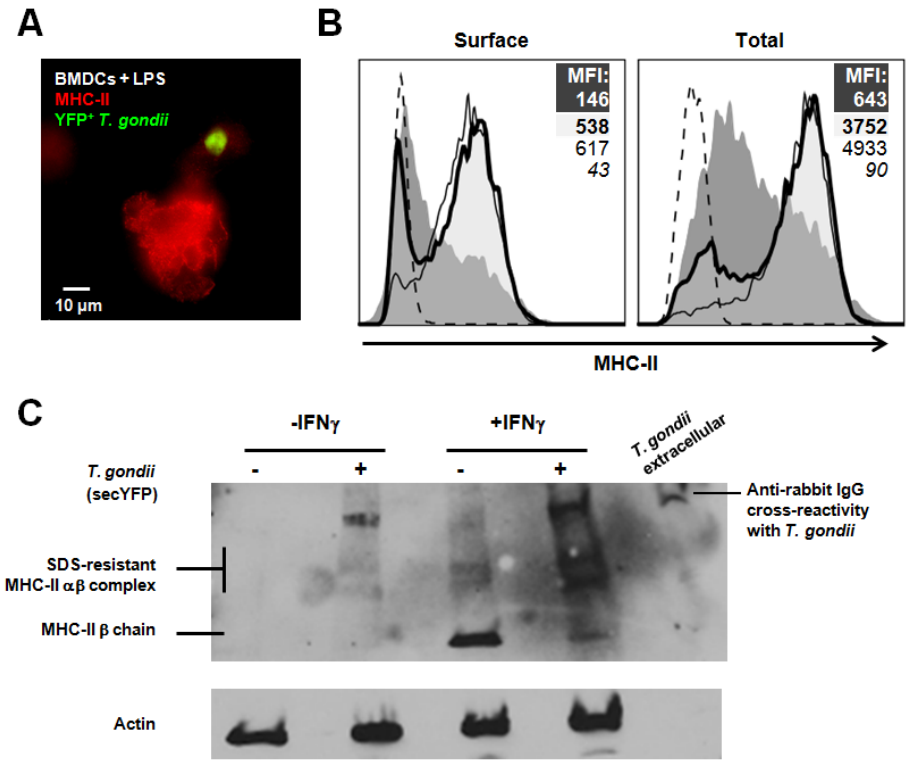

Figure 4.1: Although their expression is decreased, MHC-II molecules are still detected in *T. gondii*-infected cells. (A) BMDCs were infected with YFP-expressing parasites, stimulated overnight with LPS, fixed, and stained for MHC-II. Microscopic observations revealed that MHC-II molecules could still be detected in the infected cell (top) still, although at levels quite reduced compared to the non-infected cells (bottom). (B) Flow cytometry analysis of IFNγ-stimulated BMMΦ show that MHC-II molecules were detected in infected cells (Tg^+, filled gray curve) both at the surface and intracellularly (total staining). Also, non-infected cells within an infected culture (Tg^-, bold shaded curve) displayed lower MHC-II levels compared to the control non-infected culture (Tg^0, thin curve), suggesting that either parasite molecules are being released or that infected cells secret factors that inhibit MHC-II expression of the neighbouring cells. Staining with isotype-matched control antibodies are shown by the dashed curve. Mean fluorescence intensity (MFI) values are indicated for each population (i.e. italicized for isotype control, standard font for Tg^0 control cells, bold font for Tg^- cells, and white font in dark box for Tg^+ cells). (C) Western blotting was performed on infected BMMΦ cultures that were stimulated with 100 U/ml IFNγ or left non-stimulated, and sorted by FACS according to their infection status (YFP^- or YFP^+). Although reduced compared to IFNγ-stimulated non-infected cells, MHC-II β chain as well as SDS-resistant, mature MHC-IIαβ complexes were detected in infected cells. This last observation suggest that, although transcription is inhibited, MHC-II molecules can still be synthesized and that other post-translational mechanisms come into play to block antigen presentation.

Colocalization experiments revealed that Ii molecules accumulated predominantly in the endoplasmic reticulum (ER) of infected cells (Figure 4.3A), but were detected to a lesser extent in the Golgi and early endosomes (EE) (Figure 4.3B and 4.3C). No colocalization was observed in $LC3^+$ (autophagosomes) nor $CD63^+$ (lysosomes) compartments (Figure 4.4A and 4.4B). These observations

suggest that the majority of Ii molecules are withheld in early compartments, and do not seem to trickle down to mature compartments. In a model using Ltk- mouse fibroblasts stably transfected to express Ii without MHC-II molecules, which resembles what is observed in *T. gondii*-infected cells, it was shown that free Ii molecules reached lysosomal and late endocytic compartments by a route that bypassed the Golgi complex (Chervonsky and Sant 1995). Transport of free Ii to lysosomes was inhibited by 3-methyladenine, an inhibitor of the autophagic pathway, a process that can involve direct transport from the ER to lysosomes. However, in our model Ii molecules were detected in the Golgi, but not in lysosomes. Therefore, this might suggest that a different mechanism of Ii trafficking might be at play, or that amounts are too minute to be detected in our system.

4.4.3. Invariant chain (Ii) accumulation occurs intracellularly, but only slightly at the cell surface

In order to determine if the Ii molecules trafficked to the cell surface, different staining techniques for flow cytometry were carried out. When BMMΦ cultures were stained for surface Ii molecules (i.e. without permeabilization of the cell membrane), slight differences in surface Ii expression were observed between non-infected cells and -*T. gondii*-infected cells (Figure 4.5). However, when cells were stained following permeabilization with saponin, a marked increase of Ii levels was revealed in the infected cells. These flow cytometry results show that invariant chain molecules accumulate mostly intracellularly in *T.gondii*-infected BMMΦ, but did not accumulate to the same extent at the cell surface.

Since the induction of Ii expression was observed without addition of IFNγ, we wanted to verify if it was not due to endogenous secretion of TNFα and type I IFNs (α and β), cytokines that can indirectly trigger transcription of class-II genes through different signaling pathways (Melhus, Koerner et al. 1991) (Simmons, Wearsch et al. 2012). BMMΦ from TNFα and type I IFN receptor

(IFN-AR1), which desensitize cells from type I IFNs, KO mice were cultured and infected with *T. gondii*, and Ii expression within these cells was analyzed by flow cytometry (Figure 4.6). Similar to WT cells, infected KO cells displayed higher levels of Ii, arguing that the production of these cytokines are not responsible or do contribute in any significant way to the induced expression observed.

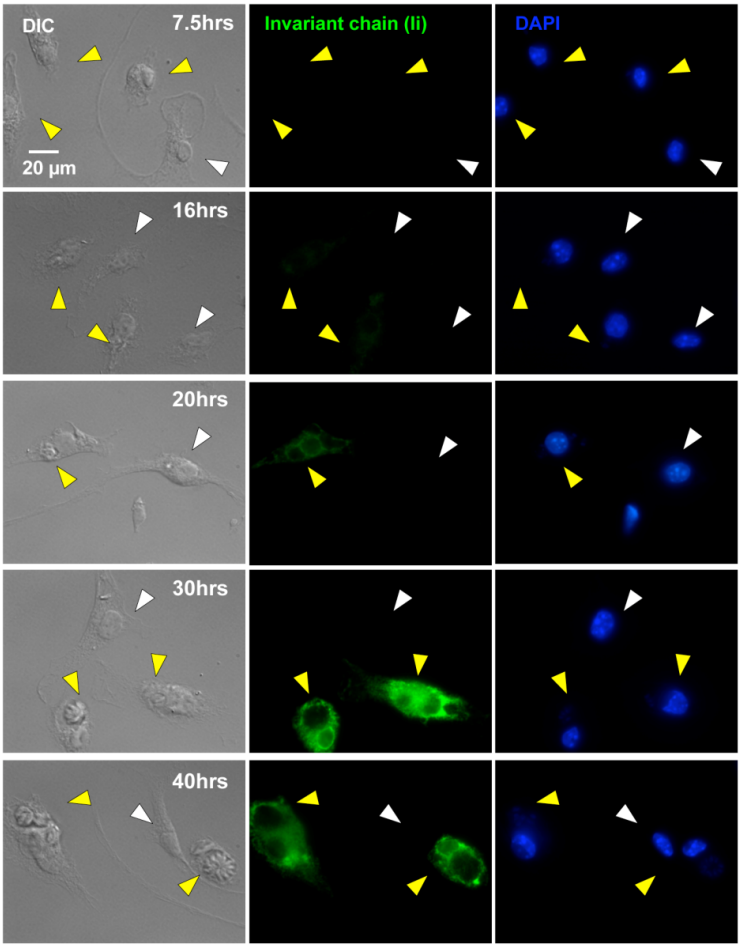

Figure 4.2: *T. gondii* up-regulates Ii protein expression in infected BMMΦ. Infected cells (yellow arrowheads) displayed an increased staining (in green) of the invariant chain in the absence of stimulation by IFNγ, as observed by deconvulution microscopy. The accumulation was observed around 20 hours post-infection, until the egress of the parasites. However, no significant levels of Ii were detected in neighboring non-infected cells (white arrowheads).

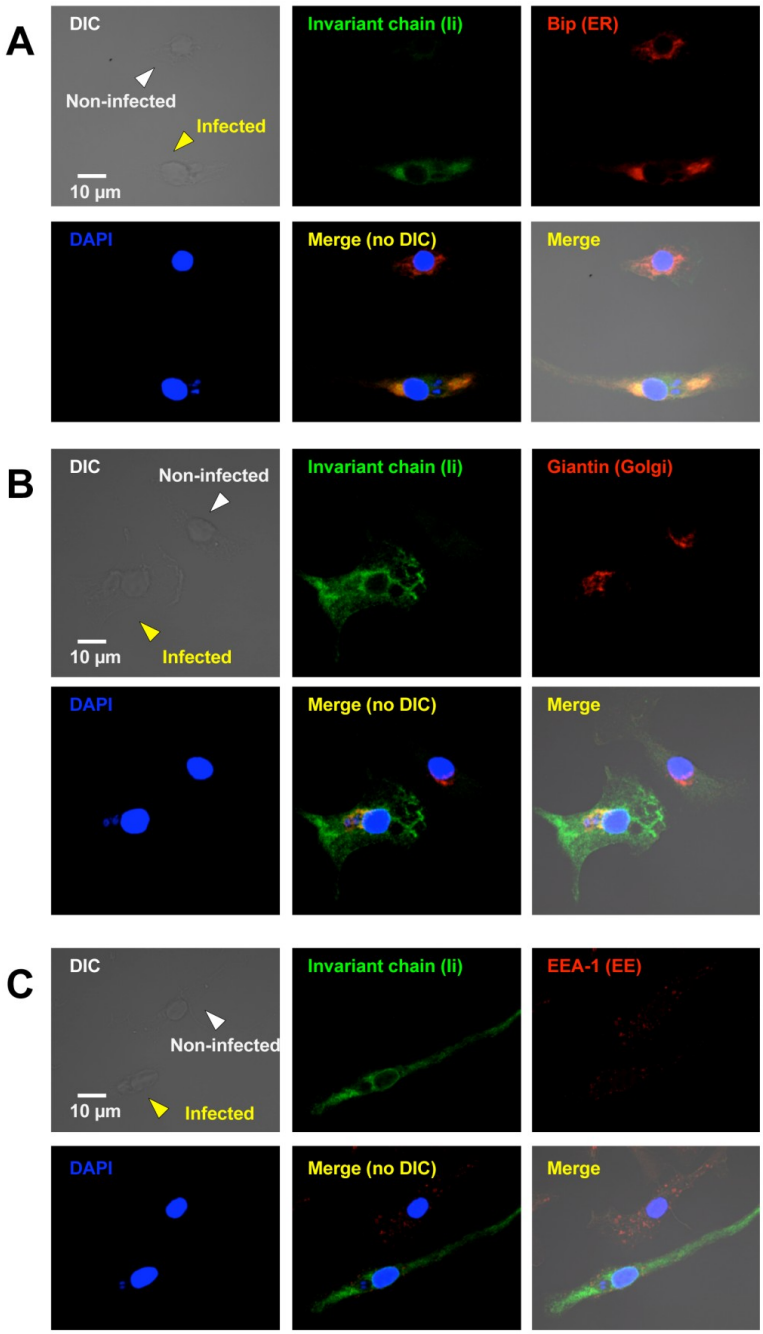

Figure 4.3: Ii accumulates mostly in the ER, but also in the Golgi and EEs in non-stimulated infected BMMΦ. Colocalization experiments for Ii (in green) were carried with different markers (A) for the ER (Bip), (B) the Golgi (Giantin), and (C) early endosomes (EEA-1) (all shown in red). These experiments revealed that the induced Ii proteins, only detected in infected cells (yellow arrows), and colocalized with Bip, an ER maker. The merged images show that the colocalization was very strong, but not complete, with a calculated colocalization coefficient (Rcoloc; where 1 is total colocalization, and 0 no colocalization) of 0.73 and a threshold split Mander's coefficient (tM; where total pixel intensity is normalized to avoid issues with absolute intensities) of 0.74 (Ii found in ER). Ii molecules were also found in the (B) Golgi (Rcoloc = 0.41, tM = 0.37) and (C) EEs (Rcoloc = 0.32, tM = 0.47) to a lesser extent. Note: DIC refers to transmitted light differential interference contrast.

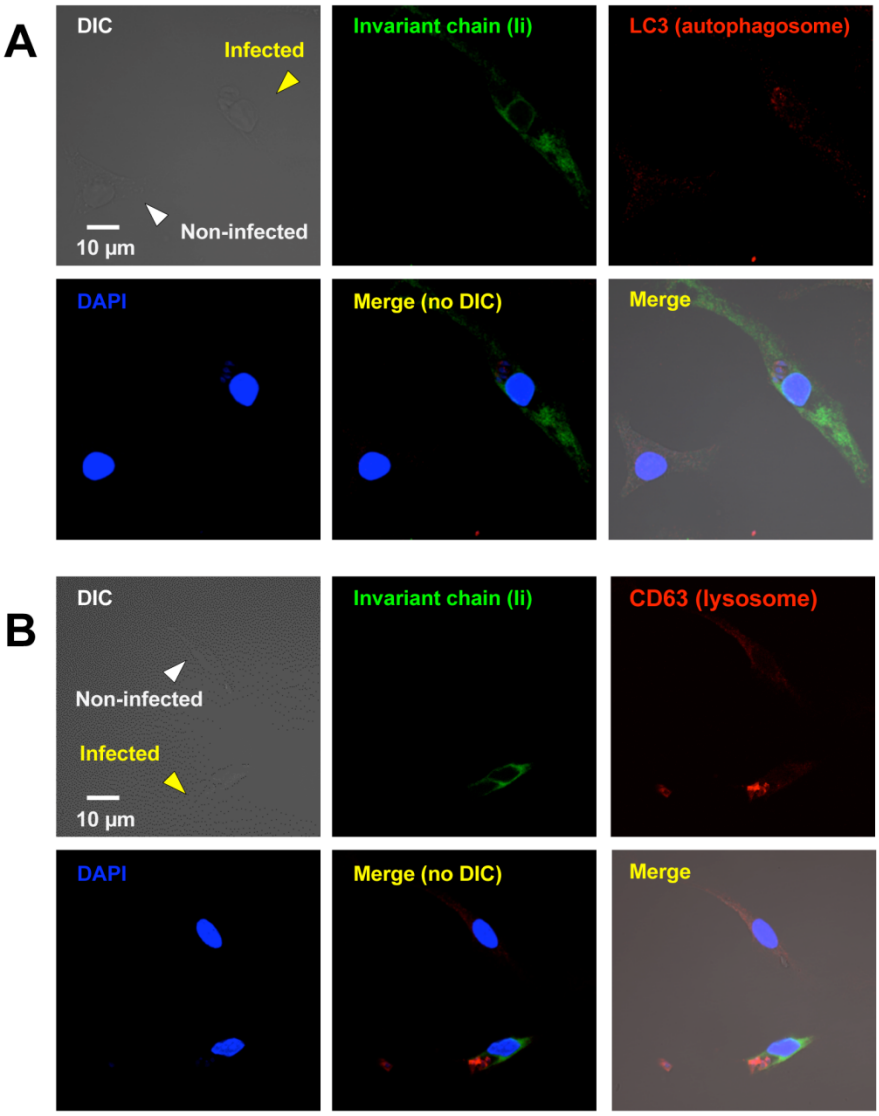

Figure 4.4: Ii does not colocalize with autophagosome or lysosome markers in infected non-stimulated BMMΦ. Colocalization experiments for Ii (in green) were carried with different markers (A) for autophagosomes (LC3), and (B) lysosomes (CD63) (all shown in red). These experiments revealed that the induced Ii proteins, only detected in infected cells (yellow arrows), do not colocalized with LC3 (Rcoloc = 0.03, tM = 0.42) nor CD63 (0.05, tM = 0.36). Taken these observations with those shown on Figure 4.2 (Chapter 4), Ii seemed to accumulate in earlier compartments of the endocytic pathway (ER, Golgi, and EEs), rather than later compartments in infected cells.

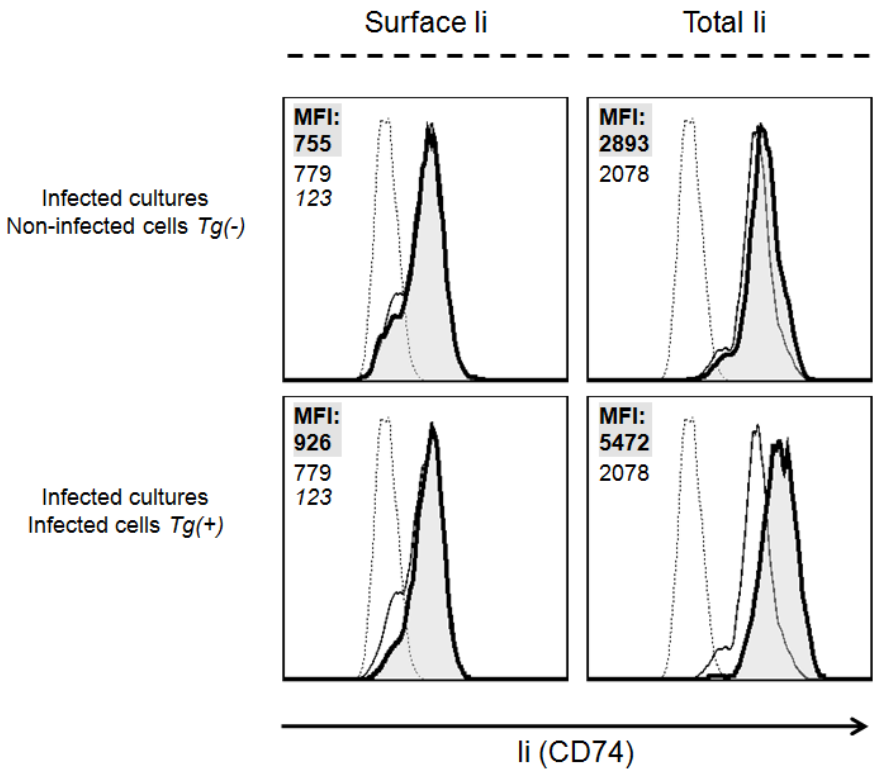

Figure 4.5: The accumulation of Ii occurs intracellularly, but only slightly at the cell surface. BMMΦ cultures were left non-infected (Tg^0, thin curves) or inoculated with CellTrace Far Red DDAO-stained parasites (Tg^- or Tg^+ as indicated, thick line, shaded curves). Cells were stained with a FITC-labelled anti-CD74 antibody either after fixation with 1% PFA, which only stained surface Ii, or after permeabilization with 0.05% saponin, staining surface and intracellular molecules, then analyzed by flow cytometry. The level of staining is reported as mean fluorescent intensity (MFI) values (upon left corner on graphs), as indicated for each population (i.e. italicized for isotype control, standard font for Tg^0 control cells, and bold font for Tg^- and Tg^+ cells). First, no significant differences were observed between non-infected cells (from non-infected or infected cultures, top left graph), while only a slight increase was observed in infected cells (lower left graph) when stained for surface molecules only. However, when cells were permeabilized beforehand, we observed a significant increased of labeling in the infected cells compared to non-infected cells (bottom right graph), indicating that the accumulation was mostly confined to intracellular compartments.

4.4.4. Ii accumulation is triggered by both type I and type II strains and requires active parasite invasion

There is increasing evidence showing significant differences between the type I or virulent, and type II or avirulent strains of *Toxoplasma gondii* regarding the modulation of the immune responses and signaling pathways. For instance, it has been shown that polymorphisms in the secreted rhoptry kinases ROP16 and ROP18 account for virulence and host-pathogen interaction differences between

type I and types II and III (Saeij, Boyle et al. 2006). A single polymorphic amino acid in ROP16 has been shown to lead to differential activation of STAT3 and STAT6, important anti-inflammatory transcription factors, by type I and type II strains (Ong, Reese et al. 2010), (Jensen, Wang et al. 2011). Also, dense granule protein GRA15 from type I and III strains has been shown to alternatively activate infected macrophages, while type II GRA15 activates NF-κB and leads to classically activate infected macrophages (Jensen, Wang et al. 2011). Therefore, we needed to verify if the induction and accumulation of Ii was type-specific. Ii accumulation was observed in BMMΦ infected with either type I RH or type II Pru strains in the absence of IFNγ (Figure 4.7A). Furthermore, active parasite replication was not required, since BMMΦ infected with uracil-deprived *ΔcpsII*, a uracil-auxotroph strain (Fox and Bzik 2002), displayed accumulated intracellular Ii (Figure 4.7B). However, cells treated with parasite lysates or that had phagocytosed heat-killed parasites did not express elevated Ii levels (Figure 4.7C) arguing that active host cell invasion by live parasites is required. These last observations contrast with what is observed for MHC-II inhibition, whereby active invasion is not required and non-infected bystander cells within an infected culture are inhibited to some extent (Stutz, Kessler et al. 2012), and parasite lysates display inhibitory activity (Lang, Algner et al. 2006), suggesting different mechanisms are involved in the inhibition of MHC-II and the induction of Ii.

4.4.5. Induction and accumulation of the invariant chain in infected cells in the absence of IFNγ is specific to infection by *T. gondii*, and is not observed during infection with other intracellular pathogens

To verify if the induction of the expression and accumulation of Ii molecules is specific to *T. gondii* infection or a generalized phenotype to infection by intracellular pathogens, BMMΦ were infected with two other intracellular pathogens *Leishamania donovani* and *Salmonella enterica* Typhimurium, both known to inhibit MHC-II expression (Reiner, Ng et al. 1987), (Kwan, McMaster et al. 1992), (Mitchell, Mastroeni et al. 2004), stained for Ii, and observed by

microscopy. In the absence of IFNγ, both pathogens failed to induce the expression Ii in the host macrophage cells (Figures 4.8A and 4.8B). This last observation suggests that the phenotype seen in *T. gondii*-infected cells is specific to the latter.

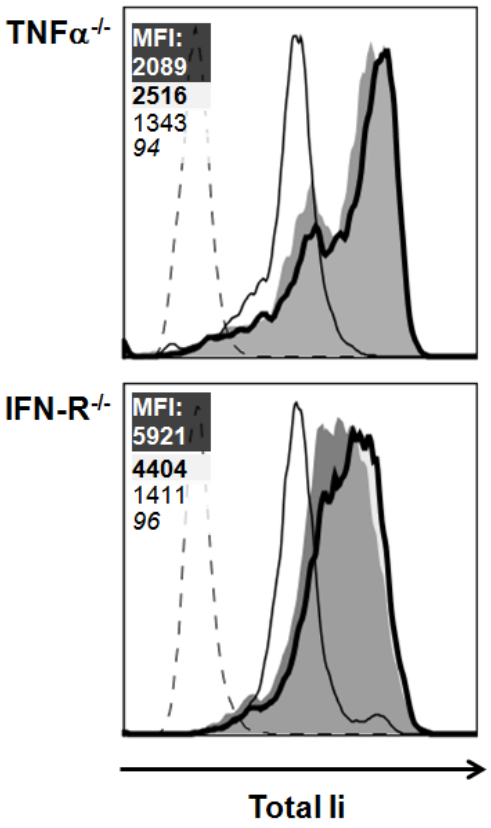

Figure 4.6: Ii induction in infected BMMΦ occurs in the absence of endogenous production of TNFα and type I IFNs. WT, TNFα$^{-/-}$ and IFN-R$^{-/-}$ BMMΦ cultures were left non-infected or infected with CellTrace Far Red DDAO-stained. WT non-infected control cultures (Tg^{0}, thin curves) and infected cells (bold shaded curves) are shown as a reference for the KO cells (filled gray curves). All cultures were left non-stimulated, stained for Ii after permeabilization, and analyzed by flow cytometry. Expression of Ii was induced in infected TNFα$^{-/-}$ and IFN-R$^{-/-}$ macrophages at similar levels compared to the WT counterparts, arguing that endogenous expression of TNFα and type I IFNs, if any, is not involved in the induced Ii expression seen in infected cells. Isotype control is indicated by the dashed curve. Mean fluorescence intensity (MFI) values are indicated for each population (i.e. italicized for isotype control, standard font for non-infected control cells, bold font for infected WT cells, and white font in dark box for infected KO cells).

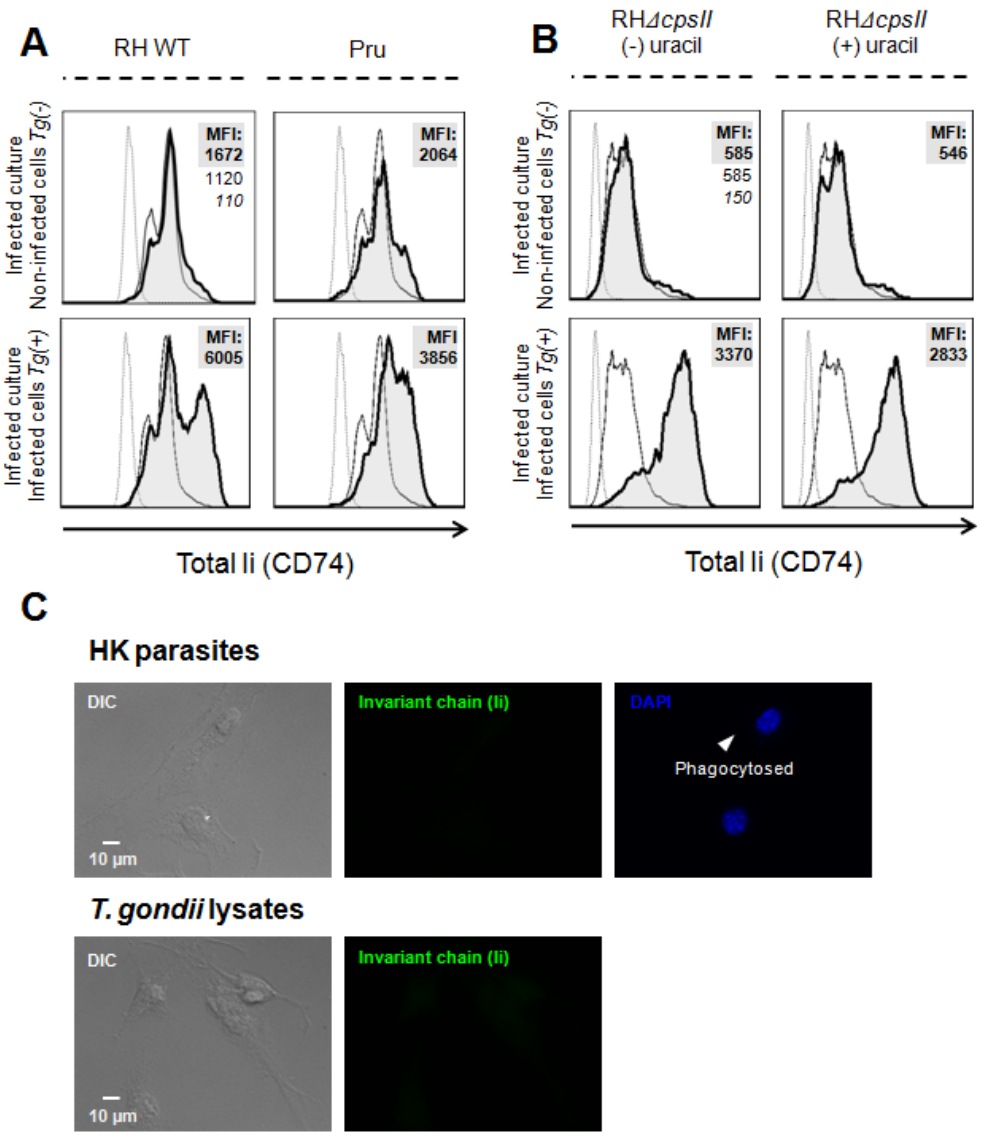

Figure 4.7: Ii accumulation is triggered by both type I and type II strains and does not require active parasite replication, while it is not caused by *T. gondii* lysates and HK parasites. (A) BMMΦ cultures were infected with either type I RH WT (left graphs) or with type II Pru (right graphs) tachyzoites. Cells were permeabilized, stained for total Ii proteins, and analyzed by flow cytometry. Although the accumulation of Ii was slightly weaker in Pru-infected cells (bottom right graph), both types of *T. gondii* induces Ii at higher levels than non-infected cells. Isotype control is indicated by the dashed curve. Mean fluorescence intensity (MFI) values are indicated for each population (i.e. italicized for isotype control, standard font for non-infected control cells, and bold font for infected cells). (B) When BMMΦ were infected with the uracil-auxotroph mutant RH*ΔcpsII,* the accumulation of Ii was observed, even when the parasites were depraved of exogenous uracil in the culture and were not able to replicate (lower right graph, bold shaded curve). No significant differences were reported when the parasites were supplied exogenous uracil and allowed to replicate (lower right graph, bold shaded curve) compared to uracil-deprived infections. Again, induction of the invariant chain was not seen in non-infected cells, even within infected cultures (top left and right graphs). (C) However, live parasites seemed to be required for the induction of Ii, since BMMΦ fed HK parasites (top panel) or treated with *T. gondii* lysates (lower panel) did not displayed elevated levels of Ii.

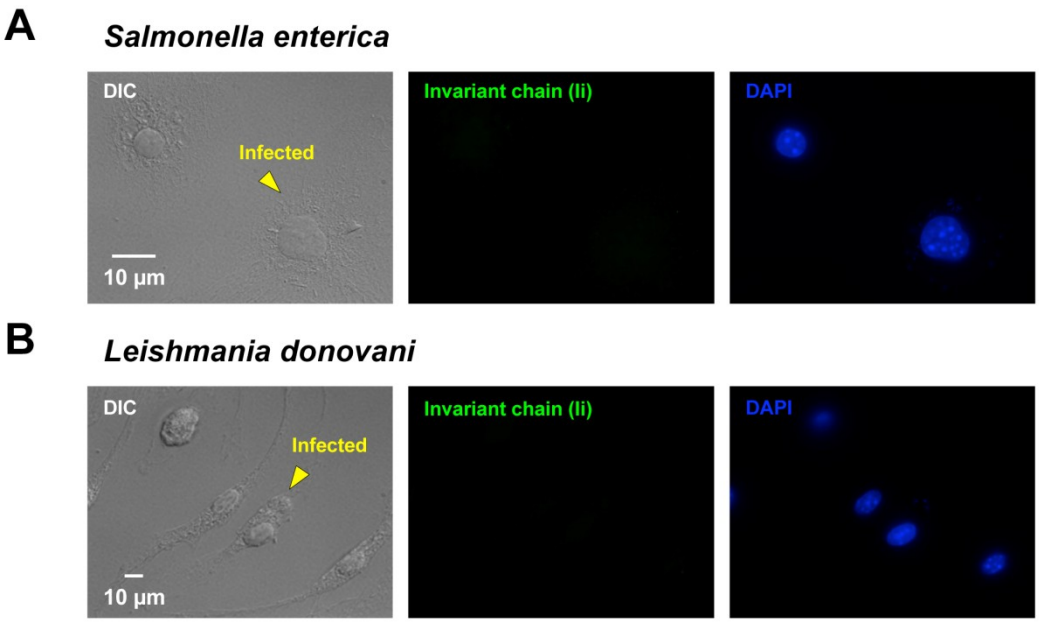

Figure 4.8: Other intracellular pathogens, *Leishmania* and *Salmonella*, do not cause Ii accumulation in infected cells. (A) BMMΦ infected with *Salmonella enterica* bacteria did not display higher levels of Ii compared to non-infected cells. (B) *Leishmania donovani*, an intracellular protozoan parasite, did not cause Ii accumulation in infected BMMΦ as seen in *T. gondii*-infected cells (see Figure 4.2).

4.4.6. Infection by *T. gondii* inhibits transcription of MHC-II (H2) and H2-DM genes, but induces transcription of the Ii gene

According to the current literature, *T. gondii* inhibits IFNγ-induced transcription of MHC-II and other related genes in infected cells (Luder, Lang et al. 2003) (Lang, Algner et al. 2006) (Kim, Fouts et al. 2007), yet we were observing an induced expression of Ii. Therefore, we assessed the transcriptional profile of different MHC-II-related genes (MHC-II, Ii, and H2-DM) in *T. gondii*-infected cells. BMMΦ cultures were infected with yellow fluorescent protein (YFP)-expressing parasites for 4 hours, left non-stimulated or stimulated with 100 U/ml IFNγ for 20 hours, and then sorted by flow cytometry according to their infection status. Samples were collected and real-time (RT) PCR was performed to measure mRNA levels of different genes involved in the MHC-II antigen presentation. First, IFNγ-induced transcription of MHC-II genes (H2-Aα, H2-Aβ1, H2-Eβ1) and H2-DM (H2-DMα, H2-DMβ1/2) was inhibited in infected

cells (Figure 4.9), as previously reported in the literature (Luder, Lang et al. 1998), (Kim, Fouts et al. 2007). Similarly, mRNA levels of both transcript variants, p41 and p31 isoforms, of Ii were lower in IFNγ-treated infected cells than levels in non-infected cells of the same cultures, in accordance with previous reports. However, transcription of both Ii isoforms was induced in infected cells left untreated compared to non-infected cells, while the other MHC-II related genes were not, revealing an unusual discoordinated expression of these genes. In fact, the murine Ii promoter consist of promoter and enhancer elements both unique to Ii and shared with other class-II genes (Zhu and Jones 1990), which could explain the differential mRNA expression between MHC-II genes and the Ii in infected cells. In other words, *T. gondii* infection could trigger a transcriptional cascade that elicits DNA elements unique to Ii, but suppress any additional IFNγ-induced transcription.

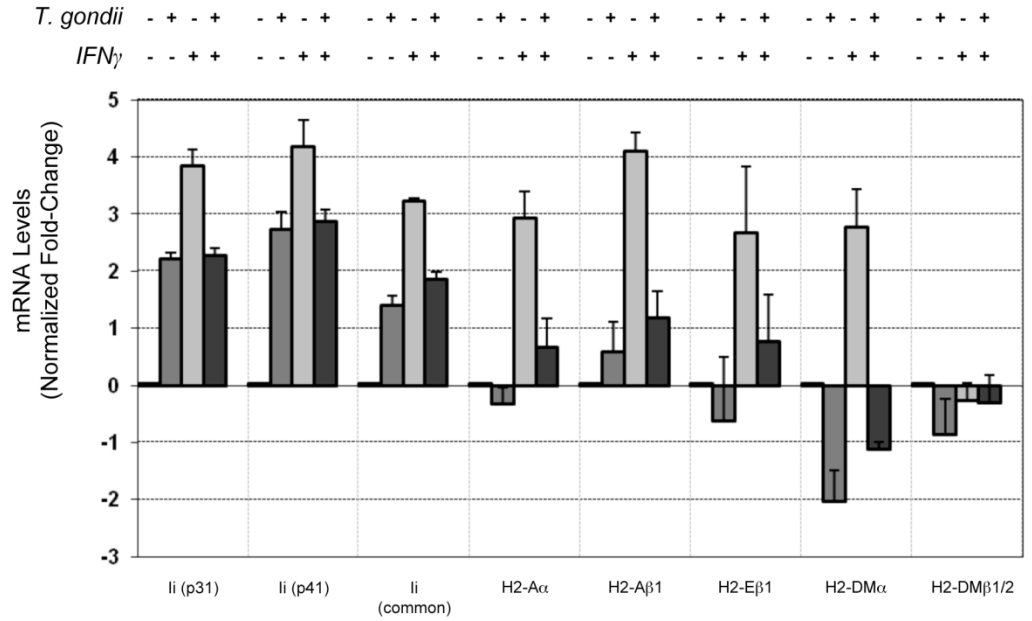

Figure 4.9: *T. gondii* induces transcription of both Ii isoforms p41 and p31 in the absence of IFNγ, while inhibiting transcription of MHC-II genes. RT-PCR analysis was performed on FACS-sorted infected BMMΦ cultures, left non-stimulated or stimulated with IFNγ. Interferon gamma-induced transcription of MHC-II genes (H2-Aα, H2-Aβ1, H2-Eβ1) was inhibited in infected cells. Also, mRNA levels of both transcript variants, p41 and p31 isoforms, of Ii were lower in IFNγ-treated infected cells compared to levels in non-infected cells of the same cultures. However, transcription of both Ii isoforms was induced in infected cells left untreated compared to non-infected cells, while the other MHC-II related genes were not. Data was calculated using the $2^{-\Delta\Delta Ct}$ method, whereby the non-infected non-stimulated cells were used to calculate normalized fold-change.

4.4.7. Accumulation of Ii in infected BMDCs, and reduced expression of H2-DM inhibit MHC-II presentation of endogenous, parasite-derived antigens in the context of MHC-II

To assess if the accumulation of the invariant chain and the inhibition of H2-DM had any impact on MHC-II antigen presentation, an experimental design exploiting the Eα model antigen and YAe antibody system was carried out (Itano, McSorley et al. 2003) (Murphy, Lo et al. 1989) (Dzierszinski and Hunter 2008). When WT BMDCs were pulsed with exogenous Eα peptide, the cells presented the antigen on MHC-II, while the ability of $Ii^{-/-}$ and H2-$DM^{-/-}$ cells to present the antigen was markedly impaired (Figure 4.10). Wild-type and $Ii^{-/-}$ cells infected with control parasites, expressing RFP only, no Eα-loaded MHC-II molecules were detected. WT, $Ii^{-/-}$, and H2-$DM^{-/-}$BMDCs were able to present the parasite-derived Eα peptide after internalizing HK Eα-expressing parasites. When WT and H2-$DM^{-/-}$ BMDCs were infected with live parasites expressing Eα in their cytosol or secreting the antigen in the parasitophorous vacuole, presentation of the parasite-derived antigen on MHC-II molecules was very low, which is in agreement with previous reports on the ability of *T. gondii* to inhibit antigen presentation by the infected host cell (Luder, Lang et al. 1998) (Luder, Walter et al. 2001) (McKee, Dzierszinski et al. 2004). Conversely, infected $Ii^{-/-}$ cells were able to present the parasite-derived Eα peptide on MHC-II molecules. Both WT and $Ii^{-/-}$ BMDCs, when infected with the control RFP-only expressing parasite, were still able to present exogenously derived Eα peptide provided after infection, while H2-$DM^{-/-}$ cells' ability to present the antigen remained very low, presumably a phenotype due to an impaired inability to displaced CLIP from the MHC-II groove inherent to the lack of H2-DM molecules. The ability of presenting the antigen was actually enhanced when $Ii^{-/-}$ cells were infected compared to non-infected cells. Taken collectively, these results indicate that the accumulation of the invariant chain induced by the parasite inhibits MHC-II presentation of parasite-derived or endogenously acquired antigens, but not exogenous antigens, while inhibition or complete absence of H2-DM plays a role

in the dampening of the presentation of endogenous, parasite-derived and exogenous antigens.

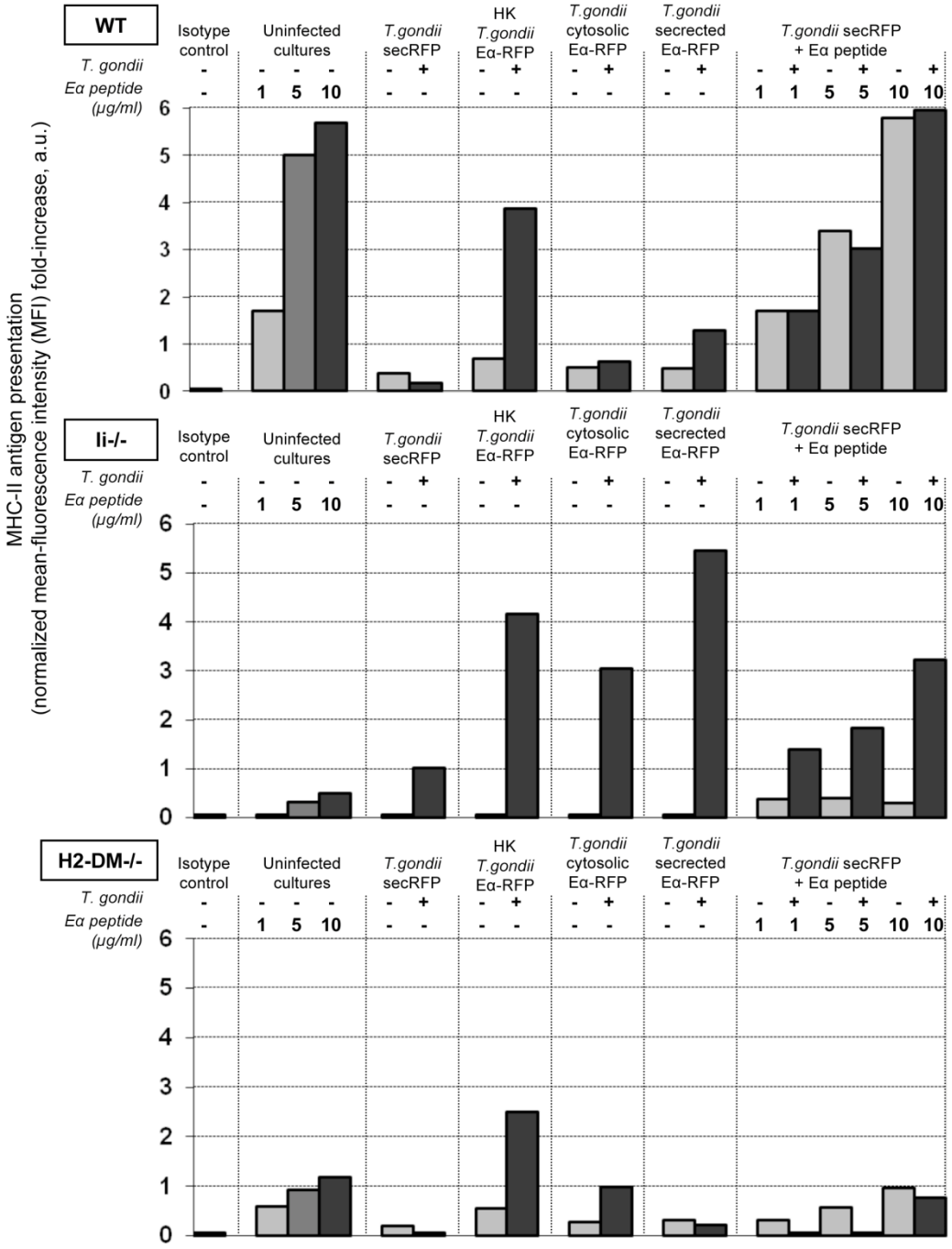

Figure 4.10: (see legend page 112)

Figure 4.10: The accumulation of Ii in infected BMDCs, and reduced expression of H2-DM inhibits presentation of endogenously-acquired, parasite-derived antigens in the context of MHC-II. The Eα model antigen and YAe antibody system was used to measure antigen presentation in the context of MHC-II by flow cytometry. Wild-type BMDCs pulsed with exogenous Eα peptide were able to present the peptide on MHC-II, while the ability of $Ii^{-/-}$ cells to present the antigen was markedly reduced. No presentation of the peptide was observed when cells were infected with the control parasite strain expressing RFP only. Both WT and $Ii^{-/-}$ BMDCs were able to present the parasite-derived Eα peptide after internalizing HK Eα-expressing parasites. In contrast, when WT BMDCs were infected with live parasites expressing Eα in their cytosol or secreting the antigen in the PV, presentation of the parasite-derived antigen on MHC-II molecules quite reduced. On the other hand, $Ii^{-/-}$ BMDCs infected with the latter strains were able to present the parasite-derived Eα peptide on MHC-II molecules. Both WT and $Ii^{-/-}$ BMDCs, when infected with the control RFP-only expressing parasite, were still able to present exogenously derived Eα peptide provided after infection. Here, data are presented as normalized mean fluorescence intensity (MFI) fold-increase. MFI values were calculated using the FlowJo analysis software, and were normalized to the MFI value obtained for the isotype control, which determined normal background fluorescence, and expressed as fold-increase

4.4.8. Accumulation of Ii is observed in *T. gondii*-infected cells in vivo and affects parasite dissemination, while Ii and H2-DM differentially impacts $CD4^+$ T cell activation and IFNγ production

To verify if the accumulation of Ii in infected cells observed *in vitro* was relevant during an *in vivo* infection, we analyzed by flow cytometry $CD11b^+$ (macrophages) and $CD11c^+$ CD8α- (myeloid dendritic cells) cell subsets from the mesenteric lymph nodes (MLN) of acutely infected WT C57BL/6 mice. Parasites used to infect these mice intraperitoneally (IP) expressed RFP in order to identify infected cells from non-infected cells by flow cytometry. Like *in vitro*, infected macrophages and myeloid DCs from infected mice expressed higher levels of the invariant chain, compared to non-infected cells from the same organ (Figure 4.11A), conferring relevance to the previous results.

Next, to assess the impact of the presence or absence of Ii and H2-DM on $CD4^+$ T cell priming and activation during acute infection, $CD4^+$ T cells were collected from MLN and spleens of acutely infected WT, $Ii^{-/-}$, and $H2\text{-}DM^{-/-}$ mice. Flow cytometry analysis revealed that a higher proportion of $CD3\varepsilon^+$ $CD4^+$ lymphocytes displayed a $CD25^{hi}$ $CD44^{hi}$ $CD62L^{low}$ phenotype, corresponding to an activated state, in $Ii^{-/-}$ compared to WT animals (64% of $CD62L^{low}$ versus 38%, respectively), while the opposite was observed in $H2\text{-}DM^{-/-}$ mice, whereby a

lower proportion of $CD4^+$ T cells displayed an activated phenotype (9% of $CD62L^{low}$) (Figure 4.11B). When measuring serum IFNγ levels by ELISA during acute infection, levels were higher in $Ii^{-/-}$ mice compared to WT mice (Figure 4.11C). As for H2-$DM^{-/-}$ mice, IFNγ levels were slightly, but not significantly lower than in WT animals. To verify if the increased T cell activation and IFNγ production observed in $Ii^{-/-}$ mice was not due to an increased parasite replication rate, RT-PCR analysis was performed on MLN from acutely infected mice to measure parasite burden. Parasite loads were actually around 25 times greater in $Ii^{-/-}$ compared to WT and H2-$DM^{-/-}$ mice (Figure 4.11D). However, *in vitro* analysis revealed no difference in parasite replication rate or egress time in infected WT BMMΦ or $Ii^{-/-}$ BMMΦ (Figure 4.12). Therefore, the increased parasite burden in MLN of infected $Ii^{-/-}$ mice could be due to an increased dissemination of the parasites towards the secondary lymphoid organs, where antigen presentation, $CD4^+$ T cell priming and activation, and finally IFNγ production could be enhanced. On the other hand, parasitemia levels within MLN of acutely infected H2-$DM^{-/-}$ mice were similar to those in WT animals (Figure 4.11D).

Since both Ii and H2-DM play a major role in the MHC-II pathway, we assessed the impact of lacking both molecules on the course of infection. To do so, double knock-out mice were generated by breeding $Ii^{-/-}$ and H2-$DM^{-/-}$ single knock-out strains, and then by breeding the heterozygote progeny. Activation profiles of $CD3\varepsilon^+$ $CD4^+$ T cell were higher (78% of $CD62L^{low}$), but serum IFNγ levels in double KO mice were comparable to WT controls during acute toxoplasmosis (Figures 4.11B and 4.11C). However, similarly to $Ii^{-/-}$ single knock-outs, parasitemia levels in draining lymph nodes were greatly higher than in WT mice or H2-$DM^{-/-}$ single KO (around 18 times higher), supporting the possibility that Ii affects the motility of infect cells and their ability to migrate to lymphoid organs (Figure 4.11D).

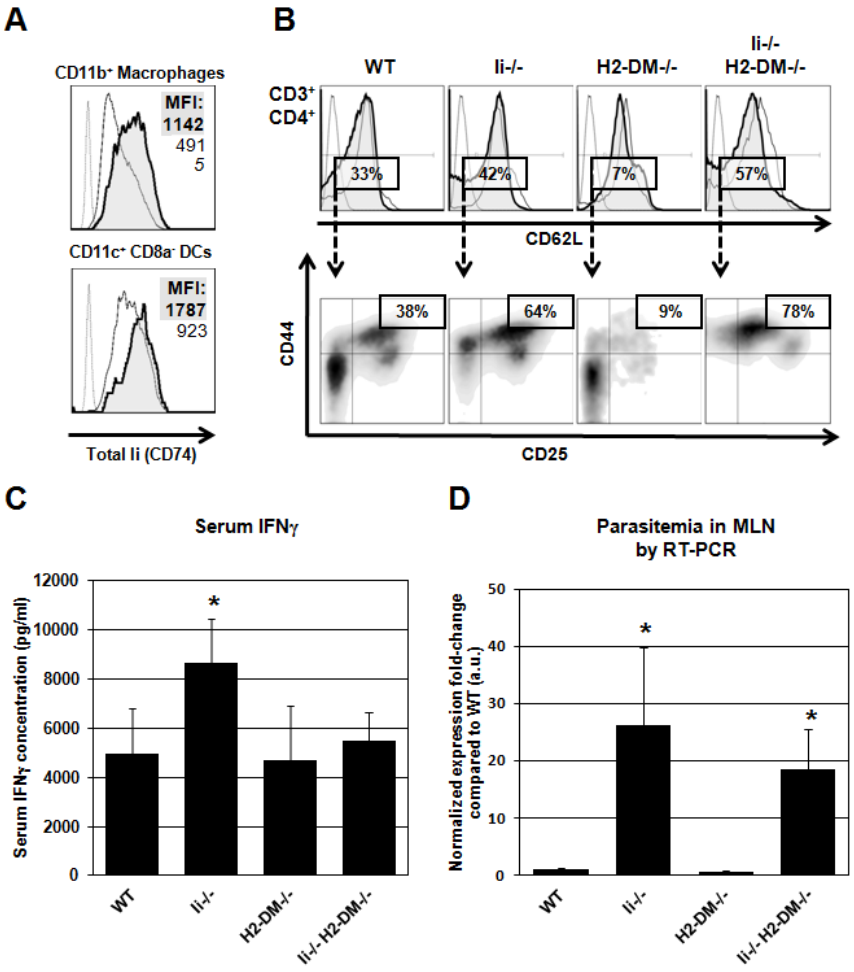

Figure 4.11: Ii accumulation in *T. gondii*-infected cells is observed *in vivo* and has an impact on parasite dissemination, while Ii and H2-DM modulate CD4$^+$ T cell activation, and IFNγ production during acute infection. (A) Flow cytometry analysis was performed on cells collected from the MLN of WT C57BL/6 mice, 5 days after I.P. infection. CD11b$^+$ (macrophages) and CD11c$^+$ CD8α- (myeloid DCs) cell subsets were identified, and staining for Ii (CD74) was observed. Infected macrophages and myeloid DCs (thick line shaded curve), expressed higher levels of Ii, compared to non-infected cells (solid curve) from the same organ, confirmed by higher MFI values (top right corner). Isotype control is shown by a dotted curve. (B) Flow cytometry analysis of CD4$^+$ T cells collected from MLN and spleens of acutely infected WT, Ii$^{-/-}$, H2-DM$^{-/-}$, and double KO (Ii$^{-/-}$ H2-DM$^{-/-}$) mice was performed. First, CD3ε$^+$ CD4$^+$ positive cells were identified. Then, we gated on CD62L expressing, either high or low, and analyzed the expression of CD25 and CD44 on the CD62L^{low} populations. This gating strategy revealed that a higher proportion of CD3ε$^+$ CD4$^+$ lymphocytes displayed a CD25^{hi} CD44^{hi} CD62L^{low} phenotype, corresponding to an activated state, in Ii$^{-/-}$ mice and double KOs compared to WT animals, while H2-DM$^{-/-}$ showed a lower proportion of this subpopulation. (C) To measure IFNγ levels, we collected serum from acutely infected mice. We measured IFNg by ELISA, using an eBioscience Mouse IFN-gamma ELISA Ready-SET-Go! Kit. Interferon gamma levels were higher in Ii$^{-/-}$ mice compared to WT mice, while H2-DM$^{-/-}$ and double KOs were similar to controls. Values are expressed as pictograms per millilitre. (D) Real-time PCR was performed on gDNA purified from MLN of acutely infected mice. The *T. gondii* B1 gene was amplified to measure parasite load. Ct values were normalized using the mouse β-actin gene, and the $2^{-\Delta\Delta Ct}$ method was used to calculate fold-increase, where reference values were those of the infected WT mice. Lack of Ii seemed to favor increase local parasitemia in MLN, while H2-DM did not seem to have effect.

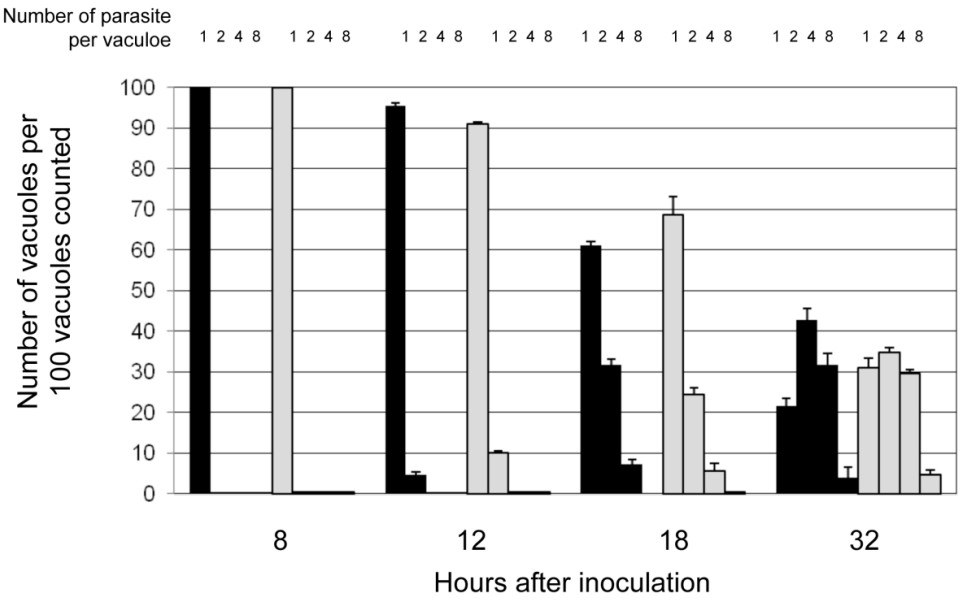

Figure 4.12: *In vitro* replication rate of parasites in infected BMM is not affected by the presence or absence of Ii. WT and $Ii^{-/-}$ BMMΦ cultures were plated on glass coverslips, infected with RH WT parasites at an MOI of 3:1, and fixed with 3.7% PFA at the indicated times after inoculation (8, 12, 18, and 32 hours post-inoculation). The number of parasites per vacuole was counted in 100 vacuoles for each type point, and repeated twice by counting vacuoles from different coverslips in order to calculate statistical error bars. Each bar represents the number of vacuoles that contained the indicated number of parasites (1, 2, 4, or 8). No significant differences were observed in the replication rate of parasites within WT BMMΦ (black bars) compared to $Ii^{-/-}$ BMMΦ (grey bars).

4.4.9. Absence of H2-DM leads to a higher cyst burden in the brains of chronically infected animals, while absence of both Ii and H2-DM proves fatal during chronic, but not acute infection

Although there were differences in the immune response in the acute phase of the infection, all KO strains, whether single or double knock-outs, were able to survive acute toxoplasmosis. However, brain cyst loads varied significantly depending of the genotype (Figure 4.13A). Quantitative PCR analysis revealed that $H2\text{-}DM^{-/-}$ had approximately 6 times more cysts compared to WT controls. While no significant differences were observed between WT and $Ii^{-/-}$ mice, cyst burdens in double KO mice was 30-fold higher. Histological sections of the infected brains reflected these previous observations (Figure 4.13B). In the case of WT and $Ii^{-/-}$, single, isolated cysts were spotted, while large clusters of

cysts were observed in H2-DM$^{-/-}$ and double KOs. Interestingly, all Ii$^{-/-}$ H2-DM$^{-/-}$ KO mice, although having survived acute toxoplasmosis, invariably died a few days into the chronic phase even though they were infected with a usually non-lethal dose of type II strain (Figure 4.13C). From day 20 post-infection, animals displayed neurological symptoms such as twitching, lethargy, and uncoordinated movement shortly before they succumbed to the infection, which could suggest reactivation of encysted parasites.

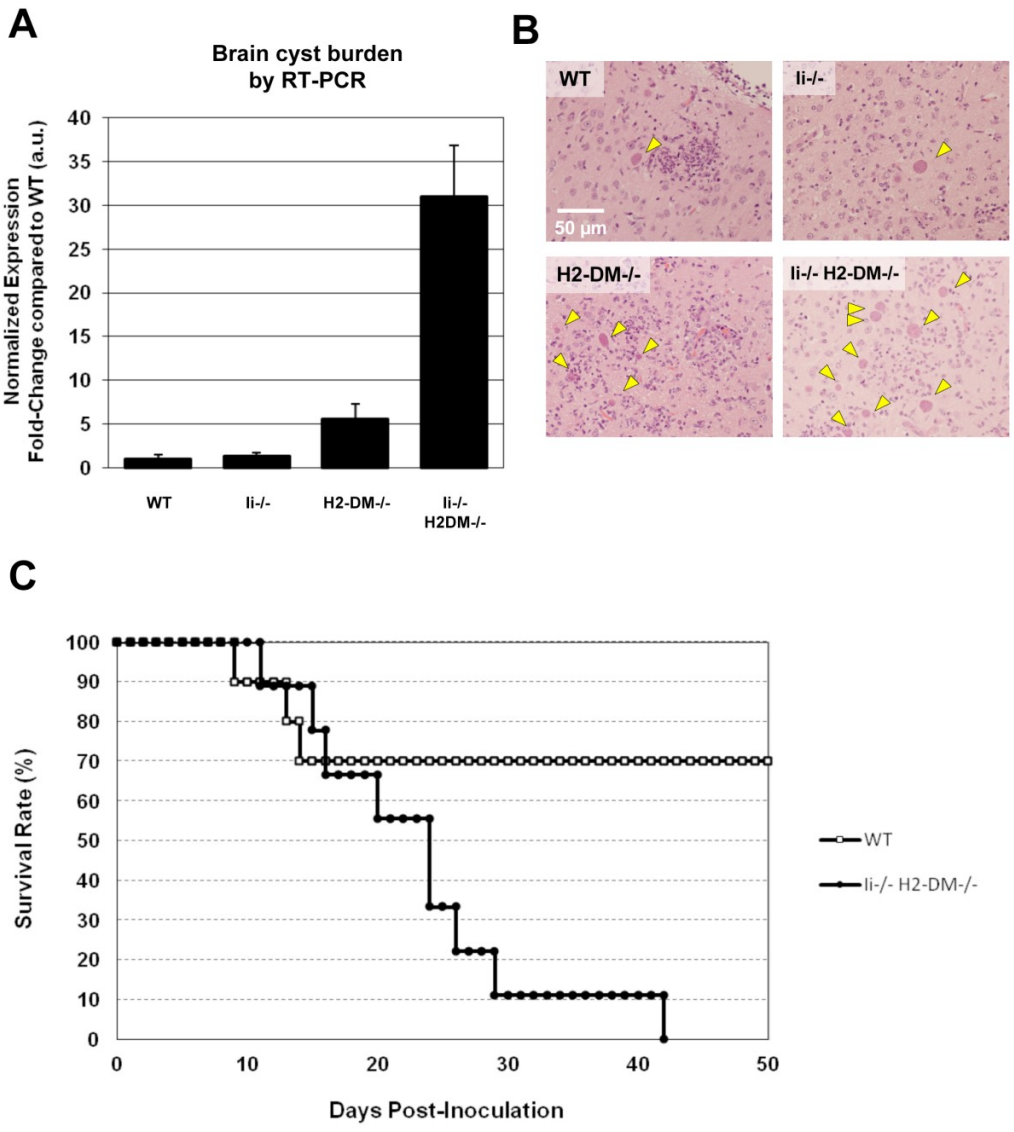

Figure 4.13: (see legend on page 119)

Figure 4.13: The absence of Ii does not affect cyst numbers at the chronic stage of infection, while absence of H2-DM increases the burden, and absence of both Ii and H-2DM proves fatal. Mice were infected with 10^3 PruΔ tachyzoites I.P. (A) RT-PCR analysis of chronically infected brains (20 P.I.) revealed that H2-DM$^{-/-}$ mice had 5-7, and double KO mice had around 30 times more cysts than WT controls or Ii$^{-/-}$ mice. (B) Histological assessment of brain sections (25 days P.I. shown here) provided visual confirmation of the increased cyst burden in the former two KO strains. Interestingly, cysts were found to be clustered in H2-DM$^{-/-}$ and double KO mice, while no overwhelming inflammation was apparent at later time points. (C) All double KOs (Ii$^{-/-}$ H2-DM$^{-/-}$) succumbed to the infection shortly into the chronic phase.

4.4.10. Both p41 and p31 isoforms, as well as the proteolytic product p10 accumulate in infected BMMΦ, while the accumulation of proteolytic intermediates follows a different pattern in infected BMDCs

In an attempt to characterize the underlying molecular mechanism of the phenotype previously observed *in vitro*, we assess the sequential proteolytic processing of the invariant chain in infected cells. By means of fluorescence activated cell sorting (FACS), non-stimulated or IFNγ-stimulated BMMΦ and BMDCs cultures infected with a transgenic parasite secreting the yellow fluorescent protein (YFP) in the PV were sorted, whereby infected and non-infected cells were collected separately. Western blot analysis on these samples revealed different patterns in the processing of Ii. First, both p41 and p31 isoforms were induced in infected BMMΦ in the absence of IFNγ (Figure 4.14A). Non-infected IFNγ-stimulated cells showed high levels of both isoforms, and the infected cells contained comparatively lower levels, but still significant levels of these proteins. However, both the non-stimulated and IFNγ-stimulated infected cells contained an increased accumulation of the p10 proteolytic intermediate compared to non-infected cells, suggesting a bias in the enzymatic processing of the invariant chain. On the other hand, both p41 and p31 isoforms were readily detected in infected BMDCs, but levels of the p10 cleavage product in infected cells, non-stimulated or stimulated, were similar to those seen in non-stimulated non-infected cells, while levels were higher in IFNγ-primed non-infected cells (Figure 4.14B). Collectively, these observations suggest that the processing of the invariant chain was biased in *T. gondii*-infected cells, but occurred differently in the different host cell type.

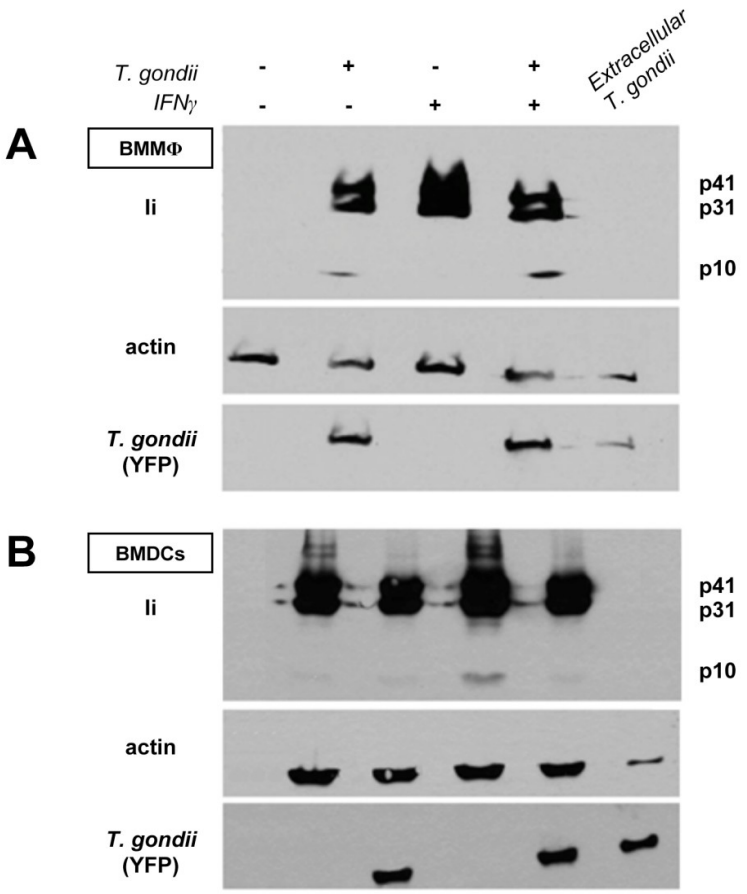

Figure 4.14: Accumulation of both p41 and p31 isoforms is observed in T. gondii-infected BMMΦ and BMDCs, and proteolytic processing is biased in infected cells, but follows a different pattern in the BMDCs. (A) Western blot analysis performed on FACS-sorted infected BMMΦ cultures, left non-stimulated or stimulated with IFNγ, revealed that both p41 and p31 isoforms were induced in infected BMMΦ in the absence of IFNγ. Non-infected IFNγ-stimulated cells showed high levels of both isoforms, and the infected cells contained comparatively lower levels. However, both the non-stimulated and IFNγ-stimulated infected cells contained an increased accumulation of the p10 proteolytic intermediate compared to non-infected cells, suggesting a bias in the enzymatic processing of the invariant chain. (B) Both p41 and p31 isoforms were detected in infected BMDCs, but levels of the p10 cleavage product in infected cells, stimulated or not, were similar to those seen in non-stimulated non-infected cells, while levels were higher in IFNγ-primed non-infected cells.

4.4.11. *T. gondii* modulates the enzymatic activity of several host proteases, cathepsins and legumain, involved in antigen degradation and Ii processing in infected BMMΦ and BMDCs

Given the bias in invariant chain processing observed by Western blotting, we measured the enzymatic activities by fluorometric measurements of legumain or asparaginyl endopeptidase (AEP), involved in the initial cleavage of the p41

and p31 isoforms to yield the p22 proteolytic product, and cathepsins (Cat) L and S, involved in the cleavage of p22 to yield p10, and p10 to CLIP (Hsing and Rudensky 2005). Enzymatic activities of all three enzymes were lowered in *T. gondii*-infected BMMΦ compared to non-infected cells (Figure 4.15). However, only Cat L activity was diminished, while Cat S and AEP activities were increased in infected BMDCs. The different phenotype between macrophages and dendritic cells partly reflects basic differences in their biology, notably with regards to Ii processing and the use of certain proteases (Bryant and Ploegh 2004).

Since the p41 isoform of Ii is known to act as an inhibitor of some cathepsins, notably Cat L (Bevec, Stoka et al. 1996), (Mihelic, Dobersek et al. 2008), we measured the enzymatic activities in $Ii^{-/-}$ BMMΦ and BMDCs and observed the same pattern. Hence, the accumulation of Ii caused by *T. gondii* infected cells does not explain the inhibition of these proteases. These proteases require optimal pH for their autocatalytic activation which is brought upon maturation and acidification of the endosomal compartments. Hence, the possibility that infection by *T. gondii* has a more general affect on the endosomal biology that would alter the functions of these pH-sensitive proteases could explain the modulation of some of these host proteases.

T. gondii possesses at least two identified cysteine peptidase inhibitors, known as cystatins, toxostatins 1 and 2, and both have been shown to inhibit *Toxoplasma* cysteine proteases TgCPB and TgCPL (Huang, Que et al. 2009). Also, toxostatin 1 was able to inhibit human cathepsins B and L in cell-free extracts. Although their subcellular localisation or their access to host cell compartments have not been confirmed, we wanted to verify whether the biased Ii proteolysis was due to the inhibitory activity of these cystatins on host proteases. BMMΦ cultures were infected with either toxostatin 1 (Δcys1) or 2 (Δcys2) knock-out strains, and Ii expression was assessed by flow cytometry and Western blotting. Similarly to infection with WT parasites, both KO strains were able to induce Ii expression in the infected cells without IFNγ stimulation (Figure 4.16A). Western blot analyses revealed an identical pattern. In other words, both p31 and

p41 isoforms were induced in cells infected with the KOs, while the p10 proteolytic product accumulated, arguing that the bias in Ii processing and host protease activity was not restored in the absence of parasite inhibitors of cathepsins (Figure 4.16B).

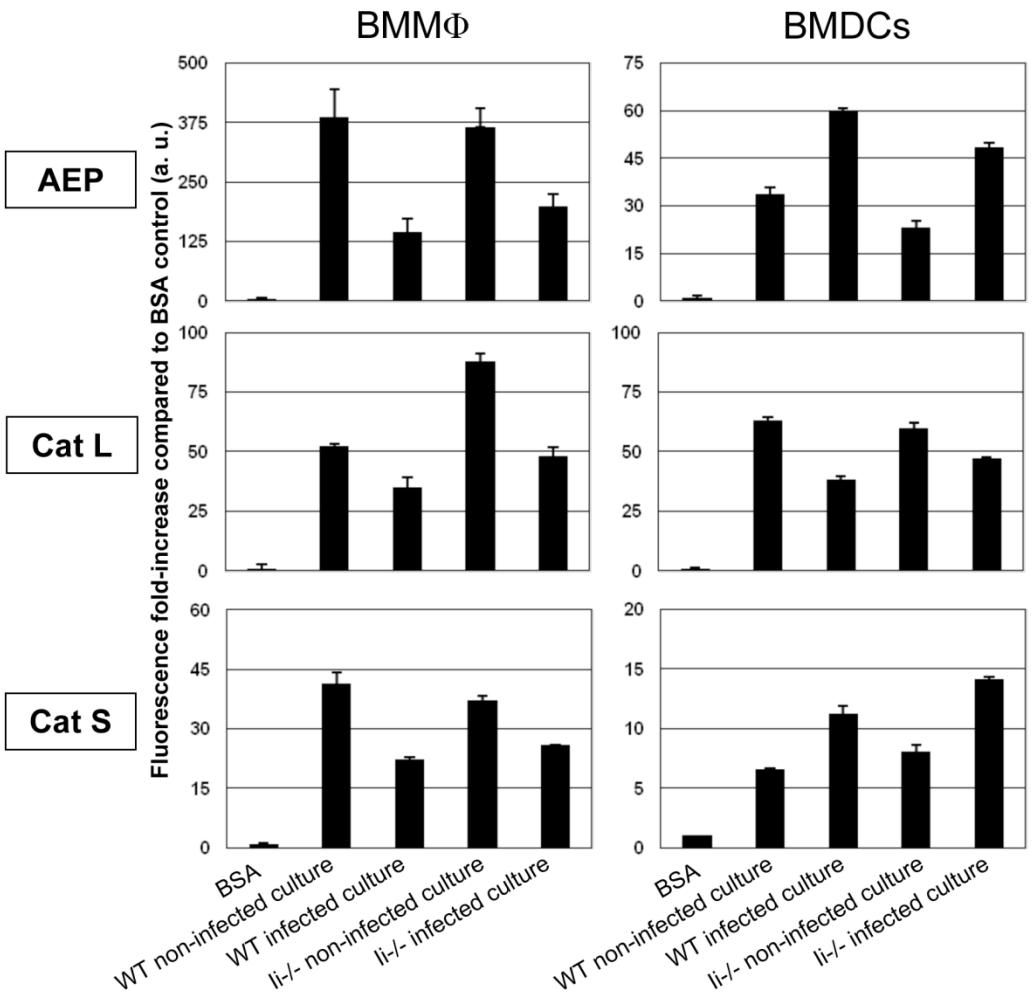

Figure 4.15: *T. gondii* modulates the enzymatic activity of AEP, Cat L and Cat S. Enzymatic activities of AEP, Cat L and Cat S were measured by fluorometric measurements. Enzymatic activities of all three enzymes were lowered in *T. gondii*-infected WT and $Ii^{-/-}$ BMMΦ compared to non-infected cells. As for infected BMDCs, only Cat L activity was diminished, while Cat S and AEP activities were increased, both in WT and $Ii^{-/-}$ cells. Values are reported as fluorescence fold-increased, where background fluorescence of the BSA mixed with the different enzyme substrates is used to normalize values.

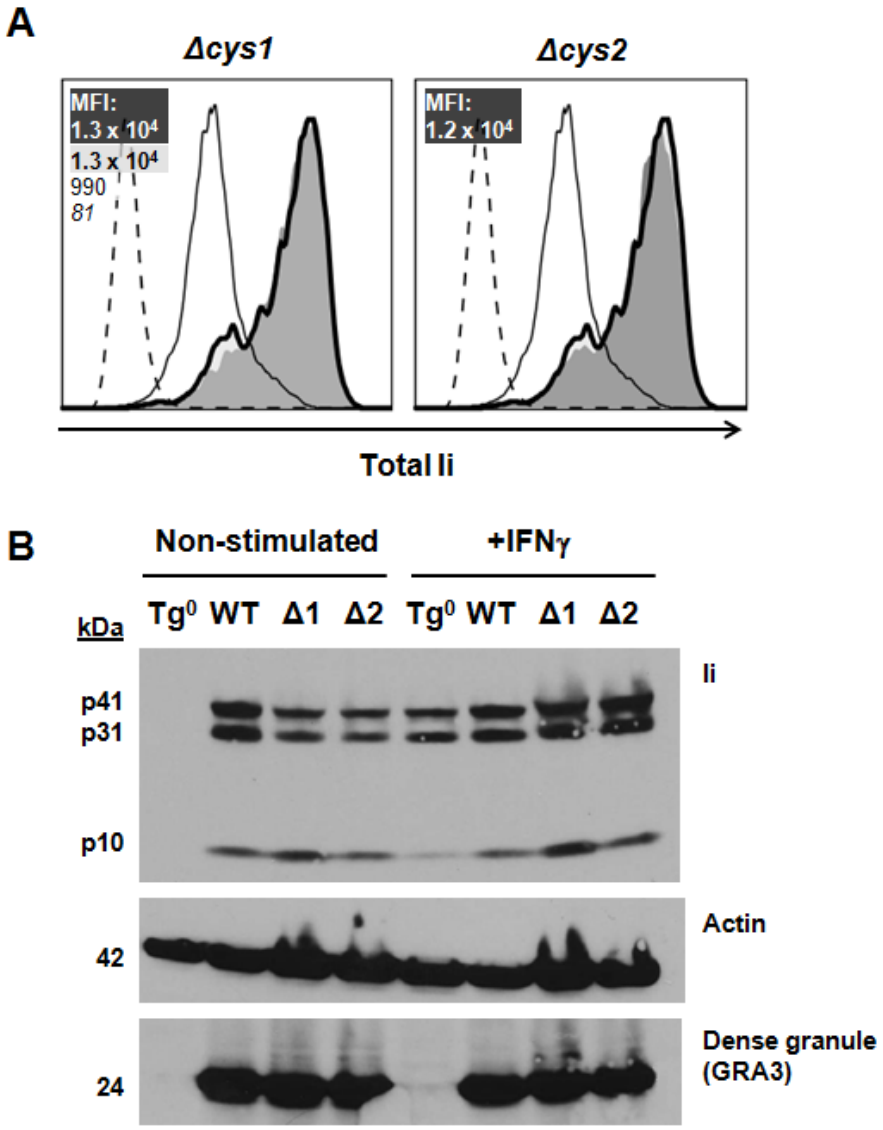

Figure 4.16: ***T. gondii*** **cystatins do not affect Ii processing.** (A) WT BMMΦ were infected with either left non-infected (Tg^0, solid curve), infected with RH WT (bold shaded curve), Δcys1 or Δcys2 (filled gray curves) parasites for 6 hours, left non-stimulated for 18 hours, stained for Ii, and analyzed by flow cytometry. Ii expression was induced in cells infected with cystatin KOs at almost identical levels as seen in cells infected with WT parasites. Isotype control is indicated by the dashed curve. Mean fluorescence intensity (MFI) values are indicated for each population (i.e. italicized for isotype control, standard font for non-infected control cells, bold font for infected WT cells, and white font in dark box for infected KO cells). (B) Western blotting was performed on BMMΦ cultures (10^6 per lane) either left non-infected, infected with RH WT, Δcys1, or Δcys2 parasites at an MOI of 8:1, left non-stimulated or stimulated with 100 U/ml IFNγ for 18 hours. Probing for Ii revealed that both p31 and p41 Ii isoforms were induced, and that the p10 proteolytic product accumulated at similar levels in all infected cells, higher than seen in non-infected cells (Tg^0), indicating that *T. gondii* cystatins are not involved in the bias observed in the processing of Ii. Actin was probed as a loading control, while probing for GRA3 was performed to verify the cultures were similarly infected.

4.4.12. *T. gondii* affects endosomal acidification in infected cells in the absence of IFNγ

Since the presence or absence of the invariant chain in infected cells did not affect the inhibition of the different host proteases involved in Ii processing and antigen degradation, we sought to determine if *T. gondii* has a more upstream effect on the endocytic pathway. One of the key events for endosomal maturation and functions is the acidification of the antigen-containing compartments (Trombetta and Mellman 2005). Therefore, we measured the acidification of endosomal compartments by flow cytometry containing internalized fluorescently-labelled 3 μm beads (Savina, Vargas et al. 2010) in *T.* gondii-infected cells. BMMΦ cultures were either infected with RFP-expressing parasites or left non-infected, then stimulated with IFNγ or left non-stimulated for 20 hours. Then, the different cultures were pulsed for 15 minutes to allow internalization of the beads, thoroughly washed, and analyzed by flow cytometry at different time points over the course of 2 hours. In the absence or presence of the invariant chain, acidification of the endosomal compartments containing the internalized beads was reduced in cells in infected cultures compared to cells from control non-infected cultures in the absence of IFNγ stimulation (Figure 4.17). In the case of non-infected cultures, endosomal pH was approximately at ~7.5 at the start of the chase, gradually decreasing to ~pH 6, while in infected cultures endosomal pH began at ~7.5, but only dropped to a pH of ~7 (WT) or ~6.6 ($Ii^{-/-}$). On the other hand, acidification was restored in the different cultures when stimulated with IFNγ. Starting pH values were between 6.5-7 and acidified down to pH ~5.8-6 in all cells (both from non-infected and infected cultures).

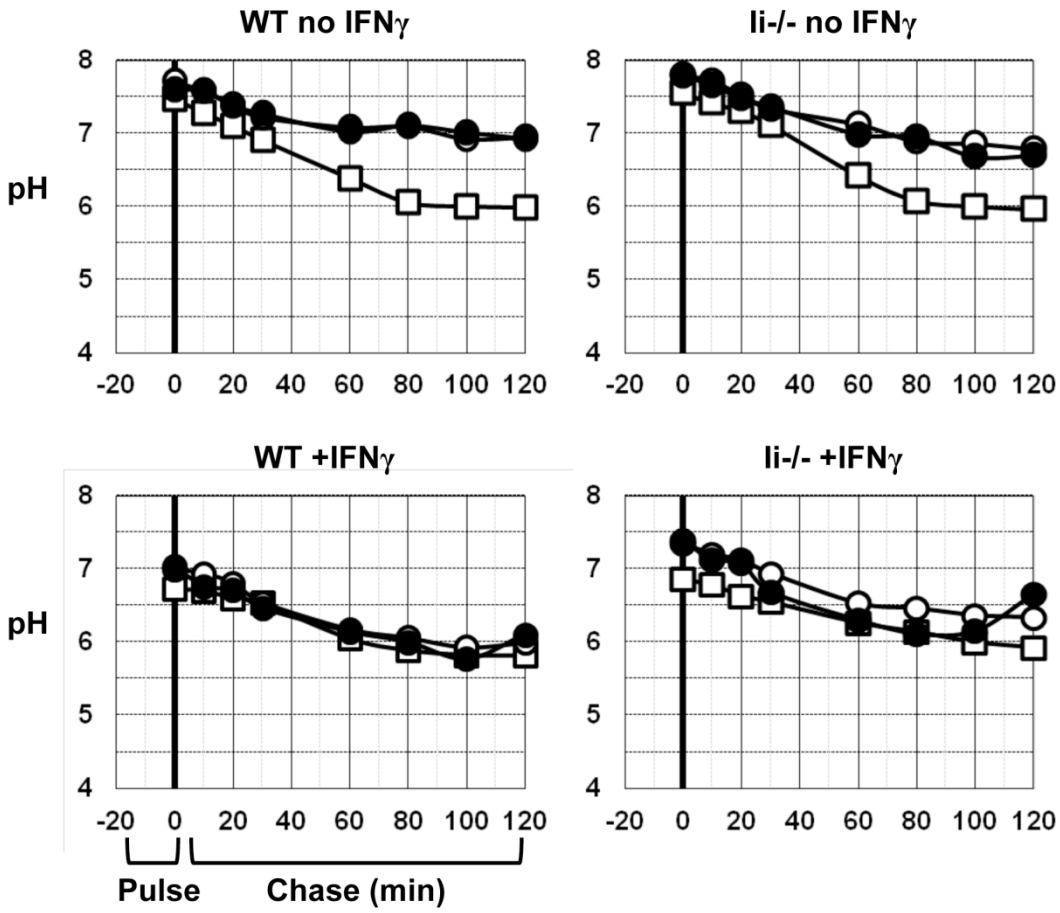

Figure 4.17*: T. gondii* affects endosomal acidification in infected BMMΦ in the absence of IFNγ. Acidification of endosomal compartments was measured by flow cytometry using 3 μm microsphere beads conjugated to pH-sensitive FITC and pH-insensitive FP647. BMMΦ cultures, either infected or non-infected, were pulsed for 15 minutes at 37°C to allow internalization of the beads. After several washed in ice-cold PBS, cells were placed into culture, and small aliquots were analyzed by flow cytometry at different time points (0, 10, 20, 30, 60, 80, 100, and 120 minutes) over a 2 hour chase. In the absence or presence of the invariant chain (top left and right graphs), acidification of the endosomal compartments containing the internalized beads was reduced in infected cells (black filled circles) and non-infected cells (empty circles) in infected cultures compared to cells from control non-infected cultures (empty squares) in the absence of IFNγ stimulation. On the other hand, acidification was practically identical between the different cultures when stimulated with IFNγ (lower left and right graphs). To generate a standard curve, a series of samples was resuspended in CO_2-independent medium adjusted to a fix pH value, ranging from 3 to 8.5 with 0.5 increments, and these samples were then analyzed by flow cytometry. Ratio of FITC / FP647 MFI values were plotted against the known pH values of the standard controls. From this standard curves, we were able to extrapolate and calculate pH values for our experimental samples.

4.5. Discussion

4.5.1. Impacts of the modulation of Ii and H2-DM by *T. gondii* on MHC-II antigen presentation

Although IFNγ is the major effector molecule during toxoplasmosis, it is only produced three days after initial infection during the course of a natural infection by *T. gondii*. This short period before the mounting of an adequate immune response allows the parasite to subvert many function of the immune system, thereby gaining a head start to establish a successful infection. In the present study, we found that *T. gondii* induces the transcription and protein synthesis of the MHC-II associated invariant chain in the absence of IFNγ in infected cells, both *in vitro* and *in vivo*. In contrast, MHC-II and H2-DM expression is inhibited in infected cells, arguing for an uncoordinated expression of these components. This phenotype is not observed in cells infected with other intracellular pathogens *Leishmania donovani* and *Salmonella enterica* Typhimurim, known to inhibit MHC-II expression (Figures 4.8A and 4.8B). This demonstrates that it is not a generalized response to invading pathogens, but a phenotype triggered by *T. gondii* specifically. The induction of Ii requires active invasion by live parasites since it is not observed with either phagocytozed HK parasites or lysates, nor is it seen in the neighboring non-infected cells. Parasite replication is not necessary to generate the effect. These observations suggest that the induced expression of Ii either requires parasite effector molecules to be released from within the PV, or that specific host reactions occur only when a viable PV is formed.

It has been shown that bacterial pathogen *Helicobacter pylori* is able to up-regulate surface CD74 (or Ii) expression on gastric epithelial cells in a IL-8-dependent manner, and to bind to this surface receptor to ensure attachment to the gastric wall (Beswick, Das et al. 2005). Surface CD74 also acts as a receptor for macrophage migration inhibitory factor (MIF), a pro-inflammatory cytokine, and binding of MIF to CD74 initiates the MAPK signaling pathway (Leng, Metz et al. 2003). Although it might be tempting to attribute such a role for Ii accumulation,

the increased amounts of Ii molecules are overwhelmingly detected intracellularly, but not to the same extent at the surface of infected cells (Figure 4.6), which would prove unlikely that MIF signaling is enhanced. Surprisingly, $Ii^{-/-}$ (or $CD74^{-/-}$) mice are not more susceptible to infection, while it was reported that $MIF^{-/-}$ mice are more susceptible to toxoplasmosis suffering greater liver damage, more brain cysts, and produce less proinflammatory cytokines (Flores, Saavedra et al. 2008). It is possible that in our study, the benefits of the lack of Ii, i.e. enhanced antigen presentation and increased IFNγ levels, may overweigh the detrimental effects of an impaired MIF-induced response.

In our study with *T.* gondii, the *in vitro* system exploiting the Eα model antigen and the YAe antibody system shows that the accumulation of the invariant chain in infected BMDCs inhibits presentation of endogenously-acquired parasite-derived antigens on MHC-II molecules (Figure 4.10). This phenotype represents a novel mechanism of MHC-II antigen presentation subversion by an intracellular protozoan, and constitutes an additional necessary post-translational layer of regulation by *T. gondii* that complements the inhibition observed at the level of transcription. In the absence of H2-DM, MHC-II-restricted antigen presentation of both exogenous and endogenous parasite-derived antigens is greatly compromised. In light of these results, it appears that *T. gondii* infection induces two opposing patterns: inducing Ii expression to act as a dominant negative, and inhibiting H2-DM to exacerbate deficient antigen presentation.

Although the exact mechanism of how the accumulation of the invariant chain blocks the presentation of endogenous parasite-derived antigens remains elusive, presentation of endogenous antigens from the cytosol or other compartments on MHC-II molecules has been demonstrated, and involves autophagy or TAP-mediated mechanisms (Munz 2004), (Trombetta and Mellman 2005). Therefore, accumulation of the invariant chain in infected cells could potential affect the delivery to or loading of antigens onto MHC-II molecules through these mechanisms. Other studies have shown that endosomal trafficking in cells expressing high levels of Ii was slowed down (Romagnoli, Layet et al.

1993), (Gregers, Nordeng et al. 2003), which could have an impact on antigen delivery to late endocytic compartments and processing, and consequently antigen loading on MHC-II molecules.

It was demonstrated that the human immunodeficiency virus (HIV) type 1 Nef protein can mediate surface MHC-II down-regulation while up-regulating CD74 expression (Stumptner-Cuvelette, Morchoisne et al. 2001) (Schindler, Wurfl et al. 2003) (Keppler, Tibroni et al. 2006). Also, Vpu and the envelop protein gp41 were both shown to directly bind CD74 and initiate a signaling cascade (Hussain, Wesley et al. 2008) (Zhou, Lu et al. 2011). Of relevance here, it was proposed that the binding of Vpu to the cytoplasmic tail of CD74 could prevent MHC-II maturation by preventing its trafficking to the surface, and consequently, interfere with presentation of antigens to $CD4^+$ T cells. So far, no evidence has been found to suggest that a *T. gondii* molecule binds in a similar fashion.

How could the accumulation of Ii in infected cells affect the presentation of parasite-derived antigens? It is possible that, in the absence of Ii, the groove of newly synthesized MHC-II molecules is left vacant and may bind to peptides derived from the ER not normally presented instead of endosomal compartments. Another study with $Ii^{-/-}$ mice showed that the absence of Ii facilitated the presentation of endogenously synthesized peptides by splenic pAPCs (Bodmer, Viville et al. 1994). Furthermore, mass spectrometry analyses of MHC-II-bound peptides from Ii-negative and Ii-expressing pAPCs revealed differences in the antigen repertoire (Muntasell, Carrascal et al. 2004). With regards to *T. gondii*, parasite antigens have been detected in the ER of infected host cells (Goldszmid, Coppens et al. 2009) which could render them available to be loaded on MHC-II in the absence of Ii and explain the results obtained in our study. This may explain why the accumulation is overwhelmingly in the ER, rather than downstream compartments. In contrast, such a mechanism could compromise antigen presentation in H2-$DM^{-/-}$ cells, whereby increased Ii levels ensure occupation of the MHC-II groove and the absence of H2-DM limits removal of Ii.

Also, the absence of both Ii and H2-DM, like in double KO mice, likely leaves the groove open for peptides to bind without H2-DM removing or editing them, which would explain the phenotypic similarities observed between $Ii^{-/-}$ and double KO animals.

4.5.2. Implications of the modulation of Ii and H2-DM by *T. gondii* on parasite dissemination and $CD4^+$ T cell activation during the acute phase, and cyst burden and survival during the chronic phase of infection.

The increased migration of *T. gondii*-infected cells towards lymphoid organs in $Ii^{-/-}$ mice during acute infection revealed significant mechanisms of parasite dissemination (Figure 4.11D). Elegant work with dendritic cells has demonstrated that Ii interacts with the actin-based motor protein myosin II and affects motility (Faure-Andre, Vargas et al. 2008). In this study, WT DCs were found to alternate between high and low motility, while $Ii^{-/-}$ DCs moved in a faster and uniform fashion. In other words, Ii negatively regulates DC motility to allow efficient sampling of the environment for antigens by the cell. In this regard, it is possible that by increasing the amount of the invariant chain, *T. gondii* slows down infected cells from heading towards lymphoid organs, where an adequate immune response could be mounted. This possibility is further supported by an increased $CD4^+$ T cell activation and IFNγ production in $Ii^{-/-}$ mice (Figures 4.11B and 11C). Since no such role in motility has been attributed to H2-DM, the absence of any differences in parasitemia levels in lymphoid organs between WT and H2-$DM^{-/-}$ mice fits in this model. The smaller proportion of activated $CD4^+$ T cells and the slightly lower IFNγ levels in H2-$DM^{-/-}$ mice during the acute phase of infection may reflect the diminished ability to present MHC-II-restricted antigens, as seen in the *in vitro* YAe experiments, and lead to a suboptimal activation of T cells. Since the double KO mice display a phenotype more similar to $Ii^{-/-}$ mice than that of H2-$DM^{-/-}$, this could suggest that the absence of Ii has a dominant effect over the absence of H2-DM, and may reveal important insights on the mechanism at play.

An interesting study, investigating MHC-II cancer vaccines and tumor-reactive type 1 $CD4^+$ T cells, reported strikingly similar phenotypes in the absence of Ii (Thompson, Srivastava et al. 2008). In this study, they had engineered human mammary carcinoma cells (MCF10) to express CIITA, MHC-II, CD80 (for co-activation), and Ii or Ii siRNA to block expression. Antigen presentation assays revealed that cells lacking Ii were more efficient at priming co-cultured $CD4^+$ T cells, inducing the production of twice as more IFNγ and the expansion of 1.5-2 fold more T cells. They also noticed that Ii-negative and Ii-expressing cells activated overlapping, but distinct repertoires of $CD4^+$ T cells, suggesting that different epitopes were being presented by MHC-II molecules.

Although $Ii^{-/-}$, H2-$DM^{-/-}$, and double KO mice survive the acute phase of infection, significant differences were observed at the chronic stage. It was initially discovered that MHC-I gene haplotypes and $CD8^+$ T cells determined cyst numbers (Brown and McLeod 1990). Here, *in vivo* infection trials suggest that cyst numbers were affected by the presence or absence Ii and H2-DM, typically associated with MHC-II antigen presentation. One could hypothesize that lower $CD4^+$ T helper cell activation would also affect the intensity and quality of the help provided to $CD8^+$ effector T cells in H2-$DM^{-/-}$, and thus cause a decreased destruction of parasites and increased cyst numbers. However, the production of IFNγ in H2-$DM^{-/-}$ and double KOs at similar levels to those of WT mice, and the elevated cyst numbers in double KOs despite high $CD4^+$ T cell activation, might complicate this assumption. The absence of H2-DM could skew antigens being presented away from immunodominant epitopes, and lacking both Ii and H2-DM, which would leave the MHC-II groove free, could change the epitope profiles as well. Although an immune response is generated, the protection against encysting parasites could be impaired in these mice. This possibility is reminiscent of two studies carried out with *Leishmania* that showed that the lack of H2-DM changes the epitopes being presented, skewing the response away from the immunodominant rLACK (158-173) to two novel LACK epitopes (33-48 and 261-276) (Nanda and Bikoff 2005) (Kamala and Nanda 2009). However, this skewed response proved to be protective against

leishmaniasis. In addition, H2-DM$^{-/-}$ and Ii$^{-/-}$ H2-DM$^{-/-}$ mice produced IFNγ and IL-17, but not IL-4 nor IL-10. Although the biology of *Leishmania* and *Toxoplasma* are obviously different, the profile of other cytokines during infection may differ substantially in our toxoplasmosis model, as well.

At the moment, the precise molecular mechanisms of why only the double KO mice succumb invariably within a few weeks of chronic infection remains unclear. Although naïve CD4$^+$ T cells require prolonged antigenic stimulation in order to differentiate into effector and memory cells (Obst, van Santen et al. 2005), it is believed that the persistence of resting memory CD4$^+$ T cells does not require sustained MHC-II presentation, but rather IL-7 and IL-15 (van Leeuwen, Sprent et al. 2009). Following the same hypothesis, it is possible that the cytokine environment in the different KO strains could contribute to the presence of different T cell pools and to the control or failed control of encysted parasites. Also, presentation of a different set of antigens in the chronic phase compared to the acute phase could require a different pool of CD4$^+$ T cells to control encysted parasites, which are not being primed in double KO mice. Obviously, it would be of great interest to further characterize the immunological state later in the chronic stage of infection with these KO models, and either validate or disprove this hypothesis.

4.5.3. Molecular mechanisms of Ii processing and endosomal biology during *T. gondii* infection

Dissecting the molecular mechanism of the invariant chain processing revealed that important host endosomal proteases involved in Ii degradation and antigen processing are differentially modulated by *T. gondii* depending on the cell type (Figure 4.15). It is known that different cell types, including macrophages and dendritic cells, preferentially utilize different proteases depending on their activation state (Hsing and Rudensky 2005). For instance, macrophages switch from CatL to CatS upon IFNγ stimulation, while conventional DCs consistently

rely on CatS. These differences could explain the differential processing of Ii observed by Western blotting of infected BMMΦ and BMDCs (Figures 4.14A and 4.14B). However, the accumulation of Ii does not an effect on the modulation of these proteases (Figure 4.15), since the same pattern was observed infected $Ii^{-/-}$ cells. Conversely, incomplete degradation of Ii has been shown to disrupt normal MHC-II trafficking patterns and block surface expression. One study had shown that by inhibiting cysteine proteases using leupeptin, a protease inhibitor, caused an accumulation of the p10 cleavage product in lysosomal structures and blocked transfer of MHC-II molecules to the surface; removal of the inhibitor completely reverted these effects (Brachet, Raposo et al. 1997). We also show that endogenous *T. gondii* cysteine protease inhibitors, toxostatins 1 and 2, do not appear to play a role in inhibiting host proteases, at least no those that partake in Ii degradation (Figure 4.16). Since these proteases require an acidified environment and as an assessment of endosomal maturation, we measured the pH of the endosomal pathway in infected cells by flow cytometry and found that acidification of the compartments containing internalized beads is reduced in infected cultures (Figure 4.17A), but is restored when IFNγ is added to the cultures (Figure 4.17B). The acidification of the endosomes/phagosomes is necessary to activate the resident aspartic and cysteine proteases, and hence for optimal antigen processing and Ii proteolysis (Hsing and Rudensky 2005). However, the different endosomal proteases have different pH profiles (Riese and Chapman 2000). For instance, cathepsin S has a rather broad pH profile and can be activated in early compartments, capable of degrading Ii and antigens within EEs through mature endolysosomes (Driessen, Bryant et al. 1999). On the under hand, cathepsins B and L, are unstable at neutral pH and hence are only active in more mature compartments (Quraishi, Nagler et al. 1999) (Turk, Dolenc et al. 1999). Moreover, acidification of endosomal compartments was shown to be important for H2-DM functions, whereby the catalysis rate of peptide exchange is accelerated at around pH 5, corresponding to late endosomes or MIIC, but not at pH 7 (Sloan, Cameron et al. 1995). Under normal conditions, this pH-dependency ensures a timely regulated maturation of MHC-II and peptide

loading. Hence, disturbance of this regulated process by *T. gondii* surely has significant consequences on the entire endocytic pathway biology.

Collectively, our results show that *Toxoplasma gondii* inhibits MHC-II-restricted antigen presentation through multiple mechanisms including a transcriptional inhibition of IFNγ-induced class II genes, a post-translational layer of regulation involving Ii as dominant negative, and perturbation of endosomal processes such as acidification and enzymatic activities of resident proteases, all in the attempt to subvert host immune functions and establish chronic infection.

Chapter 5. Conclusions

Over the past several years, the protozoan parasite *Toxoplasma gondii* has become a useful model for the study of not only apicomplexans, but also intracellular parasitism in general. The parasite's broad range of natural hosts (Dubey, Storandt et al. 1999) (Tenter, Heckeroth et al. 2000) (Dubey 2004), its malleability to genetic manipulation and the availability of numerous bioinformatical tools (Roos, Donald et al. 1994) (Donald and Roos 1995) (Kissinger, Gajria et al. 2003) (Kim and Weiss 2004) (Gajria, Bahl et al. 2008), its ability to infect any nucleated cells (Kim and Weiss 2004), and its induction of a strong Th1-type, cell-mediated immune response (Suzuki, Orellana et al. 1988) (Gazzinelli, Hakim et al. 1991) (Denkers and Gazzinelli 1998) are all characteristics that make *T. gondii* a suitable and convenient model to study different biological phenomena.

Of particular interest, as previously discussed in this thesis, *Toxoplasma gondii* has evolved numerous strategies to subvert host immune functions in order to establish a successful chronic infection. This immune subversion has been explicitly demonstrated by numerous studies showing the parasite's ability to lower NO production by inhibiting the inducible nitric oxide synthase (iNOS) transcription (Seabra, de Souza et al. 2002) (Luder, Algner et al. 2003), inhibit transcription of interferon-inducible p47 GTPases (IRG) (Butcher, Greene et al. 2005), inhibit production of pro-inflammatory cytokines like IL-12 and TNFα (Aliberti, Serhan et al. 2002) (Butcher, Kim et al. 2005), induce anti-inflammatory cytokines like IL-10 (Khan, Matsuura et al. 1995) via the STAT3/6 pathway (Butcher, Kim et al. 2005), TGFβ (Bermudez, Covaro et al. 1993), and IFNα and β (Diez, Galdeano et al. 1989), and disturb signaling pathway components such as NF-κB (Shapira, Harb et al. 2005), MAPK (Kim, Butcher et al. 2004), and STAT1 (Zimmermann, Murray et al. 2006).

Work in our laboratory has focused on antigen presentation, specifically MHC-II-restricted antigen presentation since it represents a necessary step for the generation of parasite-specific $CD4^+$ T helpers cells. This lymphocyte subset was

shown to be essential for the maintenance of $CD8^+$ T cell effector immunity against *T. gondii* (Gazzinelli, Hakim et al. 1991) (Casciotti, Ely et al. 2002), notably in the brain of chronically infected animals and directly contributing to the resistance against toxoplasmic encephalitis, a role most exemplified in $CD4^+$ T cell-deficient patients (ex: AIDS patients) (Lutjen, Soltek et al. 2006).

The work detailed in this thesis stems out from previous studies that had shown a transcriptional inhibition of MHC-II genes and protein synthesis by the parasite (Luder, Lang et al. 1998) (Luder, Lang et al. 2003) (Lang, Algner et al. 2006), and an impeded MHC-II-restricted antigen presentation and $CD4^+$ T cell activation (Luder, Walter et al. 2001) (McKee, Dzierszinski et al. 2004). In this body of work, we further contributed to the established knowledge by addressing two important aspects regarding the inhibition of MHC-II expression and antigen presentation by *T. gondii*.

The first aspect to be addressed was to identify the parasite molecules involved in the inhibition of IFNγ-induced MHC-II expression in professional antigen presenting cells. The characterization of secretory molecules in *T. gondii* and apicomplexans in general has proven to be of great interest with major implications in chemotherapeutic and vaccine designs, cell biology, disease outcome, and so on and so forth. Also, the biochemical procedures outlined in this thesis may provide important tools for future experiments wishing to characterize other secreted molecules and subcellular structures in *T. gondii* as well as other apicomplexan parasites. Although we did not identify the specific molecules that directly inhibit MHC-II expression, we provide a list of 24 potential candidates to be validated and bring forth compelling evidence that the causative molecules originate from secretory organelles. It is readily conceivable to test and confirm any of these candidates by generating knock-out strains using the KU80 system (Fox, Ristuccia et al. 2009), for example. However, generating knock-outs can lead to unexpected issues with parasite viability or fitness, especially when infecting immune cells that possess effector mechanisms able to eliminate intracellular pathogens. For instance, a particular knock-out strain

could be more sensitive to destruction without actually lacking the gene involved in MHC-II inhibition, and the infected host cell could be able to mature and express MHC-II at normal levels after eliminating the parasite. This scenario would lead to a false interpretation on the role of certain genes. Therefore, complementary approaches would be required in this case to confirm or discount certain genes; synthesizing recombinant proteins and testing these directly on host cells could help validate the phenotype.

Although the forward genetic screen presented possible shortcomings, the overall design should not be discarded. Indeed, the pitfalls stem out mostly from the specific biological phenomenon studied, i.e. MHC-II inhibition, and could be used to address other aspects of the parasite's biology. In other words, this strategy is by no means doomed to fail, but rather could provide a powerful methodology to identify the function of other genes in other settings.

The second aspect investigated was *T. gondii*'s ability to inhibit antigen presentation in infected cells. We uncovered a novel mechanism that involves the induction of the MHC-II-associated invariant chain (Ii) to block the presentation of parasite-derived endogenous on MHC-II molecules. This is the first report that links the induction of Ii by an intracellular pathogen to specifically block antigen presentation. The exact molecular mechanisms were not clearly defined, but surely this represents an immensely important question to address in future endeavors. In addition, these findings led us to characterize a more global effect of infection on host endosomal biology (acidification, protease activity, etc.), which offers an extended view of the profound changes *T. gondii* induced when infecting a host cell and highlights how well the parasite has evolutionarily adapted to its intracellular niche.

Furthermore, our *in vivo* studies highlighted the contribution of two major components of the MHC-II pathway, namely Ii and H2-DM, in the development of an immune response against toxoplasmosis. It would prove invaluable to determine the exact epitope and $CD4^+$ T cell population repertoires elicited in the different mouse strains, and how they determine the fate of the infection.

Adoptive cell transfer could also be an attractive approach to determine the role of these cell populations. For example, would transferring pAPCs or T cells from Ii KO mice improve the response in H2-DM KOs, increasing T cell activation and reducing cyst burden? The activation and the effector functions of $CD8^+$ T cells should be assessed in this system as well in order to draw a more global picture of the cell-mediated immune responses during acute toxoplasmosis.

Our *in vitro* studies not only assessed the impacts of Ii and H-2DM on the immune response, but also on parasite dissemination. Host cell motility upon infection could be assessed by more direct techniques, such as transwell assay or time-lapse video microscopy (Bahnson, Athanassiou et al. 2005), comparing infected WT and $Ii^{-/-}$ cell motility for example. In our studies, we limited the measurements to lymphoid organs, but alternatively, measuring parasite dissemination by bioluminescence-based imaging could give important information as to migration throughout the body in the different knock-out mouse strains (Saeij, Boyle et al. 2005).

Our studies mainly focused on the acute and the early onset of the chronic phase of the infection. Since we observed a significant incidence on brain cyst burden and survival, defining T cell memory development, persistence, and activity by flow cytometry phenotyping and cytokine environment profiling, and subsequent challenge with types I, II, or III parasites in our experimental model are only some of the possibilities that would provide interesting clues on the dynamics of the immune response during chronic toxoplasmosis.

In conclusion, the results detailed herein provide tremendous insight on key biological features of *Toxoplasma gondii*, specifically its immune subversion strategies with regards to antigen presentation. Importantly, these findings can be extrapolated to other parasites, and to some extent, to other intracellular pathogens, in order to guide future research. Although the great diversity of these microbes, some immune subversion strategies they rely on undoubtedly share common characteristics. Ultimately, identifying the mechanisms devised by these pathogens to subvert host immune functions will be instrumental in understanding

disease and virulence. Finally, the knowledge acquired throughout this project will potentially contribute to the rational design of T cell-based vaccines or chemotherapeutic alternatives, and surely to the field of parasitology.

References

Abgrall, S., C. Rabaud, et al. (2001). "Incidence and risk factors for toxoplasmic encephalitis in human immunodeficiency virus-infected patients before and during the highly active antiretroviral therapy era." Clin Infect Dis **33**(10): 1747-1755.

Adams, L. B., J. B. Hibbs, Jr., et al. (1990). "Microbiostatic effect of murine-activated macrophages for *Toxoplasma gondii*. Role for synthesis of inorganic nitrogen oxides from L-arginine." J Immunol **144**(7): 2725-2729.

Ahn, H. J., S. Kim, et al. (2006). "Interactions between secreted GRA proteins and host cell proteins across the paratitophorous vacuolar membrane in the parasitism of *Toxoplasma gondii*." Korean J Parasitol **44**(4): 303-312.

Ajzenberg, D., A. L. Banuls, et al. (2004). "Genetic diversity, clonality and sexuality in *Toxoplasma gondii*." Int J Parasitol **34**(10): 1185-1196.

Alexander, D. L., J. Mital, et al. (2005). "Identification of the moving junction complex of *Toxoplasma gondii*: a collaboration between distinct secretory organelles." PLoS pathogens **1**(2): e17.

Alexander, W. S. and D. J. Hilton (2004). "The role of suppressors of cytokine signaling (SOCS) proteins in regulation of the immune response." Annu Rev Immunol **22**: 503-529.

Aliberti, J., C. Reis e Sousa, et al. (2000). "CCR5 provides a signal for microbial induced production of IL-12 by CD8 alpha+ dendritic cells." Nat Immunol **1**(1): 83-87.

Aliberti, J., C. Serhan, et al. (2002). "Parasite-induced lipoxin A4 is an endogenous regulator of IL-12 production and immunopathology in *Toxoplasma gondii* infection." J Exp Med **196**(9): 1253-1262.

Alimonti, J. B., T. B. Ball, et al. (2003). "Mechanisms of CD4+ T lymphocyte cell death in human immunodeficiency virus infection and AIDS." J Gen Virol **84**(Pt 7): 1649-1661.

Amprey, J. L., J. S. Im, et al. (2004). "A subset of liver NK T cells is activated during *Leishmania donovani* infection by CD1d-bound lipophosphoglycan." J Exp Med **200**(7): 895-904.

Angus, C. W., D. Klivington-Evans, et al. (2000). "Immunization with a DNA plasmid encoding the SAG1 (P30) protein of *Toxoplasma gondii* is immunogenic and protective in rodents." J Infect Dis **181**(1): 317-324.

Araujo, F. G. (1992). "Depletion of CD4+ T cells but not inhibition of the protective activity of IFN-gamma prevents cure of toxoplasmosis mediated by drug therapy in mice." J Immunol **149**(9): 3003-3007.

Bahnson, A., C. Athanassiou, et al. (2005). "Automated measurement of cell motility and proliferation." BMC Cell Biol **6**(1): 19.

Barnden, M. J., J. Allison, et al. (1998). "Defective TCR expression in transgenic mice constructed using cDNA-based alpha- and beta-chain genes under the control of heterologous regulatory elements." Immunol Cell Biol **76**(1): 34-40.

Barral, D. C. and M. B. Brenner (2007). "CD1 antigen presentation: how it works." Nat Rev Immunol **7**(12): 929-941.

Beckman, E. M., S. A. Porcelli, et al. (1994). "Recognition of a lipid antigen by CD1-restricted alpha beta+ T cells." Nature **372**(6507): 691-694.

Beghetto, E., H. V. Nielsen, et al. (2005). "A combination of antigenic regions of *Toxoplasma gondii* microneme proteins induces protective immunity against oral infection with parasite cysts." J Infect Dis **191**(4): 637-645.

Behnke, M. S., A. Khan, et al. (2011). "Virulence differences in *Toxoplasma* mediated by amplification of a family of polymorphic pseudokinases." Proc Natl Acad Sci U S A **108**(23): 9631-9636.

Bermudez, L. E., G. Covaro, et al. (1993). "Infection of murine macrophages with *Toxoplasma gondii* is associated with release of transforming growth factor beta and downregulation of expression of tumor necrosis factor receptors." Infect Immun **61**(10): 4126-4130.

Besteiro, S., A. Michelin, et al. (2009). "Export of a *Toxoplasma gondii* rhoptry neck protein complex at the host cell membrane to form the moving junction during invasion." PLoS pathogens **5**(2): e1000309.

Beswick, E. J., S. Das, et al. (2005). "*Helicobacter pylori*-induced IL-8 production by gastric epithelial cells up-regulates CD74 expression." J Immunol **175**(1): 171-176.

Bevec, T., V. Stoka, et al. (1996). "Major histocompatibility complex class II-associated p41 invariant chain fragment is a strong inhibitor of lysosomal cathepsin L." J Exp Med **183**(4): 1331-1338.

Bikoff, E. K., L. Y. Huang, et al. (1993). "Defective major histocompatibility complex class II assembly, transport, peptide acquisition, and CD4+ T cell selection in mice lacking invariant chain expression." J Exp Med **177**(6): 1699-1712.

Blackman, M. J. and L. H. Bannister (2001). "Apical organelles of Apicomplexa: biology and isolation by subcellular fractionation." Mol Biochem Parasitol **117**(1): 11-25.

Blum, H., H. Beier, et al. (1987). "Improved Silver Staining of Plant-Proteins, Rna and DNA in Polyacrylamide Gels." Electrophoresis **8**(2): 93-99.

Bodmer, H., S. Viville, et al. (1994). "Diversity of endogenous epitopes bound to MHC class II molecules limited by invariant chain." Science **263**(5151): 1284-1286.

Bonifacino, J. S. and L. M. Traub (2003). "Signals for sorting of transmembrane proteins to endosomes and lysosomes." Annu Rev Biochem **72**: 395-447.

Bonnet, F., C. Lewden, et al. (2005). "Opportunistic infections as causes of death in HIV-infected patients in the HAART era in France." Scand J Infect Dis **37**(6-7): 482-487.

Boothroyd, J. C. and J. F. Dubremetz (2008). "Kiss and spit: the dual roles of *Toxoplasma* rhoptries." Nat Rev Microbiol **6**(1): 79-88.

Boss, J. M. and P. E. Jensen (2003). "Transcriptional regulation of the MHC class II antigen presentation pathway." Curr Opin Immunol **15**(1): 105-111.

Boyer, K. and R. McLeod (2002). Principles and Practice of Pediatric Infectious Diseases. S. Long, Proeber, C and Pickering L. New York, Churchill Livingstone**:** 1303-1322.

Brachet, V., G. Raposo, et al. (1997). "Ii chain controls the transport of major histocompatibility complex class II molecules to and from lysosomes." J Cell Biol **137**(1): 51-65.

Bradley, P. J. and J. C. Boothroyd (1999). "Identification of the pro-mature processing site of *Toxoplasma* ROP1 by mass spectrometry." Molecular and biochemical parasitology **100**(1): 103-109.

Bradley, P. J., C. L. Hsieh, et al. (2002). "Unprocessed *Toxoplasma* ROP1 is effectively targeted and secreted into the nascent parasitophorous vacuole." Molecular and biochemical parasitology **125**(1-2): 189-193.

Bradley, P. J., C. Ward, et al. (2005). "Proteomic analysis of rhoptry organelles reveals many novel constituents for host-parasite interactions in *Toxoplasma gondii*." J Biol Chem **280**(40): 34245-34258.

Braun, L., L. Travier, et al. (2008). "Purification of *Toxoplasma* dense granule proteins reveals that they are in complexes throughout the secretory pathway." Molecular and biochemical parasitology **157**(1): 13-21.

Brinkmann, V., J. S. Remington, et al. (1993). "Vaccination of mice with the protective F3G3 antigen of *Toxoplasma gondii* activates CD4+ but not CD8+ T cells and induces Toxoplasma specific IgG antibody." Mol Immunol **30**(4): 353-358.

Brown, C. R. and R. McLeod (1990). "Class I MHC genes and CD8+ T cells determine cyst number in *Toxoplasma gondii* infection." J Immunol **145**(10): 3438-3441.

Bryant, P. and H. Ploegh (2004). "Class II MHC peptide loading by the professionals." Curr Opin Immunol **16**(1): 96-102.

Bulow, R. and J. C. Boothroyd (1991). "Protection of mice from fatal *Toxoplasma gondii* infection by immunization with p30 antigen in liposomes." J Immunol **147**(10): 3496-3500.

Burg, J. L., C. M. Grover, et al. (1989). "Direct and sensitive detection of a pathogenic protozoan, *Toxoplasma gondii*, by polymerase chain reaction." J Clin Microbiol **27**(8): 1787-1792.

Busch, R., C. H. Rinderknecht, et al. (2005). "Achieving stability through editing and chaperoning: regulation of MHC class II peptide binding and expression." Immunol Rev **207**: 242-260.

Butcher, B. A., R. I. Greene, et al. (2005). "p47 GTPases regulate *Toxoplasma gondii* survival in activated macrophages." Infect Immun **73**(6): 3278-3286.

Butcher, B. A., L. Kim, et al. (2005). "IL-10-independent STAT3 activation by *Toxoplasma gondii* mediates suppression of IL-12 and TNF-alpha in host macrophages." J Immunol **174**(6): 3148-3152.

Buxton, D., K. Thomson, et al. (1991). "Vaccination of sheep with a live incomplete strain (S48) of *Toxoplasma gondii* and their immunity to challenge when pregnant." Vet Rec **129**(5): 89-93.

Cameron, P., A. McGachy, et al. (2004). "Inhibition of lipopolysaccharide-induced macrophage IL-12 production by *Leishmania mexicana* amastigotes: the role of cysteine peptidases and the NF-kappaB signaling pathway." J Immunol **173**(5): 3297-3304.

Carruthers, V. B. and L. D. Sibley (1997). "Sequential protein secretion from three distinct organelles of *Toxoplasma gondii* accompanies invasion of human fibroblasts." Eur J Cell Biol **73**(2): 114-123.

Casciotti, L., K. H. Ely, et al. (2002). "CD8(+)-T-cell immunity against *Toxoplasma gondii* can be induced but not maintained in mice lacking conventional CD4(+) T cells." Infect Immun **70**(2): 434-443.

Chen, F., A. J. Mackey, et al. (2006). "OrthoMCL-DB: querying a comprehensive multi-species collection of ortholog groups." Nucleic Acids Res **34**(Database issue): D363-368.

Chervonsky, A. and A. J. Sant (1995). "In the absence of major histocompatibility complex class II molecules, invariant chain is translocated to late endocytic compartments by autophagy." Eur J Immunol **25**(4): 911-918.

Cohen, N. R., S. Garg, et al. (2009). "Antigen Presentation by CD1 Lipids, T Cells, and NKT Cells in Microbial Immunity." Adv Immunol **102**: 1-94.

Combe, C. L., T. J. Curiel, et al. (2005). "NK cells help to induce CD8(+)-T-cell immunity against *Toxoplasma gondii* in the absence of CD4(+) T cells." Infect Immun **73**(8): 4913-4921.

Coppens, I., M. Andries, et al. (1999). "Intracellular trafficking of dense granule proteins in *Toxoplasma gondii* and experimental evidences for a regulated exocytosis." Eur J Cell Biol **78**(7): 463-472.

Couper, K. N., H. V. Nielsen, et al. (2003). "DNA vaccination with the immunodominant tachyzoite surface antigen (SAG-1) protects against adult acquired *Toxoplasma gondii* infection but does not prevent maternofoetal transmission." Vaccine **21**(21-22): 2813-2820.

Courret, N., S. Darche, et al. (2006). "CD11c- and CD11b-expressing mouse leukocytes transport single *Toxoplasma gondii* tachyzoites to the brain." Blood **107**(1): 309-316.

Courret, N., C. Frehel, et al. (2001). "Kinetics of the intracellular differentiation of *Leishmania amazonensis* and internalization of host MHC molecules by the intermediate parasite stages." Parasitology **122**(Pt 3): 263-279.

Dao, A., B. Fortier, et al. (2001). "Successful reinfection of chronically infected mice by a different *Toxoplasma gondii* genotype." Int J Parasitol **31**(1): 63-65.

Darcy, F., D. Deslee, et al. (1988). "Induction of a protective antibody-dependent response against toxoplasmosis by in vitro excreted/secreted antigens from tachyzoites of *Toxoplasma gondii*." Parasite immunology **10**(5): 553-567.

Darcy, F., D. Deslee, et al. (1988). "Induction of a protective antibody-dependent response against toxoplasmosis by in vitro excreted/secreted antigens from tachyzoites of *Toxoplasma gondii*." Parasite Immunol **10**(5): 553-567.

David Sibley, L. (2003). "Recent origins among ancient parasites." Vet Parasitol **115**(2): 185-198.

De Souza Leao, S., T. Lang, et al. (1995). "Intracellular *Leishmania amazonensis* amastigotes internalize and degrade MHC class II molecules of their host cells." J Cell Sci **108 (Pt 10)**: 3219-3231.

Debard, N., D. Buzoni-Gatel, et al. (1996). "Intranasal immunization with SAG1 protein of *Toxoplasma gondii* in association with cholera toxin

dramatically reduces development of cerebral cysts after oral infection." Infect Immun **64**(6): 2158-2166.

Denkers, E. Y. and R. T. Gazzinelli (1998). "Regulation and function of T-cell-mediated immunity during *Toxoplasma gondii* infection." Clin Microbiol Rev **11**(4): 569-588.

Denkers, E. Y., T. Scharton-Kersten, et al. (1996). "A role for CD4+ NK1.1+ T lymphocytes as major histocompatibility complex class II independent helper cells in the generation of CD8+ effector function against intracellular infection." J Exp Med **184**(1): 131-139.

Denkers, E. Y. and A. Sher (1997). "Role of natural killer and NK1+ T-cells in regulating cell-mediated immunity during *Toxoplasma gondii* infection." Biochem Soc Trans **25**(2): 699-703.

Diez, B., A. Galdeano, et al. (1989). "Relationship between the production of interferon-alpha/beta and interferon-gamma during acute toxoplasmosis." Parasitology **99 Pt 1**: 11-15.

Dittie, A. S., J. Klumperman, et al. (1999). "Differential distribution of mannose-6-phosphate receptors and furin in immature secretory granules." J Cell Sci **112 (Pt 22)**: 3955-3966.

Dobrowolski, J. M. and L. D. Sibley (1996). "*Toxoplasma* invasion of mammalian cells is powered by the actin cytoskeleton of the parasite." Cell **84**(6): 933-939.

Donald, R. G. and D. S. Roos (1994). "Homologous recombination and gene replacement at the dihydrofolate reductase-thymidylate synthase locus in *Toxoplasma gondii*." Mol Biochem Parasitol **63**(2): 243-253.

Donald, R. G. and D. S. Roos (1995). "Insertional mutagenesis and marker rescue in a protozoan parasite: cloning of the uracil phosphoribosyltransferase locus from *Toxoplasma gondii*." Proc Natl Acad Sci U S A **92**(12): 5749-5753.

Dorangeon, P. H., C. Marx-Chemla, et al. (1992). "[The risks of pyrimethamine-sulfadoxine combination in the prenatal treatment of toxoplasmosis]." J Gynecol Obstet Biol Reprod (Paris) **21**(5): 549-556.

Dougan, S. K., A. Kaser, et al. (2007). "CD1 expression on antigen-presenting cells." Curr Top Microbiol Immunol **314**: 113-141.

Driessen, C., R. A. Bryant, et al. (1999). "Cathepsin S controls the trafficking and maturation of MHC class II molecules in dendritic cells." J Cell Biol **147**(4): 775-790.

Dubey, J. P. (1986). "Toxoplasmosis." J Am Vet Med Assoc **189**(2): 166-170.

Dubey, J. P. (1998). "Advances in the life cycle of *Toxoplasma gondii*." Int J Parasitol **28**(7): 1019-1024.

Dubey, J. P. (2004). "Toxoplasmosis - a waterborne zoonosis." Vet Parasitol **126**(1-2): 57-72.

Dubey, J. P. (2008). "The history of *Toxoplasma gondii*--the first 100 years." J Eukaryot Microbiol **55**(6): 467-475.

Dubey, J. P., N. L. Miller, et al. (1970). "The *Toxoplasma gondii* oocyst from cat feces." J Exp Med **132**(4): 636-662.

Dubey, J. P., C. A. Speer, et al. (1997). "Oocyst-induced murine toxoplasmosis: life cycle, pathogenicity, and stage conversion in mice fed *Toxoplasma gondii* oocysts." J Parasitol **83**(5): 870-882.

Dubey, J. P., S. T. Storandt, et al. (1999). "*Toxoplasma gondii* antibodies in naturally exposed wild coyotes, red foxes, and gray foxes and serologic diagnosis of Toxoplasmosis in red foxes fed *T. gondii* oocysts and tissue cysts." J Parasitol **85**(2): 240-243.

Durand, B., P. Sperisen, et al. (1997). "RFXAP, a novel subunit of the RFX DNA binding complex is mutated in MHC class II deficiency." EMBO J **16**(5): 1045-1055.

Dzierszinski, F., M. Pepper, et al. (2007). "Presentation of *Toxoplasma gondii* antigens via the endogenous major histocompatibility complex class I pathway in nonprofessional and professional antigen-presenting cells." Infect Immun **75**(11): 5200-5209.

Dzierszinski, F. S. and C. A. Hunter (2008). "Advances in the use of genetically engineered parasites to study immunity to *Toxoplasma gondii*." Parasite Immunol **30**(4): 235-244.

Ellner, P. D. (1998). "Smallpox: gone but not forgotten." Infection **26**(5): 263-269.

Elsheikha, H. M. and N. A. Khan (2010). "Protozoa traversal of the blood-brain barrier to invade the central nervous system." FEMS Microbiol Rev **34**(4): 532-553.

Fan, P., F. Dong, et al. (2002). "*Chlamydia pneumoniae* secretion of a protease-like activity factor for degrading host cell transcription factors required for [correction of factors is required for] major histocompatibility complex antigen expression." Infect Immun **70**(1): 345-349.

Faure-Andre, G., P. Vargas, et al. (2008). "Regulation of dendritic cell migration by CD74, the MHC class II-associated invariant chain." Science **322**(5908): 1705-1710.

Fentress, S. J., M. S. Behnke, et al. (2010). "Phosphorylation of immunity-related GTPases by a *Toxoplasma gondii*-secreted kinase promotes macrophage survival and virulence." Cell Host Microbe **8**(6): 484-495.

Fischer, H. G., S. Stachelhaus, et al. (1998). "GRA7, an excretory 29 kDa *Toxoplasma gondii* dense granule antigen released by infected host cells." Molecular and biochemical parasitology **91**(2): 251-262.

Flores, M., R. Saavedra, et al. (2008). "Macrophage migration inhibitory factor (MIF) is critical for the host resistance against *Toxoplasma gondii*." FASEB J **22**(10): 3661-3671.

Foussard, F., M. A. Leriche, et al. (1991). "Characterization of the lipid content of *Toxoplasma gondii* rhoptries." Parasitology **102 Pt 3**: 367-370.

Fox, B. A. and D. J. Bzik (2002). "De novo pyrimidine biosynthesis is required for virulence of *Toxoplasma gondii*." Nature **415**(6874): 926-929.

Fox, B. A., J. G. Ristuccia, et al. (2009). "Efficient gene replacements in *Toxoplasma gondii* strains deficient for nonhomologous end joining." Eukaryot Cell **8**(4): 520-529.

Frenkel, J. K., J. P. Dubey, et al. (1970). "*Toxoplasma gondii* in cats: fecal stages identified as coccidian oocysts." Science **167**(3919): 893-896.

Gajria, B., A. Bahl, et al. (2008). "ToxoDB: an integrated *Toxoplasma gondii* database resource." Nucleic Acids Res **36**(Database issue): D553-556.

Gao, J., B. P. De, et al. (2001). "Human parainfluenza virus type 3 inhibits gamma interferon-induced major histocompatibility complex class II expression directly and by inducing alpha/beta interferon." J Virol **75**(3): 1124-1131.

Gazzinelli, R., Y. Xu, et al. (1992). "Simultaneous depletion of CD4+ and CD8+ T lymphocytes is required to reactivate chronic infection with *Toxoplasma gondii*." J Immunol **149**(1): 175-180.

Gazzinelli, R. T., F. T. Hakim, et al. (1991). "Synergistic role of CD4+ and CD8+ T lymphocytes in IFN-gamma production and protective immunity induced by an attenuated *Toxoplasma gondii* vaccine." J Immunol **146**(1): 286-292.

Gazzinelli, R. T., M. Wysocka, et al. (1994). "Parasite-induced IL-12 stimulates early IFN-gamma synthesis and resistance during acute infection with *Toxoplasma gondii*." J Immunol **153**(6): 2533-2543.

Gilbert, L. A., S. Ravindran, et al. (2007). "*Toxoplasma gondii* targets a protein phosphatase 2C to the nuclei of infected host cells." Eukaryot Cell **6**(1): 73-83.

Glasner, P. D., C. Silveira, et al. (1992). "An unusually high prevalence of ocular toxoplasmosis in southern Brazil." Am J Ophthalmol **114**(2): 136-144.

Glimcher, L. H. and C. J. Kara (1992). "Sequences and factors: a guide to MHC class-II transcription." Annu Rev Immunol **10**: 13-49.

Goldszmid, R. S., I. Coppens, et al. (2009). "Host ER-parasitophorous vacuole interaction provides a route of entry for antigen cross-presentation in *Toxoplasma gondii*-infected dendritic cells." J Exp Med **206**(2): 399-410.

Golkar, M., M. A. Shokrgozar, et al. (2007). "Evaluation of protective effect of recombinant dense granule antigens GRA2 and GRA6 formulated in monophosphoryl lipid A (MPL) adjuvant against *Toxoplasma* chronic infection in mice." Vaccine **25**(21): 4301-4311.

Gray, P. W. and D. V. Goeddel (1982). "Structure of the human immune interferon gene." Nature **298**(5877): 859-863.

Gregers, T. F., T. W. Nordeng, et al. (2003). "The cytoplasmic tail of invariant chain modulates antigen processing and presentation." Eur J Immunol **33**(2): 277-286.

Grigg, M. E., J. Ganatra, et al. (2001). "Unusual abundance of atypical strains associated with human ocular toxoplasmosis." J Infect Dis **184**(5): 633-639.

Gubbels, M. J., M. Lehmann, et al. (2008). "Forward genetic analysis of the apicomplexan cell division cycle in *Toxoplasma gondii*." PLoS Pathog **4**(2): e36.

Gubbels, M. J., B. Striepen, et al. (2005). "Class I major histocompatibility complex presentation of antigens that escape from the parasitophorous vacuole of *Toxoplasma gondii*." Infect Immun **73**(2): 703-711.

Guermonprez, P., J. Valladeau, et al. (2002). "Antigen presentation and T cell stimulation by dendritic cells." Annu Rev Immunol **20**: 621-667.

Hakansson, S., A. J. Charron, et al. (2001). "*Toxoplasma* evacuoles: a two-step process of secretion and fusion forms the parasitophorous vacuole." EMBO J **20**(12): 3132-3144.

Hardy, P. O., T. O. Diallo, et al. (2009). "Roles of phosphatidylinositol 3-kinase and p38 mitogen-activated protein kinase in the regulation of protein kinase C-alpha activation in interferon-gamma-stimulated macrophages." Immunology **128**(1 Suppl): e652-660.

Harper, J. M., X. W. Zhou, et al. (2004). "The novel coccidian micronemal protein MIC11 undergoes proteolytic maturation by sequential cleavage to remove an internal propeptide." International journal for parasitology **34**(9): 1047-1058.

Hartwell, L. (2008). Genetics : from genes to genomes. Boston, McGraw-Hill Higher Education.

Hehl, A. B., C. Lekutis, et al. (2000). "*Toxoplasma gondii* homologue of *Plasmodium* apical membrane antigen 1 is involved in invasion of host cells." Infect Immun **68**(12): 7078-7086.

Hemmi, S., R. Bohni, et al. (1994). "A novel member of the interferon receptor family complements functionality of the murine interferon gamma receptor in human cells." Cell **76**(5): 803-810.

Hilleman, M. R. (2000). "Vaccines in historic evolution and perspective: a narrative of vaccine discoveries." J Hum Virol **3**(2): 63-76.

Hogquist, K. A., S. C. Jameson, et al. (1994). "T cell receptor antagonist peptides induce positive selection." Cell **76**(1): 17-27.

Howe, D. K. and L. D. Sibley (1995). "*Toxoplasma gondii* comprises three clonal lineages: correlation of parasite genotype with human disease." J Infect Dis **172**(6): 1561-1566.

Hsing, L. C. and A. Y. Rudensky (2005). "The lysosomal cysteine proteases in MHC class II antigen presentation." Immunol Rev **207**: 229-241.

Huang, R., X. Que, et al. (2009). "The cathepsin L of *Toxoplasma gondii* (TgCPL) and its endogenous macromolecular inhibitor, toxostatin." Mol Biochem Parasitol **164**(1): 86-94.

Hudson, A. W. and H. L. Ploegh (2002). "The cell biology of antigen presentation." Exp Cell Res **272**(1): 1-7.

Hunter, C. A., E. Candolfi, et al. (1995). "Studies on the role of interleukin-12 in acute murine toxoplasmosis." Immunology **84**(1): 16-20.

Huotari, J. and A. Helenius (2011). "Endosome maturation." EMBO J **30**(17): 3481-3500.

Hussain, A., C. Wesley, et al. (2008). "Human immunodeficiency virus type 1 Vpu protein interacts with CD74 and modulates major histocompatibility complex class II presentation." J Virol **82**(2): 893-902.

Innes, E. A., P. M. Bartley, et al. (2009). "Veterinary vaccines against *Toxoplasma gondii*." Mem Inst Oswaldo Cruz **104**(2): 246-251.

Innes, E. A., W. R. Panton, et al. (1995). "Induction of CD4+ and CD8+ T cell responses in efferent lymph responding to *Toxoplasma gondii* infection: analysis of phenotype and function." Parasite Immunol **17**(3): 151-160.

Itano, A. A., S. J. McSorley, et al. (2003). "Distinct dendritic cell populations sequentially present antigen to CD4 T cells and stimulate different aspects of cell-mediated immunity." Immunity **19**(1): 47-57.

Jacobs, D., J. F. Dubremetz, et al. (1998). "Identification and heterologous expression of a new dense granule protein (GRA7) from *Toxoplasma gondii*." Molecular and biochemical parasitology **91**(2): 237-249.

Janeway, C. A., Jr. (2001). "How the immune system protects the host from infection." Microbes Infect **3**(13): 1167-1171.

Jauregui, L. H., J. Higgins, et al. (2001). "Development of a real-time PCR assay for detection of *Toxoplasma gondii* in pig and mouse tissues." J Clin Microbiol **39**(6): 2065-2071.

Jensen, K. D., Y. Wang, et al. (2011). "*Toxoplasma* polymorphic effectors determine macrophage polarization and intestinal inflammation." Cell Host Microbe **9**(6): 472-483.

Jiang, G., H. R. Yang, et al. (2008). "Hepatic stellate cells preferentially expand allogeneic CD4+ CD25+ FoxP3+ regulatory T cells in an IL-2-dependent manner." Transplantation **86**(11): 1492-1502.

Johnson, L. L. (1992). "A protective role for endogenous tumor necrosis factor in *Toxoplasma gondii* infection." Infect Immun **60**(5): 1979-1983.

Johnson, L. L., P. Lanthier, et al. (2004). "Vaccination protects B cell-deficient mice against an oral challenge with mildly virulent *Toxoplasma gondii*." Vaccine **22**(29-30): 4054-4061.

Johnson, L. L. and P. C. Sayles (2002). "Deficient humoral responses underlie susceptibility to *Toxoplasma gondii* in CD4-deficient mice." Infect Immun **70**(1): 185-191.

Joiner, K. A., S. A. Fuhrman, et al. (1990). "*Toxoplasma gondii*: fusion competence of parasitophorous vacuoles in Fc receptor-transfected fibroblasts." Science **249**(4969): 641-646.

Joiner, K. A. and D. S. Roos (2002). "Secretory traffic in the eukaryotic parasite *Toxoplasma gondii*: less is more." J Cell Biol **157**(4): 557-563.

Jones, T. C., S. Yeh, et al. (1972). "The interaction between *Toxoplasma gondii* and mammalian cells. I. Mechanism of entry and intracellular fate of the parasite." J Exp Med **136**(5): 1157-1172.

Jongert, E., V. Melkebeek, et al. (2008). "An enhanced GRA1-GRA7 cocktail DNA vaccine primes anti-*Toxoplasma* immune responses in pigs." Vaccine **26**(8): 1025-1031.

Jongert, E., C. W. Roberts, et al. (2009). "Vaccines against *Toxoplasma gondii*: challenges and opportunities." Mem Inst Oswaldo Cruz **104**(2): 252-266.

Kamala, T. and N. K. Nanda (2009). "Protective response to *Leishmania major* in BALB/c mice requires antigen processing in the absence of DM." J Immunol **182**(8): 4882-4890.

Kanazawa, S., T. Okamoto, et al. (2000). "Tat competes with CIITA for the binding to P-TEFb and blocks the expression of MHC class II genes in HIV infection." Immunity **12**(1): 61-70.

Karttunen, J., S. Sanderson, et al. (1992). "Detection of rare antigen-presenting cells by the lacZ T-cell activation assay suggests an expression cloning

strategy for T-cell antigens." Proc Natl Acad Sci U S A **89**(13): 6020-6024.
Kasturi, S. P. and B. Pulendran (2008). "Cross-presentation: avoiding trafficking chaos?" Nat Immunol **9**(5): 461-463.
Kaufmann, S. H. and J. Hess (1999). "Impact of intracellular location of and antigen display by intracellular bacteria: implications for vaccine development." Immunol Lett **65**(1-2): 81-84.
Kausch, A. P., T. P. Owen, Jr., et al. (1999). "Organelle isolation by magnetic immunoabsorption." Biotechniques **26**(2): 336-343.
Kaye, A. (2011). "Toxoplasmosis: diagnosis, treatment, and prevention in congenitally exposed infants." J Pediatr Health Care **25**(6): 355-364.
Keppler, O. T., N. Tibroni, et al. (2006). "Modulation of specific surface receptors and activation sensitization in primary resting CD4+ T lymphocytes by the Nef protein of HIV-1." J Leukoc Biol **79**(3): 616-627.
Kessler, H., A. Herm-Gotz, et al. (2008). "Microneme protein 8--a new essential invasion factor in *Toxoplasma gondii*." J Cell Sci **121**(Pt 7): 947-956.
Khan, I. A., K. H. Ely, et al. (1991). "A purified parasite antigen (p30) mediates CD8+ T cell immunity against fatal *Toxoplasma gondii* infection in mice." J Immunol **147**(10): 3501-3506.
Khan, I. A., T. Matsuura, et al. (1995). "IL-10 mediates immunosuppression following primary infection with *Toxoplasma gondii* in mice." Parasite Immunol **17**(4): 185-195.
Kim, K., D. Soldati, et al. (1993). "Gene replacement in *Toxoplasma gondii* with chloramphenicol acetyltransferase as selectable marker." Science **262**(5135): 911-914.
Kim, K. and L. M. Weiss (2004). "*Toxoplasma gondii*: the model apicomplexan." Int J Parasitol **34**(3): 423-432.
Kim, L., B. A. Butcher, et al. (2004). "*Toxoplasma gondii* interferes with lipopolysaccharide-induced mitogen-activated protein kinase activation by mechanisms distinct from endotoxin tolerance." J Immunol **172**(5): 3003-3010.
Kim, S. K., A. E. Fouts, et al. (2007). "*Toxoplasma gondii* dysregulates IFN-gamma-inducible gene expression in human fibroblasts: insights from a genome-wide transcriptional profiling." J Immunol **178**(8): 5154-5165.
Kissinger, J. C., B. Gajria, et al. (2003). "ToxoDB: accessing the *Toxoplasma gondii* genome." Nucleic Acids Res **31**(1): 234-236.
Koch, N., M. Zacharias, et al. (2011). "Stoichiometry of HLA class II-invariant chain oligomers." PLoS One **6**(2): e17257.
Kongsvik, T. L., S. Honing, et al. (2002). "Mechanism of interaction between leucine-based sorting signals from the invariant chain and clathrin-associated adaptor protein complexes AP1 and AP2." J Biol Chem **277**(19): 16484-16488.
Kraus, E., H. H. Kiltz, et al. (1976). "The specificity of proteinase K against oxidized insulin B chain." Hoppe Seylers Z Physiol Chem **357**(2): 233-237.

Kreisel, D., S. B. Richardson, et al. (2010). "Cutting edge: MHC class II expression by pulmonary nonhematopoietic cells plays a critical role in controlling local inflammatory responses." J Immunol **185**(7): 3809-3813.
Kropshofer, H., A. B. Vogt, et al. (1996). "Editing of the HLA-DR-peptide repertoire by HLA-DM." EMBO J **15**(22): 6144-6154.
Krupnick, A. S., A. E. Gelman, et al. (2005). "Murine vascular endothelium activates and induces the generation of allogeneic CD4+25+Foxp3+ regulatory T cells." J Immunol **175**(10): 6265-6270.
Kwak, B., F. Mulhaupt, et al. (2000). "Statins as a newly recognized type of immunomodulator." Nat Med **6**(12): 1399-1402.
Kwan, W. C., W. R. McMaster, et al. (1992). "Inhibition of expression of major histocompatibility complex class II molecules in macrophages infected with *Leishmania donovani* occurs at the level of gene transcription via a cyclic AMP-independent mechanism." Infect Immun **60**(5): 2115-2120.
Labruyere, E., M. Lingnau, et al. (1999). "Differential membrane targeting of the secretory proteins GRA4 and GRA6 within the parasitophorous vacuole formed by *Toxoplasma gondii*." Molecular and biochemical parasitology **102**(2): 311-324.
Laliberte, J. and V. B. Carruthers (2008). "Host cell manipulation by the human pathogen *Toxoplasma gondii*." Cell Mol Life Sci **65**(12): 1900-1915.
Lamarque, M. H., J. Papoin, et al. (2012). "Identification of a new rhoptry neck complex RON9/RON10 in the Apicomplexa parasite *Toxoplasma gondii*." PloS one **7**(3): e32457.
Lambert, H. and A. Barragan (2010). "Modelling parasite dissemination: host cell subversion and immune evasion by *Toxoplasma gondii*." Cell Microbiol **12**(3): 292-300.
Lambert, H., N. Hitziger, et al. (2006). "Induction of dendritic cell migration upon *Toxoplasma gondii* infection potentiates parasite dissemination." Cell Microbiol **8**(10): 1611-1623.
Landsverk, O. J., O. Bakke, et al. (2009). "MHC II and the endocytic pathway: regulation by invariant chain." Scand J Immunol **70**(3): 184-193.
Lang, C., M. Algner, et al. (2006). "Diverse mechanisms employed by *Toxoplasma gondii* to inhibit IFN-gamma-induced major histocompatibility complex class II gene expression." Microbes Infect **8**(8): 1994-2005.
Lang, C., U. Gross, et al. (2007). "Subversion of innate and adaptive immune responses by *Toxoplasma gondii*." Parasitol Res **100**(2): 191-203.
Lang, C., A. Hildebrandt, et al. (2012). "Impaired chromatin remodelling at STAT1-regulated promoters leads to global unresponsiveness of *Toxoplasma gondii*-Infected macrophages to IFN-gamma." PLoS Pathog **8**(1): e1002483.
Lange, A. and N. M. Ferguson (2009). "Antigenic diversity, transmission mechanisms, and the evolution of pathogens." PLoS Comput Biol **5**(10): e1000536.
Le Roy, E., A. Muhlethaler-Mottet, et al. (1999). "Escape of human cytomegalovirus from HLA-DR-restricted CD4(+) T-cell response is

mediated by repression of gamma interferon-induced class II transactivator expression." J Virol **73**(8): 6582-6589.
Lecoeur, H. (2002). "Nuclear apoptosis detection by flow cytometry: influence of endogenous endonucleases." Exp Cell Res **277**(1): 1-14.
Lecordier, L., C. Mercier, et al. (1999). "Transmembrane insertion of the *Toxoplasma gondii* GRA5 protein occurs after soluble secretion into the host cell." Molecular biology of the cell **10**(4): 1277-1287.
Lecordier, L., C. Mercier, et al. (1993). "Molecular structure of a *Toxoplasma gondii* dense granule antigen (GRA 5) associated with the parasitophorous vacuole membrane." Molecular and biochemical parasitology **59**(1): 143-153.
Lecordier, L., I. Moleon-Borodowsky, et al. (1995). "Characterization of a dense granule antigen of *Toxoplasma gondii* (GRA6) associated to the network of the parasitophorous vacuole." Molecular and biochemical parasitology **70**(1-2): 85-94.
Lee, E. J., Y. M. Heo, et al. (2008). "Suppressed production of pro-inflammatory cytokines by LPS-activated macrophages after treatment with *Toxoplasma gondii* lysate." Korean J Parasitol **46**(3): 145-151.
Leng, L., C. N. Metz, et al. (2003). "MIF signal transduction initiated by binding to CD74." J Exp Med **197**(11): 1467-1476.
Leriche, M. A. and J. F. Dubremetz (1991). "Characterization of the protein contents of rhoptries and dense granules of *Toxoplasma gondii* tachyzoites by subcellular fractionation and monoclonal antibodies." Mol Biochem Parasitol **45**(2): 249-259.
Levine, N. D. (1988). "Progress in taxonomy of the Apicomplexan protozoa." J Protozool **35**(4): 518-520.
Li, P., J. L. Gregg, et al. (2005). "Compartmentalization of class II antigen presentation: contribution of cytoplasmic and endosomal processing." Immunol Rev **207**: 206-217.
Lin, M. H., T. C. Chen, et al. (2000). "Real-time PCR for quantitative detection of *Toxoplasma gondii*." J Clin Microbiol **38**(11): 4121-4125.
Livak, K. J. and T. D. Schmittgen (2001). "Analysis of relative gene expression data using real-time quantitative PCR and the 2(-Delta Delta C(T)) Method." Methods **25**(4): 402-408.
Lourenco, E. V., E. S. Bernardes, et al. (2006). "Immunization with MIC1 and MIC4 induces protective immunity against *Toxoplasma gondii*." Microbes Infect **8**(5): 1244-1251.
Luder, C. G., M. Algner, et al. (2003). "Reduced expression of the inducible nitric oxide synthase after infection with *Toxoplasma gondii* facilitates parasite replication in activated murine macrophages." Int J Parasitol **33**(8): 833-844.
Luder, C. G., C. Lang, et al. (2003). "*Toxoplasma gondii* inhibits MHC class II expression in neural antigen-presenting cells by down-regulating the class II transactivator CIITA." J Neuroimmunol **134**(1-2): 12-24.
Luder, C. G., T. Lang, et al. (1998). "Down-regulation of MHC class II molecules and inability to up-regulate class I molecules in murine macrophages after infection with *Toxoplasma gondii*." Clin Exp Immunol **112**(2): 308-316.

Luder, C. G., W. Walter, et al. (2001). "*Toxoplasma gondii* down-regulates MHC class II gene expression and antigen presentation by murine macrophages via interference with nuclear translocation of STAT1alpha." Eur J Immunol **31**(5): 1475-1484.

Luers, G. H., R. Hartig, et al. (1998). "Immuno-isolation of highly purified peroxisomes using magnetic beads and continuous immunomagnetic sorting." Electrophoresis **19**(7): 1205-1210.

Luft, B. J. and J. S. Remington (1992). "Toxoplasmic encephalitis in AIDS." Clin Infect Dis **15**(2): 211-222.

Lutjen, S., S. Soltek, et al. (2006). "Organ- and disease-stage-specific regulation of *Toxoplasma gondii*-specific CD8-T-cell responses by CD4 T cells." Infect Immun **74**(10): 5790-5801.

Lutz, M. B., R. M. Suri, et al. (2000). "Immature dendritic cells generated with low doses of GM-CSF in the absence of IL-4 are maturation resistant and prolong allograft survival in vivo." Eur J Immunol **30**(7): 1813-1822.

Manoury, B., W. F. Gregory, et al. (2001). "Bm-CPI-2, a cystatin homolog secreted by the filarial parasite *Brugia malayi*, inhibits class II MHC-restricted antigen processing." Curr Biol **11**(6): 447-451.

Mantovani, R. (1999). "The molecular biology of the CCAAT-binding factor NF-Y." Gene **239**(1): 15-27.

Martin, V., A. Supanitsky, et al. (2004). "Recombinant GRA4 or ROP2 protein combined with alum or the gra4 gene provides partial protection in chronic murine models of toxoplasmosis." Clin Diagn Lab Immunol **11**(4): 704-710.

McFadden, G. I., M. E. Reith, et al. (1996). "Plastid in human parasites." Nature **381**(6582): 482.

McKee, A. S., F. Dzierszinski, et al. (2004). "Functional inactivation of immature dendritic cells by the intracellular parasite *Toxoplasma gondii*." J Immunol **173**(4): 2632-2640.

McLeod, R., K. Boyer, et al. (2006). "Outcome of treatment for congenital toxoplasmosis, 1981-2004: the National Collaborative Chicago-Based, Congenital Toxoplasmosis Study." Clin Infect Dis **42**(10): 1383-1394.

Melhus, O., T. J. Koerner, et al. (1991). "Effects of TNF alpha on the expression of class II MHC molecules in macrophages induced by IFN gamma: evidence for suppression at the level of transcription." J Leukoc Biol **49**(1): 21-28.

Mihelic, M., A. Dobersek, et al. (2008). "Inhibitory fragment from the p41 form of invariant chain can regulate activity of cysteine cathepsins in antigen presentation." J Biol Chem **283**(21): 14453-14460.

Miranda, K., D. A. Pace, et al. (2010). "Characterization of a novel organelle in *Toxoplasma gondii* with similar composition and function to the plant vacuole." Mol Microbiol **76**(6): 1358-1375.

Mishima, M., X. Xuan, et al. (2001). "Construction of recombinant feline herpesvirus type 1 expressing *Toxoplasma gondii* surface antigen 1." Mol Biochem Parasitol **117**(1): 103-106.

Mitchell, E. K., P. Mastroeni, et al. (2004). "Inhibition of cell surface MHC class II expression by *Salmonella*." Eur J Immunol **34**(9): 2559-2567.

Miyazaki, T., P. Wolf, et al. (1996). "Mice lacking H2-M complexes, enigmatic elements of the MHC class II peptide-loading pathway." Cell **84**(4): 531-541.

Molinari, M., M. Salio, et al. (1998). "Selective inhibition of Ii-dependent antigen presentation by *Helicobacter pylori* toxin VacA." J Exp Med **187**(1): 135-140.

Momburg, F., N. Koch, et al. (1986). "Differential expression of Ia and Ia-associated invariant chain in mouse tissues after in vivo treatment with IFN-gamma." J Immunol **136**(3): 940-948.

Montoya, J. G. and O. Liesenfeld (2004). "Toxoplasmosis." Lancet **363**(9425): 1965-1976.

Montoya, J. G. and J. S. Remington (1996). "Toxoplasmic chorioretinitis in the setting of acute acquired toxoplasmosis." Clin Infect Dis **23**(2): 277-282.

Montoya, J. G. and J. S. Remington (2008). "Management of *Toxoplasma gondii* infection during pregnancy." Clin Infect Dis **47**(4): 554-566.

Moreno, C. S., G. W. Beresford, et al. (1999). "CREB regulates MHC class II expression in a CIITA-dependent manner." Immunity **10**(2): 143-151.

Morisaki, J. H., J. E. Heuser, et al. (1995). "Invasion of *Toxoplasma gondii* occurs by active penetration of the host cell." J Cell Sci **108 (Pt 6)**: 2457-2464.

Mostecki, J., B. M. Showalter, et al. (2005). "Early growth response-1 regulates lipopolysaccharide-induced suppressor of cytokine signaling-1 transcription." J Biol Chem **280**(4): 2596-2605.

Muhlethaler-Mottet, A., M. Krawczyk, et al. (2004). "The S box of major histocompatibility complex class II promoters is a key determinant for recruitment of the transcriptional co-activator CIITA." J Biol Chem **279**(39): 40529-40535.

Muhlethaler-Mottet, A., L. A. Otten, et al. (1997). "Expression of MHC class II molecules in different cellular and functional compartments is controlled by differential usage of multiple promoters of the transactivator CIITA." EMBO J **16**(10): 2851-2860.

Muller, U., U. Steinhoff, et al. (1994). "Functional role of type I and type II interferons in antiviral defense." Science **264**(5167): 1918-1921.

Muntasell, A., M. Carrascal, et al. (2004). "Dissection of the HLA-DR4 peptide repertoire in endocrine epithelial cells: strong influence of invariant chain and HLA-DM expression on the nature of ligands." J Immunol **173**(2): 1085-1093.

Munz, C. (2004). "Epstein-barr virus nuclear antigen 1: from immunologically invisible to a promising T cell target." J Exp Med **199**(10): 1301-1304.

Murphy, D. B., D. Lo, et al. (1989). "A novel MHC class II epitope expressed in thymic medulla but not cortex." Nature **338**(6218): 765-768.

Nanda, N. K. and E. K. Bikoff (2005). "DM peptide-editing function leads to immunodominance in CD4 T cell responses in vivo." J Immunol **175**(10): 6473-6480.

Nanda, N. K. and A. J. Sant (2000). "DM determines the cryptic and immunodominant fate of T cell epitopes." J Exp Med **192**(6): 781-788.

Nichols, B. A. and G. R. O'Connor (1981). "Penetration of mouse peritoneal macrophages by the protozoon *Toxoplasma gondii*. New evidence for active invasion and phagocytosis." Lab Invest **44**(4): 324-335.

Niedelman, W., D. A. Gold, et al. (2012). "The Rhoptry Proteins ROP18 and ROP5 Mediate *Toxoplasma gondii* Evasion of the Murine, But Not the Human, Interferon-Gamma Response." PLoS Pathog **8**(6): e1002784.

Nielsen, H. V., S. L. Lauemoller, et al. (1999). "Complete protection against lethal *Toxoplasma gondii* infection in mice immunized with a plasmid encoding the SAG1 gene." Infect Immun **67**(12): 6358-6363.

Nimmerjahn, F., S. Milosevic, et al. (2003). "Major histocompatibility complex class II-restricted presentation of a cytosolic antigen by autophagy." Eur J Immunol **33**(5): 1250-1259.

O'Keefe, G. M., V. T. Nguyen, et al. (1999). "Class II transactivator and class II MHC gene expression in microglia: modulation by the cytokines TGF-beta, IL-4, IL-13 and IL-10." Eur J Immunol **29**(4): 1275-1285.

O'Sullivan, D. M., D. Noonan, et al. (1987). "Four Ia invariant chain forms derive from a single gene by alternate splicing and alternate initiation of transcription/translation." J Exp Med **166**(2): 444-460.

Obst, R., H. M. van Santen, et al. (2005). "Antigen persistence is required throughout the expansion phase of a CD4(+) T cell response." J Exp Med **201**(10): 1555-1565.

Odorizzi, C. G., I. S. Trowbridge, et al. (1994). "Sorting signals in the MHC class II invariant chain cytoplasmic tail and transmembrane region determine trafficking to an endocytic processing compartment." J Cell Biol **126**(2): 317-330.

Ohmori, Y. and T. A. Hamilton (2000). "Interleukin-4/STAT6 represses STAT1 and NF-kappa B-dependent transcription through distinct mechanisms." J Biol Chem **275**(48): 38095-38103.

Oksenhendler, E., I. Charreau, et al. (1994). "*Toxoplasma gondii* infection in advanced HIV infection." AIDS **8**(4): 483-487.

Ong, Y. C., M. L. Reese, et al. (2010). "*Toxoplasma* rhoptry protein 16 (ROP16) subverts host function by direct tyrosine phosphorylation of STAT6." J Biol Chem **285**(37): 28731-28740.

Pai, R. K., M. Convery, et al. (2003). "Inhibition of IFN-gamma-induced class II transactivator expression by a 19-kDa lipoprotein from *Mycobacterium tuberculosis*: a potential mechanism for immune evasion." J Immunol **171**(1): 175-184.

Peixoto, L., F. Chen, et al. (2010). "Integrative genomic approaches highlight a family of parasite-specific kinases that regulate host responses." Cell host & microbe **8**(2): 208-218.

Pennini, M. E., R. K. Pai, et al. (2006). "*Mycobacterium tuberculosis* 19-kDa lipoprotein inhibits IFN-gamma-induced chromatin remodeling of MHC2TA by TLR2 and MAPK signaling." J Immunol **176**(7): 4323-4330.

Pepper, M., F. Dzierszinski, et al. (2008). "Plasmacytoid dendritic cells are activated by *Toxoplasma gondii* to present antigen and produce cytokines." J Immunol **180**(9): 6229-6236.

Pfeifer, J. D., M. J. Wick, et al. (1993). "Phagocytic processing of bacterial antigens for class I MHC presentation to T cells." Nature **361**(6410): 359-362.

Phelps, E. D., K. R. Sweeney, et al. (2008). "*Toxoplasma gondii* rhoptry discharge correlates with activation of the early growth response 2 host cell transcription factor." Infect Immun **76**(10): 4703-4712.

Pieters, J., O. Bakke, et al. (1993). "The MHC class II-associated invariant chain contains two endosomal targeting signals within its cytoplasmic tail." J Cell Sci **106 (Pt 3)**: 831-846.

Quan, J. H., J. Q. Chu, et al. (2012). "Induction of protective immune responses by a multiantigenic DNA vaccine encoding GRA7 and ROP1 of *Toxoplasma gondii*." Clin Vaccine Immunol **19**(5): 666-674.

Quraishi, O., D. K. Nagler, et al. (1999). "The occluding loop in cathepsin B defines the pH dependence of inhibition by its propeptide." Biochemistry **38**(16): 5017-5023.

Raschke, W. C., S. Baird, et al. (1978). "Functional macrophage cell lines transformed by Abelson leukemia virus." Cell **15**(1): 261-267.

Reese, M. L., G. M. Zeiner, et al. (2011). "Polymorphic family of injected pseudokinases is paramount in *Toxoplasma* virulence." Proceedings of the National Academy of Sciences of the United States of America **108**(23): 9625-9630.

Reiner, N. E., W. Ng, et al. (1987). "Parasite-accessory cell interactions in murine leishmaniasis. II. *Leishmania donovani* suppresses macrophage expression of class I and class II major histocompatibility complex gene products." J Immunol **138**(6): 1926-1932.

Reis e Sousa, C., S. Hieny, et al. (1997). "In vivo microbial stimulation induces rapid CD40 ligand-independent production of interleukin 12 by dendritic cells and their redistribution to T cell areas." J Exp Med **186**(11): 1819-1829.

Reith, W., S. LeibundGut-Landmann, et al. (2005). "Regulation of MHC class II gene expression by the class II transactivator." Nat Rev Immunol **5**(10): 793-806.

Reith, W. and B. Mach (2001). "The bare lymphocyte syndrome and the regulation of MHC expression." Annu Rev Immunol **19**: 331-373.

Remington, J. S., R. McLeod, et al. (2000). Diseases of the fetus and newborn infant. J. S. Remington and D. O. Klein. Philadelphia, W. B. Saunders Company**:** 205-346.

Reynolds, M. G. and D. S. Roos (1998). "A biochemical and genetic model for parasite resistance to antifolates. *Toxoplasma gondii* provides insights into pyrimethamine and cycloguanil resistance in *Plasmodium falciparum*." J Biol Chem **273**(6): 3461-3469.

Riese, R. J. and H. A. Chapman (2000). "Cathepsins and compartmentalization in antigen presentation." Curr Opin Immunol **12**(1): 107-113.

Robinson, H. L. and R. R. Amara (2005). "T cell vaccines for microbial infections." Nat Med **11**(4 Suppl): S25-32.

Romagnoli, P., C. Layet, et al. (1993). "Relationship between invariant chain expression and major histocompatibility complex class II transport into early and late endocytic compartments." J Exp Med **177**(3): 583-596.

Roos, D. S., R. G. Donald, et al. (1994). "Molecular tools for genetic dissection of the protozoan parasite *Toxoplasma gondii*." Methods Cell Biol **45**: 27-63.

Roos, D. S., W. J. Sullivan, et al. (1997). "Tagging genes and trapping promoters in *Toxoplasma gondii* by insertional mutagenesis." Methods **13**(2): 112-122.

Rorman, E., C. S. Zamir, et al. (2006). "Congenital toxoplasmosis--prenatal aspects of *Toxoplasma gondii* infection." Reprod Toxicol **21**(4): 458-472.

Rosowski, E. E., D. Lu, et al. (2011). "Strain-specific activation of the NF-kappaB pathway by GRA15, a novel *Toxoplasma gondii* dense granule protein." J Exp Med **208**(1): 195-212.

Saeij, J. P., J. P. Boyle, et al. (2005). "Differences among the three major strains of *Toxoplasma gondii* and their specific interactions with the infected host." Trends Parasitol **21**(10): 476-481.

Saeij, J. P., J. P. Boyle, et al. (2006). "Polymorphic secreted kinases are key virulence factors in toxoplasmosis." Science **314**(5806): 1780-1783.

Saeij, J. P., J. P. Boyle, et al. (2005). "Bioluminescence imaging of *Toxoplasma gondii* infection in living mice reveals dramatic differences between strains." Infect Immun **73**(2): 695-702.

Saeij, J. P., S. Coller, et al. (2007). "*Toxoplasma* co-opts host gene expression by injection of a polymorphic kinase homologue." Nature **445**(7125): 324-327.

Saffer, L. D., O. Mercereau-Puijalon, et al. (1992). "Localization of a *Toxoplasma gondii* rhoptry protein by immunoelectron microscopy during and after host cell penetration." J Protozool **39**(4): 526-530.

Sant, A. J. (1994). "Endogenous antigen presentation by MHC class II molecules." Immunol Res **13**(4): 253-267.

Savina, A., P. Vargas, et al. (2010). "Measuring pH, ROS production, maturation, and degradation in dendritic cell phagosomes using cytofluorometry-based assays." Methods Mol Biol **595**: 383-402.

Scanga, C. A., J. Aliberti, et al. (2002). "Cutting edge: MyD88 is required for resistance to *Toxoplasma gondii* infection and regulates parasite-induced IL-12 production by dendritic cells." J Immunol **168**(12): 5997-6001.

Schepers, K., R. Arens, et al. (2005). "Dissection of cytotoxic and helper T cell responses." Cell Mol Life Sci **62**(23): 2695-2710.

Schindler, M., S. Wurfl, et al. (2003). "Down-modulation of mature major histocompatibility complex class II and up-regulation of invariant chain cell surface expression are well-conserved functions of human and simian immunodeficiency virus nef alleles." J Virol **77**(19): 10548-10556.

Schmidt, D. R., B. Hogh, et al. (2006). "Treatment of infants with congenital toxoplasmosis: tolerability and plasma concentrations of sulfadiazine and pyrimethamine." Eur J Pediatr **165**(1): 19-25.

Schulze, M. S. and K. W. Wucherpfennig (2012). "The mechanism of HLA-DM induced peptide exchange in the MHC class II antigen presentation pathway." Curr Opin Immunol **24**(1): 105-111.

Seabra, S. H., W. de Souza, et al. (2002). "*Toxoplasma gondii* partially inhibits nitric oxide production of activated murine macrophages." Exp Parasitol **100**(1): 62-70.

Sercarz, E. E. and E. Maverakis (2003). "Mhc-guided processing: binding of large antigen fragments." Nat Rev Immunol **3**(8): 621-629.

Shapira, S., O. S. Harb, et al. (2005). "Initiation and termination of NF-kappaB signaling by the intracellular protozoan parasite *Toxoplasma gondii*." J Cell Sci **118**(Pt 15): 3501-3508.

Sibley, L. D. and J. C. Boothroyd (1992). "Virulent strains of *Toxoplasma gondii* comprise a single clonal lineage." Nature **359**(6390): 82-85.

Sieling, P. A., D. Chatterjee, et al. (1995). "CD1-restricted T cell recognition of microbial lipoglycan antigens." Science **269**(5221): 227-230.

Simmons, D. P., P. A. Wearsch, et al. (2012). "Type I IFN drives a distinctive dendritic cell maturation phenotype that allows continued class II MHC synthesis and antigen processing." J Immunol **188**(7): 3116-3126.

Sinai, A. P. and K. A. Joiner (2001). "The *Toxoplasma gondii* protein ROP2 mediates host organelle association with the parasitophorous vacuole membrane." J Cell Biol **154**(1): 95-108.

Sloan, V. S., P. Cameron, et al. (1995). "Mediation by HLA-DM of dissociation of peptides from HLA-DR." Nature **375**(6534): 802-806.

Smiley, S. T., P. A. Lanthier, et al. (2005). "Exacerbated susceptibility to infection-stimulated immunopathology in CD1d-deficient mice." J Immunol **174**(12): 7904-7911.

Soheilian, M., M. M. Sadoughi, et al. (2005). "Prospective randomized trial of trimethoprim/sulfamethoxazole versus pyrimethamine and sulfadiazine in the treatment of ocular toxoplasmosis." Ophthalmology **112**(11): 1876-1882.

Soldati, D., J. F. Dubremetz, et al. (2001). "Microneme proteins: structural and functional requirements to promote adhesion and invasion by the apicomplexan parasite *Toxoplasma gondii*." Int J Parasitol **31**(12): 1293-1302.

St-Denis, A., F. Chano, et al. (1998). "Protein kinase C-alpha modulates lipopolysaccharide-induced functions in a murine macrophage cell line." J Biol Chem **273**(49): 32787-32792.

Starr, T. K., S. C. Jameson, et al. (2003). "Positive and negative selection of T cells." Annu Rev Immunol **21**: 139-176.

Stebbins, C. C., G. E. Loss, Jr., et al. (1995). "The requirement for DM in class II-restricted antigen presentation and SDS-stable dimer formation is allele and species dependent." J Exp Med **181**(1): 223-234.

Steimle, V., B. Durand, et al. (1995). "A novel DNA-binding regulatory factor is mutated in primary MHC class II deficiency (bare lymphocyte syndrome)." Genes Dev **9**(9): 1021-1032.

Steimle, V., L. A. Otten, et al. (1993). "Complementation cloning of an MHC class II transactivator mutated in hereditary MHC class II deficiency (or bare lymphocyte syndrome)." Cell **75**(1): 135-146.

Steinfeldt, T., S. Konen-Waisman, et al. (2010). "Phosphorylation of mouse immunity-related GTPase (IRG) resistance proteins is an evasion strategy for virulent *Toxoplasma gondii*." PLoS Biol **8**(12): e1000576.

Strubin, M., E. O. Long, et al. (1986). "Two forms of the Ia antigen-associated invariant chain result from alternative initiations at two in-phase AUGs." Cell **47**(4): 619-625.

Stumptner-Cuvelette, P., S. Morchoisne, et al. (2001). "HIV-1 Nef impairs MHC class II antigen presentation and surface expression." Proc Natl Acad Sci U S A **98**(21): 12144-12149.

Stutz, A., H. Kessler, et al. (2012). "Cell invasion and strain dependent induction of suppressor of cytokine signaling-1 by *Toxoplasma gondii*." Immunobiology **217**(1): 28-36.

Su, C., D. Evans, et al. (2003). "Recent expansion of Toxoplasma through enhanced oral transmission." Science **299**(5605): 414-416.

Suzuki, Y., M. A. Orellana, et al. (1988). "Interferon-gamma: the major mediator of resistance against *Toxoplasma gondii*." Science **240**(4851): 516-518.

Tenter, A. M., A. R. Heckeroth, et al. (2000). "*Toxoplasma gondii*: from animals to humans." Int J Parasitol **30**(12-13): 1217-1258.

Thompson, J. A., M. K. Srivastava, et al. (2008). "The absence of invariant chain in MHC II cancer vaccines enhances the activation of tumor-reactive type 1 CD4+ T lymphocytes." Cancer Immunol Immunother **57**(3): 389-398.

Ting, J. P. and J. Trowsdale (2002). "Genetic control of MHC class II expression." Cell **109 Suppl**: S21-33.

Tonkin, M. L., M. Roques, et al. (2011). "Host cell invasion by apicomplexan parasites: insights from the co-structure of AMA1 with a RON2 peptide." Science **333**(6041): 463-467.

Trombetta, E. S. and I. Mellman (2005). "Cell biology of antigen processing in vitro and in vivo." Annu Rev Immunol **23**: 975-1028.

Turk, B., I. Dolenc, et al. (1999). "Acidic pH as a physiological regulator of human cathepsin L activity." Eur J Biochem **259**(3): 926-932.

van Leeuwen, E. M., J. Sprent, et al. (2009). "Generation and maintenance of memory CD4(+) T Cells." Curr Opin Immunol **21**(2): 167-172.

Velge-Roussel, F., P. Marcelo, et al. (2000). "Intranasal immunization with *Toxoplasma gondii* SAG1 induces protective cells into both NALT and GALT compartments." Infect Immun **68**(2): 969-972.

Waldburger, J. M., S. Rossi, et al. (2003). "Promoter IV of the class II transactivator gene is essential for positive selection of CD4+ T cells." Blood **101**(9): 3550-3559.

Waldburger, J. M., T. Suter, et al. (2001). "Selective abrogation of major histocompatibility complex class II expression on extrahematopoietic cells in mice lacking promoter IV of the class II transactivator gene." J Exp Med **194**(4): 393-406.

Wearsch, P. A. and P. Cresswell (2009). Antigen processing and presentation. nri0905_antigen_poster, Nature Reviews Immunology. **1206 x 678**.

Weischenfeldt, J. and B. Porse (2008). "Bone Marrow-Derived Macrophages (BMM): Isolation and Applications." CSH Protoc **2008**: pdb prot5080.

Weiss, L. M. and K. Kim (2000). "The development and biology of bradyzoites of *Toxoplasma gondii*." Front Biosci **5**: D391-405.

Weiss, L. M. and K. Kim (2007). *Toxoplasma gondii* : the model apicomplexan : perspectives and methods. Amsterdam ; Boston, Elsevier/Academic Press.

Wright, G. D. (2007). "The antibiotic resistome: the nexus of chemical and genetic diversity." Nat Rev Microbiol **5**(3): 175-186.

Yong, E. C., E. Y. Chi, et al. (1994). "*Toxoplasma gondii* alters eicosanoid release by human mononuclear phagocytes: role of leukotrienes in interferon gamma-induced antitoxoplasma activity." J Exp Med **180**(5): 1637-1648.

Youssef, S., O. Stuve, et al. (2002). "The HMG-CoA reductase inhibitor, atorvastatin, promotes a Th2 bias and reverses paralysis in central nervous system autoimmune disease." Nature **420**(6911): 78-84.

Zhang, J. G., A. Farley, et al. (1999). "The conserved SOCS box motif in suppressors of cytokine signaling binds to elongins B and C and may couple bound proteins to proteasomal degradation." Proc Natl Acad Sci U S A **96**(5): 2071-2076.

Zhong, G., P. Fan, et al. (2001). "Identification of a chlamydial protease-like activity factor responsible for the degradation of host transcription factors." J Exp Med **193**(8): 935-942.

Zhong, G., T. Fan, et al. (1999). "*Chlamydia* inhibits interferon gamma-inducible major histocompatibility complex class II expression by degradation of upstream stimulatory factor 1." J Exp Med **189**(12): 1931-1938.

Zhou, C., L. Lu, et al. (2011). "HIV-1 glycoprotein 41 ectodomain induces activation of the CD74 protein-mediated extracellular signal-regulated kinase/mitogen-activated protein kinase pathway to enhance viral infection." J Biol Chem **286**(52): 44869-44877.

Zhu, L. and P. P. Jones (1990). "Transcriptional control of the invariant chain gene involves promoter and enhancer elements common to and distinct from major histocompatibility complex class II genes." Mol Cell Biol **10**(8): 3906-3916.

Zimmermann, S., P. J. Murray, et al. (2006). "Induction of suppressor of cytokine signaling-1 by *Toxoplasma gondii* contributes to immune evasion in macrophages by blocking IFN-gamma signaling." J Immunol **176**(3): 1840-1847.

Appendix

Gene	Sense primer	Anti-sense primer
CD74 p31	5'-ACC GAG GCT CCA CCT AAA GAG-3'	5'- TTG ACC CAG TTC CTG CCT G-3'
CD74 p41	5'-TTC CTC ACA CCA AGA GCC G -3'	5'- TGT CCA GTG GCT CAC TGC AG -3'
CD74 common	5'- GAA CCT GCA ACT GGA GAG CC -3'	5'- GGT TTG GCA GAT TTC GGA AG -3'
H2-Aα	5'- CAT CTT CCC TCC TGT GAT CAA CA -3'	5'- CAC CGT CTG CGA CTG ACT TG -3'
H2-Aβ1	5'- GGA GAC TCC GAA AGG CAT TTC -3'	5'- GCG TCC CGT TGG TGA AGT AG -3'
H2-Eβ1	5'- TGG CAG CTG TGA TCC TGT TG -3'	5'- AAA CCA TGG TCT GGA GTC TCT GA-3'
H2-DMα	5'- GGC GGT GCT CGA AGC A -3'	5'- TGT GCC GGA ATG TGT GGT T -3'
H2-DMβ1/2	5'- CTA TCC AGC GGA TGT GAC CAT -3'	5'- TGG GCT GAG CCG TCT TCT -3'

Appendix Table 1: RT-PCR primers for class II genes.